A THREE-DIMENSIONAL HYDRODYNAMIC-EUTROPHICATION MODEL (HEM-3D): DESCRIPTION OF WATER QUALITY AND SEDIMENT PROCESS SUBMODELS

(EFDC WATER QUALITY MODEL)

by

Kyeong Park, Albert Y. Kuo, Jian Shen and John M. Hamrick

Special Report in Applied Marine Science
and Ocean Engineering No. 327

School of Marine Science
Virginia Institute of Marine Science
College of William and Mary
Gloucester Point, VA 23062

January 1995

(Revised by Tetra Tech, Inc., June 2000)

Table of Contents

List of Tables

List of Figures

Acknowledgements

The mathematical model described in this report was developed as a part of the Three-Dimensional Model Project funded by the Virginia Chesapeake Bay Initiative Programs. We thank Gamble M. Sisson for helpful discussions and review of the manuscript, and James E. Bauer and Robert J. Diaz for discussions on sediment processes. We are grateful to Robert J. Byrne for his guidance and support.

1 - INTRODUCTION

Virginia Institute of Marine Science (VIMS) has been developing a general purpose three-dimensional hydrodynamic and sediment transport model, Environmental Fluid Dynamics Computer Code (EFDC; Hamrick 1992). The real-time model simulates density and topographically-induced circulation as well as tidal and wind-driven flows, and spatial and temporal distributions of salinity, temperature and sediment concentration. The model also is capable of handling the wetting and drying of shallow area, hydraulic control structures, vegetation resistance for wetlands and Lagrangian particle tracking. The information of physical transport processes, both advective and diffusive, simulated by the hydrodynamic model can be used to account for the transport of passive substances including non-conservative water quality parameters.

A water quality model with twenty-one state variables has been developed and integrated with EFDC to form a three-dimensional Hydrodynamic-Eutrophication Model (HEM-3D) of the VIMS. The model, upon receiving the information of physical transport from EFDC, simulates the spatial and temporal distributions of water quality parameters including dissolved oxygen, suspended algae (3 groups), various components of carbon, nitrogen, phosphorus and silica cycles, and fecal coliform bacteria. A sediment process model with twenty-seven state variables has also been developed. The sediment process model, upon receiving the particulate organic matter deposited from the overlying water column, simulates their diagenesis and the resulting fluxes of inorganic substances (ammonium, nitrate, phosphate and silica) and sediment oxygen demand back to the water column. The coupling of the sediment process model with the water quality model not only enhances the model's predictive capability of water quality parameters but also enables it to simulate the long-term changes in water quality conditions in response to changes in nutrient loadings. This report documents the water quality model, including the sediment process model, for the formulations of the kinetic processes being simulated and their numerical methods of solution.

The governing mass-balance equation for each of the water quality state variables may be expressed as:

$$\frac{\partial C}{\partial t} + \frac{\partial (uC)}{\partial x} + \frac{\partial (vC)}{\partial y} + \frac{\partial (wC)}{\partial z} =$$

$$\frac{\partial}{\partial x}\left(K_x \frac{\partial C}{\partial x} \right) + \frac{\partial}{\partial y}\left(K_y \frac{\partial C}{\partial y} \right) + \frac{\partial}{\partial z}\left(K_z \frac{\partial C}{\partial z} \right) + S_C \qquad (1\text{-}1)$$

C = concentration of a water quality state variable

u, v & w = velocity components in the x-, y- and z-directions, respectively

K_x, K_y & K_z = turbulent diffusivities in the x-, y- and z-directions, respectively

S_C = internal and external sources and sinks per unit volume.

The last three terms on the left-hand side (LHS) of Eq. 1-1 account for the advective transport and the first three terms on the right-hand side (RHS) of Eq. 1-1 account for the diffusive transport. These six terms for physical transport are analogous to, and thus the numerical method of solution is the same as, those in the mass-balance equation for salinity in the hydrodynamic model (Hamrick 1992). The last term in Eq. 1-1 represents the kinetic processes and external loads for each of the state variables. The present model solves Eq. 1-1 after decoupling the kinetic terms from the physical transport terms. The solution scheme for both the physical transport (Hamrick 1992) and the kinetic equations (Chapter 2 and Section 4-12) is second-order accurate. Chapter 2 describes the decoupling and the method of solution for Eq. 1-1.

The kinetic processes included in this model use the formulations in the tidal prism water quality model, TPM-VIMS (Kuo & Park 1994), which are mostly from the Chesapeake Bay three-dimensional water quality model, CE-QUAL-ICM (Cerco & Cole 1994). The kinetic sources and sinks, and external loads for each state variable are described in Chapter 4. The kinetic processes include the exchange fluxes at the sediment-water interface. A sediment process model, which was developed for the Chesapeake Bay three-dimensional modeling effort (DiToro & Fitzpatrick 1993), was slightly modified and incorporated into the tidal prism model (Kuo & Park 1994). This sediment process model is incorporated into the present model to simulate the sediment-water exchange fluxes, and is described in Chapter 5. Brief comments are given in Chapter 6.

2 - Solution Method of Governing Mass-Balance Equation

The governing mass-balance equation for water quality state variables (Eq. 1-1) consists of physical transport, advective and diffusive, and kinetic processes. When solving Eq. 1-1, the kinetic terms are decoupled from the physical transport terms. The mass-balance equation for physical transport only, which takes the same form as the salt-balance equation, is:

$$\frac{\partial C}{\partial t} + \frac{\partial (uC)}{\partial x} + \frac{\partial (vC)}{\partial y} + \frac{\partial (wC)}{\partial z} = \frac{\partial}{\partial x}\left(K_x \frac{\partial C}{\partial x} \right) + \frac{\partial}{\partial y}\left(K_y \frac{\partial C}{\partial y} \right) + \frac{\partial}{\partial z}\left(K_z \frac{\partial C}{\partial z} \right) \qquad (2\text{-}1)$$

The equation for kinetic processes only, which will be referred to as kinetic equation, is:

$$\frac{\partial C}{\partial t} = S_C \qquad (2\text{-}2)$$

which may be expressed as (see Eq. 3-20):

$$\frac{\partial C}{\partial t} = K \cdot C + R \qquad (2\text{-}3)$$

where K is kinetic rate (time^{-1}) and R is source/sink term (mass volume^{-1} time^{-1}). Equation 2-3 is obtained by linearizing some terms in the kinetic equations (Section III-10 and Appendix A), mostly Monod type expressions. Hence, K and R are known values in Eq. 2-3. Equation 2-1 is identical with, and thus its numerical method of solution is the same as, the mass-balance equation for salinity (Hamrick 1992). This chapter describes the method of solution for Eq. 1-1 in terms of interfacing Equations 2-1 and 2-3.

The hydrodynamic model employs a second-order accurate three time-level advection scheme after integrating Eq. 2-1 over a cell volume (Hamrick 1992), and thus its time step is $2 \cdot \Delta t$ where $\Delta t = t_{n+1} - t_n$. To achieve the same second-order accuracy, the solution scheme of the kinetic equation (Eq. 2-3) is derived by dividing the solution procedure over a time period of $2 \cdot \Delta t$ into two steps, alternating between explicit and implicit schemes. Figure 2-1a illustrates the solution procedure over the time period from t_{n-1} to t_{n+1}.

The first step, S1, solves Eq. 2-3 over Δt from t_{n-1} to t_n by the explicit scheme:

$$C_{-P}^{\,n} - C^{n-1} = \Delta t \cdot K^{n-1} \cdot C^{n-1} + \Delta t \cdot R^{n-1} \qquad (2\text{-}4\text{-}1)$$

which subjects the conditions at $t = t_{n-1}$, C^{n-1}, to the kinetic processes alone to give $C_{-p}^{\,n}$. The superscript designates the time step. The subscript -P designates an intermediate concentration that lacks the

physical transport over Δt, whereas the subscript +P will designate one with surplus physical transport over Δt. In Fig. 2-1, the subscript -K designates an intermediate concentration that lacks the kinetic update over Δt, whereas the subscript +K designates one with surplus kinetic update over Δt. In Fig. 2-1a, hence, $C_{-P}^{n} = C_{+K}^{n-1}$.

Next, the intermediate concentration fields, C_{+K}^{n-1}, are physically transported over $2\cdot\Delta t$ from t_{n-1} to t_{n+1} in step S2 (Fig. 2-1a) by the finite difference form of Eq. 2-1 after being integrated over the cell volume (Hamrick 1992):

$$C_{-K}^{n+1} - C_{+K}^{n-1} = 2\cdot\Delta t\cdot PT \tag{2-4-2}$$

where PT is a physical transport operator over $2\cdot\Delta t$ from t_{n-1} to t_{n+1}, and C_{-K}^{n+1} is another intermediate concentration at $t = t_{n+1}$ lacking the kinetic update over Δt from t_n to t_{n+1}. Finally, the step S3 solves Eq. 2-3 over Δt from t_n to t_{n+1} by the implicit scheme:

$$C^{n+1} - C_{+P}^{n} = \Delta t\cdot K^{n-1}\cdot C^{n+1} + \Delta t\cdot R^{n+1} \tag{2-4-3}$$

where C^{n+1} is the concentration at $t = t_{n+1}$. In the linearized kinetic equation (Eq. 2-3 or Eq. 3-20), the kinetic rate is evaluated using old conditions, i.e., K^{n-1}. Also note in Eq. 2-4-3, $C_{+P}^{n} = C_{-K}^{n+1}$ (Fig. 2-1a).

In principle, the same three-step procedure, S1, S2 and S3, may be repeated for the next time period from t_{n+1} to t_{n+3}, with the equation for the step S4 given by:

$$C_{-P}^{n+2} - C^{n+1} = \Delta t\cdot K^{n+1}\cdot C^{n+1} + \Delta t\cdot R^{n+1} \tag{2-4-4}$$

where C_{-P}^{n+2} is an intermediate concentration at $t = t_{n+2}$ lacking the physical transport over Δt from t_{n+1} to t_{n+2}. In practice, the computational steps S3 and S4 may be combined by adding Equations 2-4-3 and 2-4-4 to arrive at (Fig. 2-1b):

$$C_{-P}^{n+2} - C_{+P}^{n} = \Delta t\cdot\left(K^{n-1} + K^{n+1}\right)\cdot C^{n+1} + 2\cdot\Delta t\cdot R^{n+1} \tag{2-5}$$

which may be approximated by:

$$C_{-P}^{n+2} - C_{+P}^{n} = \Delta t\cdot K^{n}\cdot\left(C_{+P}^{n} + C_{-P}^{n+2}\right) + 2\cdot\Delta t\cdot R^{n} \tag{2-6}$$

or

$$C_{+K}^{n+1} - C_{-K}^{n+1} = \Delta t\cdot K^{n}\cdot\left(C_{-K}^{n+1} + C_{+K}^{n+1}\right) + 2\cdot\Delta t\cdot R^{n} \tag{2-7}$$

by assuming:

$$K^{n-1} + K^{n+1} \simeq 2\cdot K^{n} \tag{2-8-1}$$

$$C^{n+1} \simeq \frac{1}{2}\left(C_{+P}^{n} + C_{-P}^{n+2}\right) = \frac{1}{2}\left(C_{-K}^{n+1} + C_{+K}^{n+1}\right) \quad (2\text{-}8\text{-}2)$$

$$R^{n+1} \simeq R^{n} \quad (2\text{-}8\text{-}3)$$

Equation 2-6, or Eq. 2-7, is a second-order accurate trapezoidal solution of Eq. 2-3 over $2\cdot\Delta t$ from t_n to t_{n+2}, with the concentration at $t = t_{n+1}$ given by Eq. 2-8-2. The source/sink term R consists of external loads and sediment-water exchange fluxes (Section 4-12 and Appendix A). In model application, external loads are usually specified as a daily input and sediment-water exchange fluxes have a time scale of days and months. Since Δt in a three-dimensional real-time model is on the order of minutes, the assumption in Eq. 2-8-3 does not significantly affect the accuracy of the solution.

With the combination of computational steps S3 and S4 in Fig. 2-1a, the solution scheme for Equations 2-1 and 2-3 becomes an alternate solution of the physical transport (Eq. 2-4-2) and the kinetic processes (Eq. 2-7), as illustrated in Fig. 2-1b. Both Equations 2-4-2 and 2-7 are second-order accurate. It should be noted that the intermediate concentration with the subscripts, either ±K or ±P, are not real concentrations at their time steps. For example, C_{-K}^{n+1} and C_{+K}^{n+1} are imaginary concentrations at $t = t_{n+1}$, with the former lacking the kinetic update from t_n to t_{n+1} and the latter with surplus kinetic update from t_{n+1} to t_{n+2}. The real concentrations at $t = t_{n+1}$, C^{n+1}, may be evaluated by the average of these two (Eq. 2-8-2).

Finally, the solution scheme may be generalized into the one illustrated in Fig. 2-1c. Since the water quality kinetic processes have much longer time scales than the allowable Δt in the real-time hydrodynamic model, the kinetic equation (Eq. 2-3) may be solved not as often as the physical transport equation (Eq. 2-1). In general, then, $\theta = m\cdot(2\cdot\Delta t)$ where m is a positive integer. In Fig. 2-1c, the kinetic equation is solved once over a time interval of θ from t_n to t_{n+2m} for every m steps of computation of physical transport. It, however, should be cautioned that θ should not be large enough to cause instability by consuming all materials within a cell over a time period of θ.

The decoupling of the kinetic processes from the physical transport results in a simple and efficient computational procedure as described above (Park & Kuo submitted). The decoupling of the governing equations not only simplifies the solution scheme but also makes the model more flexible with respect to the addition of new water quality state variables and to the modification of the kinetic formulations. The solution scheme for the physical transport equation needs to be obtained and validated only once for conservative substance such as salt. Later addition of new water quality state variables or modification of the kinetic formulations would require only simple modification in the solution scheme for kinetic equations.

3 - EFDC HYDRODYNAMIC MODEL

Modeling the physics, chemistry, and biology of the receiving waters of streams, lakes, estuaries, or coastal regions requires a model that incorporates all the major processes. Transport processes for this study were simulated using the three-dimensional EFDC hydrodynamic model that includes temperature transport. The EFDC hydrodynamic model was developed by Hamrick (1992). The model formulation was based on the principles expressed by the equations of motion, conservation of volume, and conservation of mass. Quantities computed by the model included three-dimensional velocities, surface elevation, vertical viscosity and diffusivity, temperature, salinity, and density.

3.1 General

The Environmental Fluid Dynamics Code is a general purpose modeling package for simulating three-dimensional flow, transport, and biogeochemical processes in surface water systems including rivers, lakes, estuaries, reservoirs, wetlands, and coastal regions. The EFDC model was originally developed at the Virginia Institute of Marine Science for estuarine and coastal applications and is considered public domain software. In addition to hydrodynamic and salinity and temperature transport simulation capabilities, EFDC is capable of simulating cohesive and noncohesive sediment transport, near field and far field discharge dilution from multiple sources, eutrophication processes, the transport and fate of toxic contaminants in the water and sediment phases, and the transport and fate of various life stages of finfish and shellfish. Special enhancements to the hydrodynamic portion of the code, including vegetation resistance, drying and wetting, hydraulic structure representation, wave-current boundary layer interaction, and wave-induced currents, allow refined modeling of wetland marsh systems, controlled flow systems, and nearshore wave induced currents and sediment transport. The EFDC model has been extensively tested and documented for more than 20 modeling studies. The model is presently being used by a number of organizations including universities, governmental agencies, and environmental consulting firms.

The structure of the EFDC model includes four major modules: (1) a hydrodynamic model, (2) a water quality model, (3) a sediment transport model, and (4) a toxics model (see Figure 3-1). The EFDC hydrodynamic model itself, which was used for this study, is composed of six transport modules including dynamics, dye, temperature, salinity, near field plume, and drifter (see Figure 3-2). Various products of the dynamics module (i.e., water depth, velocity, and mixing) are directly coupled to the water quality, sediment transport, and toxics models as shown in the following figures. Schematic diagrams for the water quality model, the sediment transport model, and the toxics model are shown in Figures 3-3, 3-4, and 3-5, respectively.

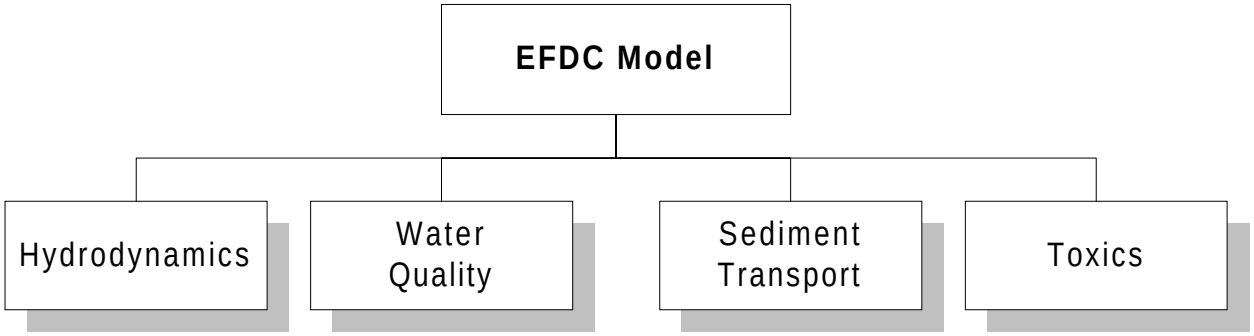

Figure 3-1. Primary modules of the EFDC model.

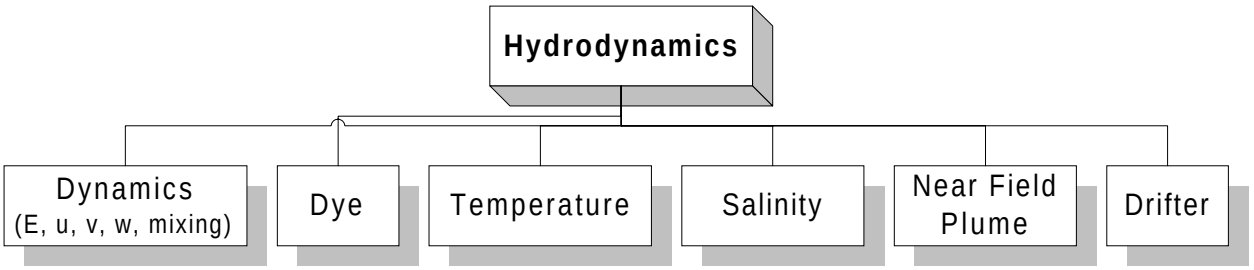

Figure 3-2. Structure of the EFDC hydrodynamic model.

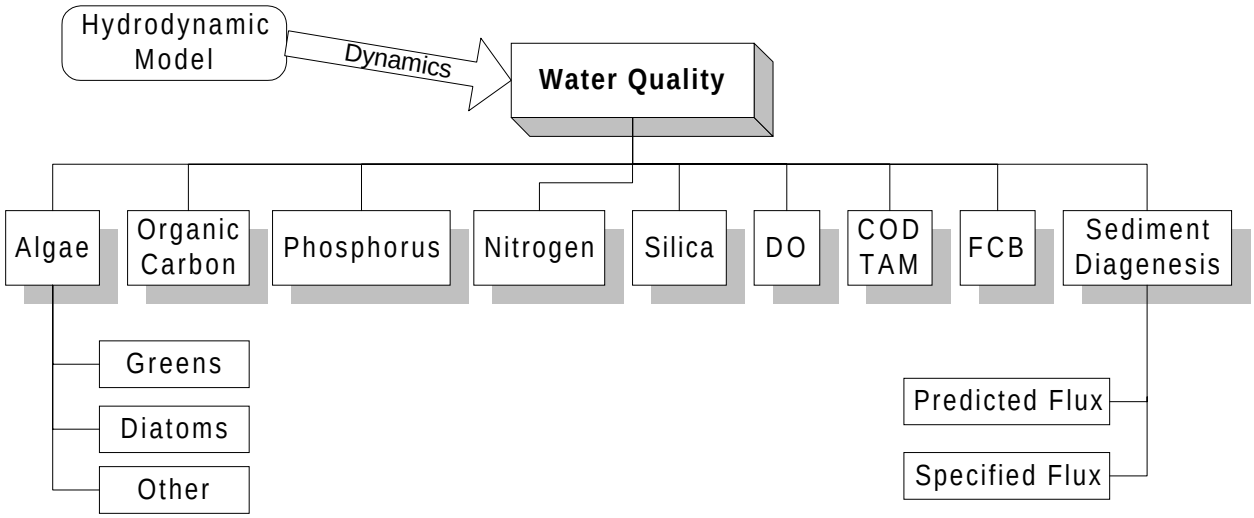

Figure 3-3. Structure of the EFDC water quality model.

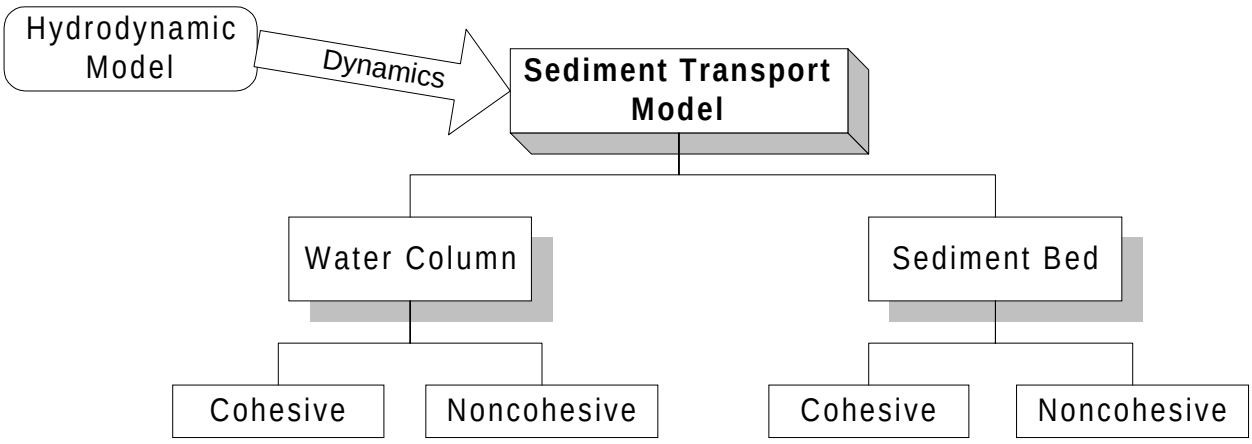

Figure 3-4. Structure of the EFDC sediment transport model.

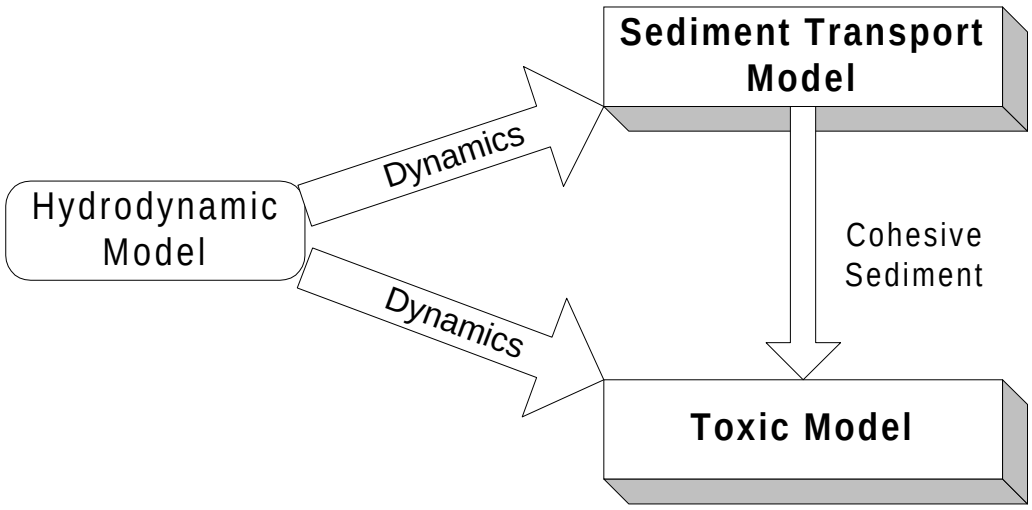

Figure 3-5. Structure of the EFDC toxics model.

3.2 Hydrodynamics and Salinity and Temperature Transport

The physics of the EFDC model and many aspects of the computational scheme are equivalent to the widely used Blumberg-Mellor model (Blumberg and Mellor 1987). The EFDC model solves the three-dimensional, vertically hydrostatic, free surface, turbulent averaged equations of motions for a variable density fluid. Dynamically coupled transport equations for turbulent kinetic energy, turbulent length scale, salinity, and temperature are also solved. The two turbulence parameter transport equations implement the Mellor-Yamada level 2.5 turbulence closure scheme (Mellor and Yamada 1982; Galperin et al. 1988). The EFDC model uses a stretched or sigma vertical coordinate and Cartesian, or curvilinear, orthogonal horizontal coordinates.

The numerical scheme employed in EFDC to solve the equations of motion uses second order accurate spatial finite differencing on a staggered or C grid. The model's time integration employs a second order accurate three-time level, finite difference scheme with an internal-external mode splitting procedure to separate the internal shear or baroclinic mode from the external free surface gravity wave or barotropic mode. The external mode solution is semi-implicit and simultaneously computes the two-dimensional (2-D) surface elevation field by a preconditioned conjugate gradient procedure. The external solution is completed by the calculation of the depth average barotropic velocities using the new surface elevation field. The model's semi-implicit external solution allows large time steps that are constrained only by the stability criteria of the explicit central difference or high order upwind advection scheme (Smolarkiewicz and Margolin 1993) used for the nonlinear accelerations. Horizontal boundary conditions for the external mode solution include options for simultaneously specifying the surface elevation only, the characteristic of an incoming wave (Bennett and McIntosh 1982), free radiation of an outgoing wave (Bennett 1976; Blumberg and Kantha 1985), or the normal volumetric flux on arbitrary portions of the boundary. The EFDC model's internal momentum equation solution, at the same time step as the external solution, is implicit with respect to vertical diffusion. The internal solution of the momentum equations is in terms of the vertical profile of shear stress and velocity shear, which results in the simplest and most accurate form of the baroclinic pressure gradients and eliminates the over determined character of alternate internal mode formulations. Time splitting inherent in the three-time-level scheme is controlled by periodic insertion of a second order accurate two-time-level trapezoidal step. EFDC is also readily configured as a 2-D model in either the horizontal or vertical planes.

The EFDC model implements a second order accurate in space and time, mass conservation fractional step solution scheme for the Eulerian transport equations for salinity, temperature, suspended sediment, water quality constituents, and toxic contaminants. The transport equations are temporally integrated at the same time step or twice the time step of the momentum equation solution (Smolarkiewicz and Margolin 1993). The advective step of the transport solution uses either the central

difference scheme used in the Blumberg-Mellor model or a hierarchy of positive definite upwind difference schemes. The highest accuracy upwind scheme, second order accurate in space and time, is based on a flux-corrected transport version Smolarkiewicz's multidimensional positive-definite advection transport algorithm (Smolarkiewicz and Clark, 1986; Smolarkiewicz and Grabowski 1990), which is monotonic and minimizes numerical diffusion. The horizontal diffusion step, if required, is explicit in time, whereas the vertical diffusion step is implicit. Horizontal boundary conditions include time variable material inflow concentrations, upwind outflow, and a damping relaxation specification of climatological boundary concentration. The NOAA Geophysical Fluid Dynamics Laboratory's atmospheric heat exchange model (Rosati and Miyakoda 1988) is implemented for the temperature transport equation.

3.3 Sediment Transport

The EFDC code is capable of simulating the transport and fate of multiple size classes of cohesive and noncohesive suspended sediment including bed deposition and resuspension. Water column transport is based on the same high order advection-diffusion scheme used for salinity and temperature. A number of options are included for the specification of settling velocities. For the transport of multiple size classes of cohesive sediment, an optional flocculation model (Burban et al. 1989, 1990) can be activated. Sediment mass conservative deposited bed formulations are included for both cohesive and noncohesive sediment. The deposited bed may be represented by a single layer or multiple layers. The multiple bed layer option provides a time since deposition versus vertical position in the bed relationship to be established. Water column/sediment bed interface elevation changes can be optionally incorporated into the hydrodynamic continuity equation. An optional one-dimensional (1-D) in the vertical, bed consolidation calculation can be performed for cohesive beds.

3.4 Water Quality and Eutrophication Simulation

The EFDC code includes two internal eutrophication submodels for water quality simulation (Park et al. 1995). The simple or reduced eutrophication model is functionally equivalent to the WASP5 EUTRO model (Ambrose et al. 1993). The complex or full eutrophication model is functionally equivalent to the CE-QUAL-ICM or Chesapeake Bay Water Quality model (Cerco and Cole 1993). Both water column eutrophication models are coupled to a functionally equivalent implementation of the CE-QUAL-ICM sediment diagenesis or biogeochemical processes model (DiToro and Fitzpatrick 1993). The eutrophication models can be executed simultaneously with the hydrodynamic component of EFDC, or EFDC simulated hydrodynamic transport fields can be saved, allowing the EFDC code to be executed in a water quality only simulation mode.

The computational scheme used in the internal eutrophication models employs a fractional step extension of the same advective and diffusive algorithms used for salinity and temperature, which

guarantee positive constituent concentrations. A novel ordering of the reaction sequence in the reactive source and sink fractional step allows the linearized reactions to be solved implicitly, further guaranteeing positive concentrations. The eutrophication models accept an arbitrary number of point and nonpoint source loadings as well as atmospheric and ground water loadings.

In addition to the internal eutrophication models, the EFDC model can be externally linked to the WASP5 model. In the external linking mode, the EFDC model generates WASP5 input files describing cell geometry and connectivity as well as advective and diffusive transport fields. For estuary simulation, the transport fields may be intratidally time averaged or intertidally time averaged using the averaging procedure described by Hamrick (1994).

3.5 Toxic Contaminant Transport and Fate

The EFDC code includes two internal submodels for simulating the transport and fate of toxic contaminants. A simple, single contaminant submodel can be activated from the master input file. The simple model accounts for water and suspended sediment phase transport with equilibrium partitioning and a lumped first order reaction. Contaminant mass per unit area in the sediment bed is also simulated. The second, more complex, submodel simulates the transport and fate of an arbitrary number of reacting contaminants in the water and sediment phases of both the water column and sediment bed. In this mode, the contaminant transport and fate simulation is functionally similar to the WASP5 TOXIC model (Ambrose et al. 1993), with the added flexibility of simulating an arbitrary number of contaminants, and the improved accuracy of utilizing more complex three-dimensional physical transport fields in a highly accurate numerical transport scheme. Water-sediment phases interaction may be represented by equilibrium or nonlinear sorption processes. In this mode, the multilayer sediment bed formulation is active, with sediment bed water volume and dissolved contaminant mass balances activated to allow contaminants to reenter the water column by sediment resuspension, pore water expulsion due to consolidation, and diffusion from the pore water into the water column. The complex contaminant model activates a subroutine describing reaction processes with appropriate reaction parameters provided by the toxic reaction processes input file.

3.6 Finfish and Shellfish Transport

The EFDC code includes the capability of simulating the transport and fate of various life stages of finfish and shellfish. In addition to advection and diffusion by the ambient flow, mortality, predation, toxicity, and swimming behavior are simulated. Organism age and ambient environment queued vertical and horizontal swimming and settling is simulated. Environmental queues include light intensity, temperature, salinity, and tidal phases.

3.7 Near-Field Discharge Dilution and Mixing Zone Analysis

In addition to the far-field transport and fate simulation capability incorporated into the EFDC code's water quality and toxic contaminant modules, the code includes a near-field discharge dilution and mixing zone module. The near field model is based on a Lagrangian buoyant jet and plume model (Frick 1984; Lee and Cheung 1990) and allows representation of submerged single and multiple port diffusers and buoyant surface jets. The near field model provides analysis capabilities similar to CORMIX (Jirka and Doneker 1991; Jirka and Akar 1991) while offering two distinct advantages. The first advantage is that a more realistic representation of ambient current and stratification conditions, provided directly by the EFDC hydrodynamic module, is incorporated into the analysis. The second advantage is that multiple discharges and multiple near field analysis times may be specified to account for varying ambient current and stratification conditions. For example, the analysis of 10 discharges under six ambient conditions each would require 60 executions of CORMIX, while the entire analysis of the 60 situations would be produced in a single EFDC simulation. The near-field simulation may be executed in two modes. The first provides virtual source information for representing the discharges in a standard EFDC far field transport and fate simulation. In the second mode the near-field and far-field transport are directly coupled, using a virtual source formulation, to provide simultaneous near and far field transport and fate simulation.

3.8 Spill Trajectory and Search and Rescue Simulation

In addition to the Eulerian transport equation formulation used for far field analysis and the Lagrangian jet and plume module used for near field analysis, the EFDC code incorporates a number of Lagrangian particle transport formulations based on an implicit trilinear interpolation scheme (Bennett and Clites 1987). The first formulation allows release of neutrally buoyant or buoyant drifters at user specified locations and times. This formulation is useful in simulating spill trajectories, search and rescue operations, and oceanographic instrument drifters. The second formulation releases drifters in each three-dimensional model cell at a specified sequence of times and calculates the generalized Lagrangian mean velocity field (Andrews and McIntyre 1978) relative to a user-specified averaging interval.

3.9 Wetland, Marsh, and Tidal Flat Simulation Extension

The EFDC model provides a number of enhancements for the simulation of flow and transport in wetlands, marshes, and tidal flats. The code allows for drying and wetting in shallow areas by a mass conservative scheme. The drying and wetting formulation is coupled to the mass transport equations in a manner that prevents negative concentrations of dissolved and suspended materials. A number of alternatives are in place in the model to simulate general discharge control structures such as weirs, spillways, culverts, and water surface elevation activated pumps. The effect of submerged and emergent plants is incorporated into the turbulence closure model and flow resistance formulation. Plant density

and geometric characteristics of individual and composite plants are required as input for the vegetation resistance formulation. A simple soil moisture model, allowing rainfall infiltration and soil water loss due to evapotranspiration under dry conditions, is implemented. To represent narrow channels and canals in wetland, marsh and tidal flat systems, a subgrid scale channel model is implemented. The subgrid channel model allows a 1-D network in the horizontal channels to be dynamically coupled to the two-dimensional horizontal grid representing the wetland, marsh, or tidal flat system. Volume and mass exchanges between 2-D wetland cells and the 1-D channels are accounted for. The channels may continue to flow when the 2-D wetland cells become dry.

3.10 Nearshore Wave-Induced Currents and Sediment Transport Extensions

The EFDC code includes a number of extensions for simulation of nearshore wave-induced currents and noncohesive sediment transport. The extensions include a wave-current boundary layer formulation similar to that of Grant and Madsen (1986); modifications of the hydrodynamic model's momentum equations to represent wave period averaged Eulerian mean quantities; the inclusion of the three-dimensional wave-induced radiation or Reynold's stresses in the momentum equations; and modifications of the velocity fields in the transport equations to include advective transport by the wave-induced Stoke's drift. High frequency surface wave fields are provide by an external wave refraction-diffraction model or by an internal mild slope equation submodel similar to that of Madsen and Larsen (1987). The internal refraction-diffraction computation is executed on a refined horizontal grid coincident with the main model's horizontal grid.

3.11 User Interface

The EFDC modeling package's user interface is based on text input file templates. This choice was selected in the interest of maintaining model portability across a range of computing platforms and readily allows the model user to modify input files using most text editing software. The text interface also allows modification of model files on remote computing systems and in hetrogeneous network environments. All input files have standard templates available with the EFDC code and in the digital version of the user's manual. The file templates include extensive built-in documentation and an explanation of numerical input data quantities. Actual numerical input data are inserted into the text template in a flexible free format as internally specified in the file templates. Extensive checking of input files is implemented in the code and diagnostic on screen messages indicate the location and nature of input file errors. All input files involving dimensional data have unit conversion specifications for the Meters-Kilograms-Seconds (MKS) international system of units used internally in the model.

3.12 Preprocessing Software

The EFDC modeling package includes a grid generating preprocessor code, GEFDC, which is used to construct the horizontal model grid, and interpolate bathymetry and initial fields such as water surface elevation, salinity, to the grid cells. EFDC inputs files specifying the grid geometry and initial fields are generated by the preprocessor. The preprocessor is capable of generating Cartesian and curvilinear-orthogonal grids using a number of grid generation schemes (Mobley and Stewart 1980; Ryskin and Leal 1983; Kang and Leal 1992).

3.13 Program Configuration

The EFDC code exists in only one generic version. A model application is specified entirely by information in the input files. To minimize memory requirements for specific applications, an executable file is created by adjusting the appropriate variable array size in the model's parameter file and compiling the source code. The EFDC model can be configured to execute all or a portion of a model application in reduced spatial dimension mode including 2-D depth or width averaged and 1-D cross section averaged. The number of layers used in the 3-D mode or 2-D width averaged mode is readily changed by one line of model input. Model grid sections specified as 2-D width averaged are allowed to have depth varying widths to provide representations equivalent to those of 2-D width averaged estuarine and reservoir models such as CE-QUAL-W2 (Cole and Buchak 1994).

3.14 Run-Time Diagnostics

The EFDC modeling package includes extensive built-in run-time diagnostics that may be activated in the master input file by the model user. Representative diagnostics include records of maximum CFL numbers, times and locations of negative depths, a variety of volume and mass balance checks, and global mass and energy balances. An on screen print of model variables in a specified cell can be activated during modeling execution. The model generates a number of log files that allow additional diagnostics of any run-time problems encountered during the set-up of a new application.

3.15 Model Output Options

A wide variety of output options are available for the EFDC model, including (1) specification of output files for horizontal plane and vertical plane transect plotting of vector and scalar field at a specified time; (2) the generation of time series of model variables at selected locations and time intervals; (3) grab sample simulation at specified times and locations; and (4) the specification of least squares analysis of selected model variables at a defined location over a specified interval. A general three-dimensional output option allows saving of all major model variables in a compressed-file format at specified times. A restart file is generated at user-specified intervals during model execution.

3.16 Postprocessing, Graphics, and Visualization

The generic model output files can be readily processed by a number of third party graphics and visualization software packages, often without the need for intermediate processing (Rennie and Hamrick 1992). The availability of the source code to the user allows the code to be modified for specific output options. Graphics and visualization software successfully used with EFDC output include: APE, AVS, IDL, Mathematica, MatLab, NCAR Graphics, PV-Wave, Techplot, SiteView, Spyglass Transform and Slicer, Voxelview, and GrADS. The model developer currently uses Spyglass and Voxelview and a number of postprocessor applications are available for special image enhancement for these products.

3.17 Documentation

Extensive documentation of the EFDC model is available. Theoretical and computational aspects of the model are described by Hamrick (1992). The model user's manual (Hamrick 1996) provides details on use of the GEFDC preprocessor and set-up of the EFDC input files. Input file templates are also included. A number of papers describe model applications and capabilities (Hamrick 1992b; Hamrick 1994; Moustafa and Hamrick 1994; Hamrick and Wu 1996; and Wu et al. 1996).

3.18 Computer Requirements

The EFDC modeling system is written in FORTRAN 77. The few nonstandard VAX FORTRAN language extensions in the code are supported by a wide variety of ANSI standard FORTRAN 77 compilers. The generic or universal source code has been compiled and executed on most UNIX workstations (DEC Alpha, Hewlett-Packard, IBM RISC6000, Silicon Graphics, Sun and Sparc compatibles) Cray and Convex supercomputers, and PC compatible and Macintosh personal computers. Absoft, Lahey, and Microsoft compilers are supported on PC compatibles, while Absoft, Language Systems, and Motorola compilers are supported on Macintosh and compatible systems.

4 - EFDC WATER QUALITY MODEL

4.1 Introduction

The central issues in the water quality model are primary production of carbon by algae and concentration of dissolved oxygen. Primary production provides the energy required by the ecosystem to function. However, excessive primary production is detrimental since its decomposition in the water and sediments consumes oxygen. Dissolved oxygen is necessary to support the life functions of higher organisms and is considered an indicator of the health of estuarine systems. In order to predict primary production and dissolved oxygen, a large suite of model state variables is necessary (Table 4-1). The nitrate state variable in the model represents the sum of nitrate and nitrite nitrogen. The three variables (salinity, water temperature, and total suspended solids) needed for computation of the above 21 state variables are provided by the EFDC hydrodynamic model. The interactions among the state variables is illustrated in Figure 4-1. The kinetic processes included in the EFDC water quality model are mostly from the Chesapeake Bay three-dimensional water quality model, CE-QUAL-ICM (Cerco & Cole 1994). The kinetic sources and sinks as well as the external loads for each state variable are described in Sections 4.3 to 4.11. The kinetic processes include the exchange of fluxes at the sediment-water interface, including sediment oxygen demand, which are explained in Section 5 (EFDC Sediment Process Model) of this report. The description of the EFDC water column water quality model in this section is from Park et al. (1995).

Table 4-1. EFDC model water quality state variables.

1) cyanobacteria	12) labile particulate organic nitrogen
2) diatom algae	13) dissolved organic nitrogen
3) green algae	14) ammonia nitrogen
4) refractory particulate organic carbon	15) nitrate nitrogen
5) labile particulate organic carbon	16) particulate biogenic silica
6) dissolved organic carbon	17) dissolved available silica
7) refractory particulate organic phosphorus	18) chemical oxygen demand
8) labile particulate organic phosphorus	19) dissolved oxygen
9) dissolved organic phosphorus	20) total active metal
10) total phosphate	21) fecal coliform bacteria
11) refractory particulate organic nitrogen	22) macroalgae

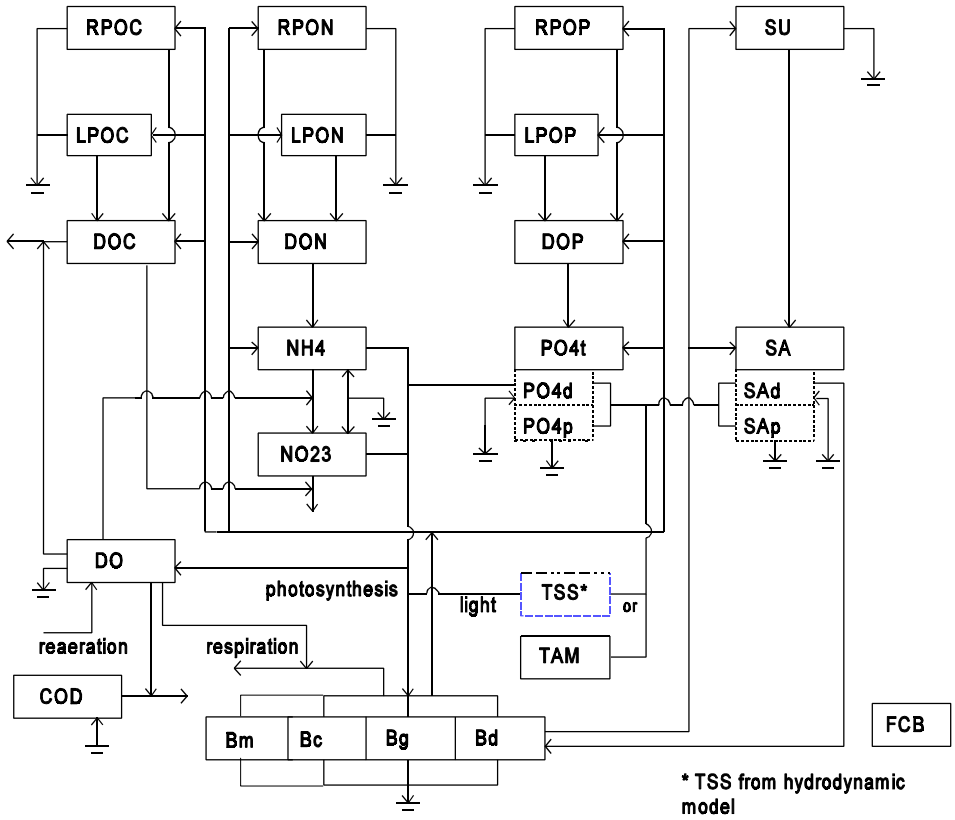

Figure 4-1. Schematic diagram for the EFDC water column water quality model.

4.1.1 Algae

Algae are grouped into four model classes: cyanobacteria, diatoms, greens, and macroalgae. The grouping is based upon the distinctive characteristics of each class and upon the significant role the characteristics play in the ecosystem. Cyanobacteria, commonly called blue-green algae, are characterized by their abundance (as picoplankton) in saline water and by their bloom-forming characteristics in fresh water. Cyanobacteria are unique in that some species fix atmospheric nitrogen although nitrogen fixers are not believed to be predominant in many river systems. Diatoms are distinguished by their requirement of silica as a nutrient to form cell walls. Diatoms are large algae characterized by high settling velocities. Settling of spring diatom blooms to the sediments may be a significant source of carbon for sediment oxygen demand. Algae that do not fall into the preceding two groups are lumped into the heading of green algae. Green algae settle at a rate intermediate between

cyanobacteria and diatoms and are subject to greater grazing pressure than cyanobacteria. Macroalgae are almost always attached to a stable substrate and are therefore most abundant in the areas of harbors and near shore. Many stream systems are characterized by various rooted macrophytes and periphyton. All species of macroalgae considered in this model have been lumped into a single class of macroalgae. Because of their attachment to the substrate, they are limited to growing in the bottom water-column layer and are not subject to physical transport.

4.1.2 Organic Carbon

Three organic carbon state variables are considered: dissolved, labile particulate, and refractory particulate. Labile and refractory distinctions are based upon the time scale of decomposition. Labile organic carbon decomposes on a time scale of days to weeks whereas refractory organic carbon requires more time. Labile organic carbon decomposes rapidly in the water column or the sediments. Refractory organic carbon decomposes slowly, primarily in the sediments, and may contribute to sediment oxygen demand years after deposition.

4.1.3 Nitrogen

Nitrogen is first divided into organic and mineral fractions. Organic nitrogen state variables are: dissolved organic nitrogen, labile particulate organic nitrogen, and refractory particulate organic nitrogen. Two mineral nitrogen forms are considered: ammonium and nitrate. Both are utilized to satisfy algal nutrient requirements although ammonium is preferred from thermodynamic considerations. The primary reason for distinguishing the two is that ammonium is oxidized by nitrifying bacteria into nitrate. This oxidation can be a significant sink of oxygen in the water column and sediments. An intermediate in the complete oxidation of ammonium, nitrite, also exists. Nitrite concentrations are usually much less than nitrate and for modeling purposes nitrite is combined with nitrate. Hence the nitrate state variable actually represents the sum of nitrate plus nitrite.

4.1.4 Phosphorus

As with carbon and nitrogen, organic phosphorus is considered in three states: dissolved, labile particulate, and refractory particulate. Only a single mineral form, total phosphate, is considered. Total phosphate exists as several states within the model ecosystem: dissolved phosphate, phosphate sorbed to inorganic solids, and phosphate incorporated in algal cells. Equilibrium partition coefficients are used to distribute the total among the three states.

4.1.5 Silica

Silica is divided into two state variables: available silica and particulate biogenic silica. Available silica is primarily dissolved and can be utilized by diatoms. Particulate biogenic silica cannot

be utilized. In the model, particulate biogenic silica is produced through diatom mortality. Particulate biogenic silica undergoes dissolution to available silica or else settles to the bottom sediments.

4.1.6 Chemical Oxygen Demand

In the context of this study, chemical oxygen demand is the concentration of reduced substances that are oxidizable by inorganic means. The primary component of chemical oxygen demand is sulfide released from sediments. Oxidation of sulfide to sulfate may remove substantial quantities of dissolved oxygen from the water column.

4.1.7 Dissolved Oxygen

Dissolved oxygen is required for the existence of higher life forms. Oxygen availability determines the distribution of organisms and the flows of energy and nutrients in an ecosystem. Dissolved oxygen is a central component of the water quality model.

4.1.8 Total Active Metal

Both phosphate and dissolved silica sorb to inorganic solids, primarily iron and manganese. Sorption and subsequent settling is one pathway for removal of phosphate and silica from the water column. Consequently, the concentration and transport of iron and manganese are represented in the model. Limited data do not allow a complete treatment of iron and manganese chemistry, however. Rather, a single state variable, total active metal, is defined as the total concentration of metals that are active in phosphate and silica transport. Total active metal is partitioned between particulate and dissolved phases by an oxygen-dependent partition coefficient.

4.1.9 Salinity

Salinity is a conservative tracer that provides verification of the transport component of the model and facilitates examination of conservation of mass. Salinity also influences the dissolved oxygen saturation concentration and is used in the determination of kinetics constants that differ in saline and fresh water.

4.1.10 Temperature

Temperature is a primary determinant of the rate of biochemical reactions. Reaction rates increase as a function of temperature although extreme temperatures result in the mortality of organisms.

4.2 Conservation Of Mass Equation

The governing mass-balance equation for each of the water quality state variables may be expressed as:

$$\frac{\partial C}{\partial t} + \frac{\partial (uC)}{\partial x} + \frac{\partial (vC)}{\partial y} + \frac{\partial (wC)}{\partial z} =$$

$$\frac{\partial}{\partial x}\left(K_x \frac{\partial C}{\partial x} \right) + \frac{\partial}{\partial y}\left(K_y \frac{\partial C}{\partial y} \right) + \frac{\partial}{\partial z}\left(K_z \frac{\partial C}{\partial z} \right) + S_C \qquad (4\text{-}1)$$

C = concentration of a water quality state variable
u, v & w = velocity components in the x-, y- and z-directions, respectively
K_x, K_y & K_z = turbulent diffusivities in the x-, y- and z-directions, respectively
S_C = internal and external sources and sinks per unit volume.

The last three terms on the left-hand side (LHS) of Eq. 4-1 account for the advective transport and the first three terms on the right-hand side (RHS) of Eq. 4-1 account for the diffusive transport. These six terms for physical transport are analogous to, and thus the numerical method of solution is the same as, those in the mass-balance equation for salinity in the hydrodynamic model (Hamrick 1992). The last term in Eq. 4-1 represents the kinetic processes and external loads for each of the state variables. The present model solves Eq. 4-1 after decoupling the kinetic terms from the physical transport terms. The solution scheme for both the physical transport (Hamrick 1992) and the kinetic equations is second-order accurate.

The governing mass-balance equation for water quality state variables (Eq. 4-1) consists of physical transport, advective and diffusive, and kinetic processes. When solving Eq. 4-1, the kinetic terms are decoupled from the physical transport terms. The mass-balance equation for physical transport only, which takes the same form as the salt-balance equation, is:

$$\frac{\partial C}{\partial t} + \frac{\partial (uC)}{\partial x} + \frac{\partial (vC)}{\partial y} + \frac{\partial (wC)}{\partial z} = \frac{\partial}{\partial x}\left(K_x \frac{\partial C}{\partial x} \right) + \frac{\partial}{\partial y}\left(K_y \frac{\partial C}{\partial y} \right) + \frac{\partial}{\partial z}\left(K_z \frac{\partial C}{\partial z} \right) \qquad (4\text{-}2)$$

The equation for kinetic processes only, which will be referred to as kinetic equation, is:

$$\frac{\partial C}{\partial t} = S_C \qquad (4\text{-}3)$$

which may be expressed as:

$$\frac{\partial C}{\partial t} = K \cdot C + R \qquad (4\text{-}4)$$

where K is kinetic rate (time^{-1}) and R is source/sink term (mass volume^{-1} time^{-1}). Equation 4-4 is obtained by linearizing some terms in the kinetic equations, mostly Monod type expressions. Hence, K

and R are known values in Eq. 4-4. Equation 4-2 is identical to, and thus its numerical method of solution is the same as, the mass-balance equation for salinity (Hamrick 1992).

The remainder of this chapter details the kinetics portion of the mass-conservation equation for each state variable. Parameters are defined where they first appear. All parameters are listed, in alphabetical order, in an appendix. For consistency with reported rate coefficients, kinetics are detailed using a temporal dimension of days. Within the CE-QUAL-ICM computer code, kinetics sources and sinks are converted to a dimension of seconds before employment in the mass-conservation equation.

4.3 Algae

Algae, which occupies a central role in the model (Fig. 4-1), are grouped into four model state variables: cyanobacteria (blue-green algae), diatoms, green algae, and macroalgae. The subscript, **x**, is used to denote four algal groups: **c** for cyanobacteria, **d** for diatoms, **g** for green algae, and **m** for macroalgae. Sources and sinks included in the model are

- growth (production)
- basal metabolism
- predation
- settling
- external loads.

Equations describing these processes are largely the same for three algal groups with differences in the values of parameters in the equations. The kinetic equation describing these processes is:

$$\frac{\partial B_x}{\partial t} = (P_x - BM_x - PR_x)B_x + \frac{\partial}{\partial z}(WS_x \cdot B_x) + \frac{WB_x}{V} \qquad (4\text{-}5)$$

B_x = algal biomass of algal group x (g C m^{-3})

t = time (day)

P_x = production rate of algal group x (day^{-1})

BM_x = basal metabolism rate of algal group x (day^{-1})

PR_x = predation rate of algal group x (day^{-1})

WS_x = settling velocity of algal group x (m day^{-1})

WB_x = external loads of algal group x (g C day^{-1})

V = cell volume (m^3).

The model simulates the total biomass of the macroalgae rather than the size of the macroalgae; therefore, they can be treated as other groups of algae. Since macroalgae attache to the bottom, they are limited to growing in the bottom layer only and are not be transported through water movement.

4.3.1 Production (Algal Growth)

Algal growth depends on nutrient availability, ambient light and temperature. The effects of these processes are considered to be multiplicative:

$$P_x = PM_x \cdot f_1(N) \cdot f_2(I) \cdot f_3(T) \quad (4\text{-}6)$$

PM_x = maximum growth rate under optimal conditions for algal group x (day^{-1})
$f_1(N)$ = effect of suboptimal nutrient concentration ($0 \le f_1 \le 1$)
$f_2(I)$ = effect of suboptimal light intensity ($0 \le f_2 \le 1$)
$f_3(T)$ = effect of suboptimal temperature ($0 \le f_3 \le 1$).

The freshwater cyanobacteria may undergo rapid mortality in salt water, e.g., freshwater organisms in the Potomac River (Thomann et al. 1985). For the freshwater organisms, the increased mortality may be included in the model by retaining the salinity toxicity term in the growth equation for cyanobacteria:

$$P_c = PM_c \cdot f_1(N) \cdot f_2(I) \cdot f_3(T) \cdot f_4(S) \quad (4\text{-}7)$$

$f_4(S)$ = effect of salinity on cyanobacteria growth ($0 \le f_4 \le 1$).

Activation of the salinity toxicity term, $f_4(S)$, is an option in the source code.

4.3.2 Effect of Nutrients on Algal Growth

Using Liebig's "law of the minimum" (Odum 1971) that growth is determined by the nutrient in least supply, the nutrient limitation for growth of cyanobacteria and green algae is expressed as:

$$f_1(N) = minimum\left(\frac{NH4 + NO3}{KHN_x + NH4 + NO3}, \frac{PO4d}{KHP_x + PO4d}\right) \quad (4\text{-}8)$$

NH4 = ammonium nitrogen concentration (g N m^{-3})
NO3 = nitrate nitrogen concentration (g N m^{-3})
KHN_x = half-saturation constant for nitrogen uptake for algal group x (g N m^{-3})
PO4d = dissolved phosphate phosphorus concentration (g P m^{-3})
KHP_x = half-saturation constant for phosphorus uptake for algal group x (g P m^{-3}).

Some cyanobacteria, e.g., *Anabaena*, can fix nitrogen from atmosphere and thus is not limited by nitrogen. Hence, Eq. 4-8 is not applicable to the growth of nitrogen fixers.

Since diatoms require silica as well as nitrogen and phosphorus for growth, the nutrient limitation for diatoms is expressed as:

$$f_1(N) = minimum\left(\frac{NH4 + NO3}{KHN_d + NH4 + NO3}, \frac{PO4d}{KHP_d + PO4d}, \frac{SAd}{KHS + SAd}\right) \quad (4\text{-}9)$$

SAd = concentration of dissolved available silica (g Si m^{-3})

KHS = half-saturation constant for silica uptake for diatoms (g Si m^{-3}).

4.3.3 Effect of Light on Algal Growth

The daily and vertically integrated form of Steele's equation is:

$$f_2(I) = \frac{2.718 \cdot FD}{Kess \cdot \Delta z}\left(e^{-\alpha_B} - e^{-\alpha_T}\right) \quad (4\text{-}10)$$

$$\alpha_B = \frac{I_o}{FD \cdot (I_s)_x} \cdot \exp\left(-Kess\,[H_T + \Delta z]\right) \quad (4\text{-}11)$$

$$\alpha_T = \frac{I_o}{FD \cdot (I_s)_x} \cdot \exp\left(-Kess \cdot H_T\right) \quad (4\text{-}12)$$

FD = fractional daylength ($0 \le FD \le 1$)

Kess = total light extinction coefficient (m^{-1})

Δz = layer thickness (m)

I_o = daily total light intensity at water surface (langleys day^{-1})

$(I_s)_x$ = optimal light intensity for algal group x (langleys day^{-1})

H_T = depth from the free surface to the top of the layer (m).

Light extinction in the water column consists of three fractions in the model: a background value dependent on water color, extinction due to suspended particles and extinction due to light absorption by ambient chlorophyll:

$$Kess = Ke_b + Ke_{TSS} \cdot TSS + Ke_{Chl} \cdot \sum_{x=c,d,g}\left(\frac{B_x}{CChl_x}\right) \quad (4\text{-}13)$$

Ke_b = background light extinction (m^{-1})

Ke_{TSS} = light extinction coefficient for total suspended solid (m^{-1} per g m^{-3})

TSS = total suspended solid concentration (g m^{-3}) provided from the hydrodynamic model

Ke_{Chl} = light extinction coefficient for chlorophyll 'a' (m^{-1} per mg Chl m^{-3})

$CChl_x$ = carbon-to-chlorophyll ratio in algal group x (g C per mg Chl).

Since macroalgae only attach to the bottom, they are not included in computation of the light extinction. Self shading is not considered for macroalgae for the present model. For a model application

that does not simulate TSS, the Ke_{TSS} term may be set to zero and Ke_b may be estimated to include light extinction due to suspended solid.

Optimal light intensity (I_s) for photosynthesis depends on algal taxonomy, duration of exposure, temperature, nutritional status and previous acclimation. Variations in I_s are largely due to adaptations by algae intended to maximize production in a variable environment. Steel (1962) noted the result of adaptations is that optimal intensity is a consistent fraction (approximately 50%) of daily intensity. Kremer & Nixon (1978) reported an analogous finding that maximum algal growth occurs at a constant depth (approximately 1 m) in the water column. Their approach is adopted so that optimal intensity is expressed as:

$$(I_s)_x = maximum \left\{(I_o)_{avg} \cdot e^{-Kess\cdot(D_{opt})_x}, (I_s)_{\min}\right\} \quad (4\text{-}14)$$

$(D_{opt})_x$ = depth of maximum algal growth for algal group x (m)
$(I_o)_{avg}$ = adjusted surface light intensity (langleys day^{-1}).

A minimum, $(I_s)_{min}$, in Eq. 4-14 is specified so that algae do not thrive at extremely low light levels. The time required for algae to adapt to changes in light intensity is recognized by estimating $(I_s)_x$ based on a time-weighted average of daily light intensity:

$$(I_o)_{avg} = CI_a \cdot I_o + CI_b \cdot I_1 + CI_c \cdot I_2 \quad (4\text{-}15)$$

I_1 = daily light intensity one day preceding model day (langleys day^{-1})
I_2 = daily light intensity two days preceding model day (langleys day^{-1})
CI_a, CI_b & CI_c = weighting factors for I_0, I_1 and I_2, respectively: $CI_a + CI_b + CI_c = 1$.

4.3.4 Effect of Temperature on Algal Growth

A Gaussian probability curve is used to represent the temperature dependency of algal growth:

$$\begin{aligned} f_3(T) &= \exp(-KTG1_x[T - TM_x]^2) && if \quad T \le TM_x \\ &= \exp(-KTG2_x[TM_x - T]^2) && if \quad T > TM_x \end{aligned} \quad (4\text{-}16)$$

T = temperature (°C) provided from the hydrodynamic model
TM_x = optimal temperature for algal growth for algal group x (°C)
$KTG1_x$ = effect of temperature below TM_x on growth for algal group x ($°C^{-2}$)
$KTG2_x$ = effect of temperature above TM_x on growth for algal group x ($°C^{-2}$).

4.3.5 Effect of Salinity on Growth of Freshwater Cyanobacteria

The growth of freshwater cyanobacteria in salt water is limited by:

$$f_4(S) = \frac{STOX^2}{STOX^2 + S^2} \quad (4\text{-}17)$$

STOX = salinity at which Microcystis growth is halved (ppt)
S = salinity in water column (ppt) provided from the hydrodynamic model.

4.3.6 Algal Basal Metabolism

Algal biomass in the present model decreases through basal metabolism (respiration and excretion) and predation. Basal metabolism in the present model is the sum of all internal processes that decrease algal biomass, and consists of two parts; respiration and excretion. In basal metabolism, algal matter (carbon, nitrogen, phosphorus and silica) is returned to organic and inorganic pools in the environment, mainly to dissolved organic and inorganic matter. Respiration, which may be viewed as a reversal of production, consumes dissolved oxygen. Basal metabolism is considered to be an exponentially increasing function of temperature:

$$BM_x = BMR_x \cdot \exp(KTB_x[T - TR_x]) \quad (4\text{-}18)$$

BMR_x = basal metabolism rate at TR_x for algal group x (day^{-1})
KTB_x = effect of temperature on metabolism for algal group x ($^\circ C^{-1}$)
TR_x = reference temperature for basal metabolism for algal group x ($^\circ C$).

4.3.7 Algal Predation

The present model does not include zooplankton. Instead, a constant rate is specified for algal predation, which implicitly assumes zooplankton biomass is a constant fraction of algal biomass. An equation similar to that for basal metabolism (Eq. 4-18) is used for predation:

$$PR_x = PRR_x \cdot \exp(KTB_x[T - TR_x]) \quad (4\text{-}19)$$

PRR_x = predation rate at TR_x for algal group x (day^{-1}).

The difference between predation and basal metabolism lies in the distribution of the end products of the two processes. In predation, algal matter (carbon, nitrogen, phosphorus and silica) is returned to organic and inorganic pools in the environment, mainly to particulate organic matter. The predation for macroalgae is a lumped parameter that includes losses due to grazing, frond breakage and other lossest. This implicitly assumes that the losses are a fraction of the biomass.

4.3.8 Algal Settling

Settling velocities for four algal groups, WS_c, WS_d , WS_g, and WS_m, are specified as an input. Seasonal variations in settling velocity of diatoms can be accounted for by specifying time-varying WS_d.

4.4 Organic Carbon

The present model has three state variables for organic carbon: refractory particulate, labile particulate and dissolved.

4.4.1 Particulate Organic Carbon

Labile and refractory distinctions are based on the time scale of decomposition. Labile particulate organic carbon with a decomposition time scale of days to weeks decomposes rapidly in the water column or in the sediments. Refractory particulate organic carbon with a longer-than-weeks decomposition time scale decomposes slowly, primarily in the sediments, and may contribute to sediment oxygen demand years after decomposition. For labile and refractory particulate organic carbon, sources and sinks included in the model are (Fig. 4-1):

- algal predation
- dissolution to dissolved organic carbon
- settling
- external loads

The governing equations for refractory and labile particulate organic carbons are:

$$\frac{\partial RPOC}{\partial t} = \sum_{x=c,d,g,m} FCRP \cdot PR_x \cdot B_x - K_{RPOC} \cdot RPOC + \frac{\partial}{\partial z}(WS_{RP} \cdot RPOC) + \frac{WRPOC}{V} \qquad (4\text{-}20)$$

$$\frac{\partial LPOC}{\partial t} = \sum_{x=c,d,g,m} FCLP \cdot PR_x \cdot B_x - K_{LPOC} \cdot LPOC + \frac{\partial}{\partial z}(WS_{LP} \cdot LPOC) + \frac{WLPOC}{V} \qquad (4\text{-}21)$$

RPOC = concentration of refractory particulate organic carbon (g C m^{-3})

LPOC = concentration of labile particulate organic carbon (g C m^{-3})

FCRP = fraction of predated carbon produced as refractory particulate organic carbon

FCLP = fraction of predated carbon produced as labile particulate organic carbon

K_{RPOC} = dissolution rate of refractory particulate organic carbon (day^{-1})

K_{LPOC} = dissolution rate of labile particulate organic carbon (day^{-1})

WS_{RP} = settling velocity of refractory particulate organic matter (m day^{-1})

WS_{LP} = settling velocity of labile particulate organic matter (m day^{-1})

WRPOC = external loads of refractory particulate organic carbon (g C day^{-1})

WLPOC = external loads of labile particulate organic carbon (g C day^{-1}).

4.4.2 Dissolved Organic Carbon

Sources and sinks for dissolved organic carbon included in the model are (Fig. 4-1):

- algal excretion (exudation) and predation
- dissolution from refractory and labile particulate organic carbon

- heterotrophic respiration of dissolved organic carbon (decomposition)
- denitrification
- external loads

The kinetic equation describing these processes is:

$$\frac{\partial DOC}{\partial t} = \sum_{x=c,d,g,m} \left(\left[FCD_x + (1 - FCD_x) \frac{KHR_x}{KHR_x + DO} \right] BM_x + FCDP \cdot PR_x \right) \cdot B_x$$

$$+ K_{RPOC} \cdot RPOC + K_{LPOC} \cdot LPOC - K_{HR} \cdot DOC - Denit \cdot DOC + \frac{WDOC}{V} \qquad (4\text{-}22)$$

DOC = concentration of dissolved organic carbon (g C m^{-3})

FCD_x = fraction of basal metabolism exuded as dissolved organic carbon at infinite dissolved oxygen concentration for algal group x

KHR_x = half-saturation constant of dissolved oxygen for algal dissolved organic carbon excretion for group x (g O_2 m^{-3})

DO = dissolved oxygen concentration (g O_2 m^{-3})

FCDP = fraction of predated carbon produced as dissolved organic carbon

K_{HR} = heterotrophic respiration rate of dissolved organic carbon (day^{-1})

Denit = denitrification rate (day^{-1}) given in Eq. 4-34

WDOC = external loads of dissolved organic carbon (g C day^{-1}).

The remainder of this section explains each term in Equations 4-20 to 4-22.

4.4.3 Effect of Algae on Organic Carbon

The terms within summation ($\sum$) in Equations 4-20 to 4-22 account for the effects of algae on organic carbon through basal metabolism and predation.

4.4.3.1 Basal metabolism. Basal metabolism, consisting of respiration and excretion, returns algal matter (carbon, nitrogen, phosphorus and silica) back to the environment. Loss of algal biomass through basal metabolism is (Eq. 4-18):

$$\frac{\partial B_x}{\partial t} = -BM_x \cdot B_x \qquad (4\text{-}23)$$

which indicates that the total loss of algal biomass due to basal metabolism is independent of ambient dissolved oxygen concentration. In this model, it is assumed that the distribution of total loss between respiration and excretion is constant as long as there is sufficient dissolved oxygen for algae to respire. Under that condition, the losses by respiration and excretion may be written as:

$(1 - FCD_x) \cdot BM_x \cdot B_x$ due to respiration (4-24)

$$FCD_x \cdot BM_x \cdot B_x \qquad \text{due to excretion} \qquad (4\text{-}25)$$

where FCD_x is a constant of value between 0 and 1. Algae cannot respire in the absence of oxygen, however. Although the total loss of algal biomass due to basal metabolism is oxygen-independent (Eq. 4-23), the distribution of total loss between respiration and excretion is oxygen-dependent. When oxygen level is high, respiration is a large fraction of the total. As dissolved oxygen becomes scarce, excretion becomes dominant. Thus, Eq. 4-24 represents the loss by respiration only at high oxygen levels. In general, Eq. 4-24 can be decomposed into two fractions as a function of dissolved oxygen availability:

$$(1 - FCD_x)\frac{DO}{KHR_x + DO} BM_x \cdot B_x \qquad \text{due to respiration} \qquad (4\text{-}26)$$

$$(1 - FCD_x)\frac{KHR_x}{KHR_x + DO} BM_x \cdot B_x \qquad \text{due to excretion} \qquad (4\text{-}27)$$

Equation 4-26 represents the loss of algal biomass by respiration and Eq. 4-27 represents additional excretion due to insufficient dissolved oxygen concentration. The parameter KHR_x, which is defined as the half-saturation constant of dissolved oxygen for algal dissolved organic carbon excretion in Eq. 4-22, can also be defined as the half-saturation constant of dissolved oxygen for algal respiration in Eq. 4-26.

Combining Equations 4-25 and 4-27, the total loss due to excretion is:

$$\left(FCD_x + (1 - FCD_x)\frac{KHR_x}{KHR_x + DO} \right) BM_x \cdot B_x \qquad (4\text{-}28)$$

Equations 4-26 and 4-28 combine to give the total loss of algal biomass due to basal metabolism, $BM_x \cdot B_x$ (Eq. 4-23). The definition of FCD_x in Eq. 4-22 becomes apparent in Eq. 4-28; i.e., fraction of basal metabolism exuded as dissolved organic carbon at infinite dissolved oxygen concentration. At zero oxygen level, 100% of total loss due to basal metabolism is by excretion regardless of FCD_x. The end carbon product of respiration is primarily carbon dioxide, an inorganic form not considered in the present model, while the end carbon product of excretion is primarily dissolved organic carbon. Therefore, Eq. 4-28, that appears in Eq. 4-22, represents the contribution of excretion to dissolved organic carbon, and there is no source term for particulate organic carbon from algal basal metabolism in Equations 4-20 and 4-21.

4.4.3.2 Predation. Algae produce organic carbon through the effects of predation. Zooplankton take up and redistribute algal carbon through grazing, assimilation, respiration and excretion. Since

zooplankton are not included in the model, routing of algal carbon through zooplankton predation is simulated by empirical distribution coefficients in Equations 4-20 to 4-22; FCRP, FCLP and FCDP. The sum of these three predation fractions should be unity.

4.4.4 Heterotrophic Respiration and Dissolution

The second term on the RHS of Equations 4-20 and 4-21 represents dissolution of particulate to dissolved organic carbon and the third term in the second line of Eq. 4-22 represents heterotrophic respiration of dissolved organic carbon. The oxic heterotrophic respiration is a function of dissolved oxygen: the lower the dissolved oxygen, the smaller the respiration term becomes. Heterotrophic respiration rate, therefore, is expressed using a Monod function of dissolved oxygen:

$$K_{HR} = \frac{DO}{KHOR_{DO} + DO} K_{DOC} \tag{4-29}$$

$KHOR_{DO}$ = oxic respiration half-saturation constant for dissolved oxygen (g O_2 m^{-3})

K_{DOC} = heterotrophic respiration rate of dissolved organic carbon at infinite dissolved oxygen concentration (day^{-1}).

Dissolution and heterotrophic respiration rates depend on the availability of carbonaceous substrate and on heterotrophic activity. Algae produce labile carbon that fuels heterotrophic activity: dissolution and heterotrophic respiration do not require the presence of algae though, and may be fueled entirely by external carbon inputs. In the model, algal biomass, as a surrogate for heterotrophic activity, is incorporated into formulations of dissolution and heterotrophic respiration rates. Formulations of these rates require specification of algal-dependent and algal-independent rates:

$$K_{RPOC} = (K_{RC} + K_{RCalg} \sum_{x=c,d,g} B_x) \cdot \exp(KT_{HDR}[T - TR_{HDR}]) \tag{4-30}$$

$$K_{LPOC} = (K_{LC} + K_{LCalg} \sum_{x=c,d,g} B_x) \cdot \exp(KT_{HDR}[T - TR_{HDR}]) \tag{4-31}$$

$$K_{DOC} = (K_{DC} + K_{DCalg} \sum_{x=c,d,g} B_x) \cdot \exp(KT_{MNL}[T - TR_{MNL}]) \tag{4-32}$$

K_{RC} = minimum dissolution rate of refractory particulate organic carbon (day^{-1})

K_{LC} = minimum dissolution rate of labile particulate organic carbon (day^{-1})

K_{DC} = minimum respiration rate of dissolved organic carbon (day^{-1})

K_{RCalg} & K_{LCalg} = constants that relate dissolution of refractory and labile particulate organic carbon, respectively, to algal biomass (day^{-1} per g C m^{-3})

K_{DCalg} = constant that relates respiration to algal biomass (day^{-1} per g C m^{-3})

KT_{HDR} = effect of temperature on hydrolysis of particulate organic matter ($^{\circ}C^{-1}$)

TR_{HDR} = reference temperature for hydrolysis of particulate organic matter (°C)
KT_{MNL} = effect of temperature on mineralization of dissolved organic matter ($°C^{-1}$)
TR_{MNL} = reference temperature for mineralization of dissolved organic matter (°C).
Equations 4-30 to 4-32 have exponential functions that relate rates to temperature.

In the present model, the term "hydrolysis" is defined as the process by which particulate organic matter is converted to dissolved organic form, and thus includes both dissolution of particulate carbon and hydrolysis of particulate phosphorus and nitrogen. Therefore, the parameters, KT_{HDR} and TR_{HDR}, are also used for the temperature effects on hydrolysis of particulate phosphorus (Equations 4-28 and 4-29) and nitrogen (Equations 4-54 and 4-55). The term "mineralization" is defined as the process by which dissolved organic matter is converted to dissolved inorganic form, and thus includes both heterotrophic respiration of dissolved organic carbon and mineralization of dissolved organic phosphorus and nitrogen. Therefore, the parameters, KT_{MNL} and TR_{MNL}, are also used for the temperature effects on mineralization of dissolved phosphorus (Eq. 4-46) and nitrogen (Eq. 4-56).

4.4.5 Effect of Denitrification on Dissolved Organic Carbon

As oxygen is depleted from natural systems, organic matter is oxidized by the reduction of alternate electron acceptors. Thermodynamically, the first alternate acceptor reduced in the absence of oxygen is nitrate. The reduction of nitrate by a large number of heterotrophic anaerobes is referred to as denitrification, and the stoichiometry of this reaction is (Stumm & Morgan 1981):

$$4NO_3^- + 4H^+ + 5CH_2O \rightarrow 2N_2 + 7H_2O + 5CO_2 \quad (4\text{-}33)$$

The last term in Eq. 4-22 accounts for the effect of denitrification on dissolved organic carbon. The kinetics of denitrification in the model are first-order:

$$Denit = \frac{KHOR_{DO}}{KHOR_{DO} + DO} \frac{NO3}{KHDN_N + NO3} AANOX \cdot K_{DOC} \quad (4\text{-}34)$$

$KHDN_N$ = denitrification half-saturation constant for nitrate (g N m^{-3})
AANOX = ratio of denitrification rate to oxic dissolved organic carbon respiration rate .

In Eq. 4-34, the dissolved organic carbon respiration rate, K_{DOC}, is modified so that significant decomposition via denitrification occurs only when nitrate is freely available and dissolved oxygen is depleted. The ratio, AANOX, makes the anoxic respiration slower than oxic respiration. Note that K_{DOC}, defined in Eq. 4-32, includes the temperature effect on denitrification.

4.5 Phosphorus

The present model has four state variables for phosphorus: three organic forms (refractory particulate, labile particulate and dissolved) and one inorganic form (total phosphate).

4.5.1 Particulate Organic Phosphorus

For refractory and labile particulate organic phosphorus, sources and sinks included in the model are (Fig. 4-1):

- algal basal metabolism and predation
- dissolution to dissolved organic phosphorus
- settling
- external loads

The kinetic equations for refractory and labile particulate organic phosphorus are:

$$\frac{\partial RPOP}{\partial t} = \sum_{x=c,d,g,m} (FPR_x \cdot BM_x + FPRP \cdot PR_x) APC \cdot B_x - K_{RPOP} \cdot RPOP + \frac{\partial}{\partial z}(WS_{RP} \cdot RPOP) + \frac{WRPOP}{V} \quad (4\text{-}35)$$

$$\frac{\partial LPOP}{\partial t} = \sum_{x=c,d,g,m} (FPL_x \cdot BM_x + FPLP \cdot PR_x) APC \cdot B_x - K_{LPOP} \cdot LPOP + \frac{\partial}{\partial z}(WS_{LP} \cdot LPOP) + \frac{WLPOP}{V} \quad (4\text{-}36)$$

RPOP = concentration of refractory particulate organic phosphorus (g P m^{-3})

LPOP = concentration of labile particulate organic phosphorus (g P m^{-3})

FPR_x = fraction of metabolized phosphorus by algal group x produced as refractory particulate organic phosphorus

FPL_x = fraction of metabolized phosphorus by algal group x produced as labile particulate organic phosphorus

FPRP = fraction of predated phosphorus produced as refractory particulate organic phosphorus

FPLP = fraction of predated phosphorus produced as labile particulate organic phosphorus

APC = mean phosphorus-to-carbon ratio in all algal groups (g P per g C)

K_{RPOP} = hydrolysis rate of refractory particulate organic phosphorus (day^{-1})

K_{LPOP} = hydrolysis rate of labile particulate organic phosphorus (day-1)

WRPOP = external loads of refractory particulate organic phosphorus (g P day^{-1})

WLPOP = external loads of labile particulate organic phosphorus (g P day^{-1}).

4.5.2 Dissolved Organic Phosphorus

Sources and sinks for dissolved organic phosphorus included in the model are (Fig. 4-1):

- algal basal metabolism and predation
- dissolution from refractory and labile particulate organic phosphorus
- mineralization to phosphate phosphorus
- external loads

The kinetic equation describing these processes is:

$$\frac{\partial DOP}{\partial t} = \sum_{x=c,d,g,m} (FPD_x \cdot BM_x + FPDP \cdot PR_x) APC \cdot B_x$$

$$+ K_{RPOP} \cdot RPOP + K_{LPOP} \cdot LPOP - K_{DOP} \cdot DOP + \frac{WDOP}{V} \quad (4\text{-}37)$$

DOP = concentration of dissolved organic phosphorus (g P m^{-3})

FPD_x = fraction of metabolized phosphorus by algal group x produced as dissolved organic phosphorus

FPDP = fraction of predated phosphorus produced as dissolved organic phosphorus

K_{DOP} = mineralization rate of dissolved organic phosphorus (day^{-1})

WDOP = external loads of dissolved organic phosphorus (g P day^{-1}).

4.5.3 Total Phosphate

For total phosphate that includes both dissolved and sorbed phosphate (Section 4.5.4), sources and sinks included in the model are (Fig. 4-1):

- algal basal metabolism, predation, and uptake
- mineralization from dissolved organic phosphorus
- settling of sorbed phosphate
- sediment-water exchange of dissolved phosphate for the bottom layer only
- external loads.

The kinetic equation describing these processes is:

$$\frac{\partial PO4t}{\partial t} = \sum_{x=c,d,g,m} (FPI_x \cdot BM_x + FPIP \cdot PR_x - P_x) APC \cdot B_x + K_{DOP} \cdot DOP$$

$$+ \frac{\partial}{\partial z}(WS_{TSS} \cdot PO4p) + \frac{BFPO4d}{\Delta z} + \frac{WPO4t}{V} \quad (4\text{-}38)$$

PO4t = total phosphate (g P m^{-3}) = PO4d + PO4p (4-39)

PO4d = dissolved phosphate (g P m^{-3})

PO4p = particulate (sorbed) phosphate (g P m^{-3})

FPI_x = fraction of metabolized phosphorus by algal group x produced as inorganic phosphorus

FPIP = fraction of predated phosphorus produced as inorganic phosphorus
WS_{TSS} = settling velocity of suspended solid (m day^{-1}), provided by the hydrodynamic model
BFPO4d = sediment-water exchange flux of phosphate (g P m^{-2} day^{-1}), applied to the bottom layer only
WPO4t = external loads of total phosphate (g P day^{-1}).

In Eq. 4-38, if total active metal is chosen as a measure of sorption site, the settling velocity of total suspended solid, WS_{TSS}, is replaced by that of particulate metal, WS_s (Sections 4.5.4 and 4.10). The remainder of this section explains each term in Equations 4-35 to 4-38, except BFPO4d which is described in Chapter 5 of this document.

4.5.4 Total Phosphate System

Suspended and bottom sediment particles (clay, silt and metal hydroxides) adsorb and desorb phosphate in river and estuarine waters. This adsorption-desorption process has been suggested to buffer phosphate concentration in water column and to enhance the transport of phosphate away from its external sources (Carritt & Goodgal 1954; Froelich 1988; Lebo 1991). To ease the computational complication due to the adsorption-desorption of phosphate, dissolved and sorbed phosphate are treated and transported as a single state variable. Therefore, the model phosphate state variable, total phosphate, is defined as the sum of dissolved and sorbed phosphate (Eq. 4-39), and the concentrations for each fraction are determined by equilibrium partitioning of their sum.

In CE-QUAL-ICM, sorption of phosphate to particulate species of metals including iron and manganese was considered based on phenomenon observed in the monitoring data from the mainstem of the Chesapeake Bay: phosphate was rapidly depleted from anoxic bottom waters during the autumn reaeration event (Cerco & Cole 1994). Their hypothesis was that reaeration of bottom waters caused dissolved iron and manganese to precipitate, and phosphate sorbed to newly-formed metal particles and rapidly settled to the bottom. One state variable, total active metal, in CE-QUAL-ICM was defined as the sum of all metals that act as sorption sites, and the total active metal was partitioned into particulate and dissolved fractions via an equilibrium partitioning coefficient (Section 4.10). Then, phosphate was assumed to sorb to only the particulate fraction of the total active metal.

In the treatment of phosphate sorption in CE-QUAL-ICM, the particulate fraction of metal hydroxides was emphasized as a sorption site in bottom waters under anoxic conditions. Phosphorus is a highly particle-reactive element, and phosphate in solution reacts quickly with a wide variety of surfaces, being taken up by and released from particles (Froelich 1988). The present model has two options, total suspended solid and total active metal, as a measure of a sorption site for phosphate, and dissolved and

sorbed fractions are determined by equilibrium partitioning of their sum as a function of total suspended solid or total active metal concentration:

$$PO4p = \frac{K_{PO4p} \cdot TSS}{1 + K_{PO4p} \cdot TSS} PO4t \quad \text{or} \quad PO4p = \frac{K_{PO4p} \cdot TAMp}{1 + K_{PO4p} \cdot TAMp} PO4t \tag{4-40}$$

$$PO4d = \frac{1}{1 + K_{PO4p} \cdot TSS} PO4t \quad \text{or} \quad PO4d = \frac{1}{1 + K_{PO4p} \cdot TAMp} PO4t$$

$$= PO4t - PO4p \tag{4-41}$$

K_{PO4p} = empirical coefficient relating phosphate sorption to total suspended solid (per g m^{-3}) or particulate total active metal (per mol m^{-3}) concentration

TAMp = particulate total active metal (mol m^{-3}).

Dividing Eq. 4-40 by Eq. 4-41 gives:

$$K_{PO4p} = \frac{PO4p}{PO4d} \frac{1}{TSS} \quad \text{or} \quad K_{PO4p} = \frac{PO4p}{PO4d} \frac{1}{TAMp} \tag{4-42}$$

where the meaning of K_{PO4p} becomes apparent, i.e., the ratio of sorbed to dissolved phosphate per unit concentration of total suspended solid or particulate total active metal (i.e., per unit sorption site available).

4.5.5 Algal Phosphorus-to-Carbon Ratio (APC)

Algal biomass is quantified in units of carbon per volume of water. In order to express the effects of algal biomass on phosphorus and nitrogen, the ratios of phosphorus-to-carbon and nitrogen-to-carbon in algal biomass must be specified. Although global mean values of these ratios are well known (Redfield et al. 1963), algal composition varies especially as a function of nutrient availability. As phosphorus and nitrogen become scarce, algae adjust their composition so that smaller quantities of these vital nutrients are required to produce carbonaceous biomass (DiToro 1980; Parsons et al. 1984). Examining the field data from the surface of upper Chesapeake Bay, Cerco & Cole (1994) showed that the variation of nitrogen-to-carbon stoichiometry was small and thus used a constant algal nitrogen-to-carbon ratio, ANC_x. Large variations, however, were observed for algal phosphorus-to-carbon ratio indicating the adaptation of algae to ambient phosphorus concentration (Cerco & Cole 1994): algal phosphorus content is high when ambient phosphorus is abundant and is low when ambient phosphorus is scarce. Thus, a variable algal phosphorus-to-carbon ratio, APC, is used in model formulation. A mean

ratio for all algal groups, APC, is described by an empirical approximation to the trend observed in field data (Cerco & Cole 1994):

$$APC = \left(CP_{prm1} + CP_{prm2} \cdot \exp[-CP_{prm3} \cdot PO4d]\right)^{-1} \quad (4\text{-}43)$$

CP_{prm1} = minimum carbon-to-phosphorus ratio (g C per g P)

CP_{prm2} = difference between minimum and maximum carbon-to-phosphorus ratio (g C per g P)

CP_{prm3} = effect of dissolved phosphate concentration on carbon-to-phosphorus ratio (per g P m^{-3}).

4.5.6 Effect of Algae on Phosphorus

The terms within summation ($\sum$) in Equations 4-35 to 4-38 account for the effects of algae on phosphorus. Both basal metabolism (respiration and excretion) and predation are considered, and thus formulated, to contribute to organic and phosphate phosphorus. That is, the total loss by basal metabolism ($BM_x \cdot B_x$ in Eq. 4-5) is distributed using distribution coefficients; FPR_x, FPL_x, FPD_x and FPI_x. The total loss by predation ($PR_x \cdot B_x$ in Eq. 4-5), is also distributed using distribution coefficients; FPRP, FPLP, FPDP and FPIP. The sum of four distribution coefficients for basal metabolism should be unity, and so is that for predation. Algae take up dissolved phosphate for growth, and algae uptake of phosphate is represented by ($-\sum P_x \cdot APC \cdot B_x$) in Eq. 4-38.

4.5.7 Mineralization and Hydrolysis

The third term on the RHS of Equations 4-35 and 4-36 represents hydrolysis of particulate organic phosphorus and the last term in Eq. 3-7 represents mineralization of dissolved organic phosphorus. Mineralization of organic phosphorus is mediated by the release of nucleotidase and phosphatase enzymes by bacteria (Chróst & Overbek 1987) and algae (Boni et al. 1989). Since the algae themselves release the enzymes and bacterial abundance is related to algal biomass, the rate of organic phosphorus mineralization is related to algal biomass in model formulation. Another mechanism included in model formulation is that algae stimulate production of an enzyme that mineralizes organic phosphorus to phosphate when phosphate is scarce (Chróst & Overbek 1987; Boni et al. 1989). The formulations for hydrolysis and mineralization rates including these processes are:

$$K_{RPOP} = \left(K_{RP} + \frac{KHP}{KHP + PO4d} K_{RPalg} \sum_{x=c,d,g} B_x\right) \cdot \exp\left(KT_{HDR}[T - TR_{HDR}]\right) \quad (4\text{-}44)$$

$$K_{LPOP} = \left(K_{LP} + \frac{KHP}{KHP + PO4d} K_{LPalg} \sum_{x=c,d,g} B_x\right) \cdot \exp\left(KT_{HDR}[T - TR_{HDR}]\right) \quad (4\text{-}45)$$

$$K_{DOP} = \left(K_{DP} + \frac{KHP}{KHP + PO4d} K_{DPalg} \sum_{x=c,d,g} B_x\right) \cdot \exp\left(KT_{MNL}[T - TR_{MNL}]\right) \quad (4\text{-}46)$$

K_{RP} = minimum hydrolysis rate of refractory particulate organic phosphorus (day^{-1})

K_{LP} = minimum hydrolysis rate of labile particulate organic phosphorus (day^{-1})

K_{DP} = minimum mineralization rate of dissolved organic phosphorus (day^{-1})

K_{RPalg} & K_{LPalg} = constants that relate hydrolysis of refractory and labile particulate organic phosphorus, respectively, to algal biomass (day^{-1} per g C m^{-3})

K_{DPalg} = constant that relates mineralization to algal biomass (day^{-1} per g C m^{-3})

KHP = mean half-saturation constant for algal phosphorus uptake (g P m^{-3})

$$= \frac{1}{3}\sum_{x=c,d,g} KHP_x \tag{4-47}$$

When phosphate is abundant relative to KHP, the rates become to be close to the minimum values with little influence from algal biomass. When phosphate becomes scarce relative to KHP, the rates increase with the magnitude of increase depending on algal biomass. Equations 4-44 to 4-46 have exponential functions that relate rates to temperature.

4.6 Nitrogen

The present model has five state variables for nitrogen: three organic forms (refractory particulate, labile particulate and dissolved) and two inorganic forms (ammonium and nitrate). The nitrate state variable in the model represents the sum of nitrate and nitrite.

4.6.1 Particulate Organic Nitrogen

For refractory and labile particulate organic nitrogen, sources and sinks included in the model are (Fig. 4-1):

- algal basal metabolism and predation
- dissolution to dissolved organic nitrogen
- settling
- external loads

The kinetic equations for refractory and labile particulate organic nitrogen are:

$$\frac{\partial RPON}{\partial t} = \sum_{x=c,d,g,m} (FNR_x \cdot BM_x + FNRP \cdot PR_x) ANC_x \cdot B_x - K_{RPON} \cdot RPON$$

$$+ \frac{\partial}{\partial z}(WS_{RP} \cdot RPON) + \frac{WRPON}{V} \tag{4-48}$$

$$\frac{\partial LPON}{\partial t} = \sum_{x=c,d,g,m} (FNL_x \cdot BM_x + FNLP \cdot PR_x) ANC_x \cdot B_x - K_{LPON} \cdot LPON$$

$$+ \frac{\partial}{\partial z}(WS_{LP} \cdot LPON) + \frac{WLPON}{V} \quad (4\text{-}49)$$

RPON = concentration of refractory particulate organic nitrogen (g N m^{-3})

LPON = concentration of labile particulate organic nitrogen (g N m^{-3})

FNR_x = fraction metabolized nitrogen by algal group x as refractory particulate organic nitrogen

FNL_x = fraction of metabolized nitrogen by algal group x produced as labile particulate organic nitrogen

FNRP = fraction of predated nitrogen produced as refractory particulate organic nitrogen

FNLP = fraction of predated nitrogen produced as labile particulate organic nitrogen

ANC_x = nitrogen-to-carbon ratio in algal group x (g N per g C)

K_{RPON} = hydrolysis rate of refractory particulate organic nitrogen (day^{-1})

K_{LPON} = hydrolysis rate of labile particulate organic nitrogen (day^{-1})

WRPON = external loads of refractory particulate organic nitrogen (g N day^{-1})

WLPON = external loads of labile particulate organic nitrogen (g N day^{-1}).

4.6.2 Dissolved Organic Nitrogen

Sources and sinks for dissolved organic nitrogen included in the model are (Fig. 4-1):

- algal basal metabolism and predation
- dissolution from refractory and labile particulate organic nitrogen
- mineralization to ammonium
- external loads

The kinetic equation describing these processes is:

$$\frac{\partial DON}{\partial t} = \sum_{x=c,d,g,m} (FND_x \cdot BM_x + FNDP \cdot PR_x) ANC_x \cdot B_x$$

$$+ K_{RPON} \cdot RPON + K_{LPON} \cdot LPON - K_{DON} \cdot DON + \frac{WDON}{V} \quad (4\text{-}50)$$

DON = concentration of dissolved organic nitrogen (g N m^{-3})

FND_x = fraction of metabolized nitrogen by algal group x produced as dissolved organic nitrogen

FNDP = fraction of predated nitrogen produced as dissolved organic nitrogen

K_{DON} = mineralization rate of dissolved organic nitrogen (day^{-1})

WDON = external loads of dissolved organic nitrogen (g N day^{-1}).

4.6.3 Ammonium Nitrogen

Sources and sinks for ammonia nitrogen included in the model are (Fig. 4-1):

- algal basal metabolism, predation, and uptake
- mineralization from dissolved organic nitrogen

- nitrification to nitrate
- sediment-water exchange for the bottom layer only
- external loads.

The kinetic equation describing these processes is:

$$\frac{\partial NH4}{\partial t} = \sum_{x=c,d,g,m} (FNI_x \cdot BM_x + FNIP \cdot PR_x - PN_x \cdot P_x) ANC_x \cdot B_x + K_{DON} \cdot DON$$

$$- Nit \cdot NH4 + \frac{BFNH4}{\Delta z} + \frac{WNH4}{V} \qquad (4\text{-}51)$$

FNI_x = fraction of metabolized nitrogen by algal group x produced as inorganic nitrogen

FNIP = fraction of predated nitrogen produced as inorganic nitrogen

PN_x = preference for ammonium uptake by algal group x ($0 \le PN_x \le 1$)

Nit = nitrification rate (day^{-1}) given in Eq. 4-59

BFNH4 = sediment-water exchange flux of ammonium (g N m^{-2} day^{-1}), applied to the bottom layer only

WNH4 = external loads of ammonium (g N day^{-1}).

4.6.4 Nitrate Nitrogen

Sources and sinks for nitrate nitrogen included in the model are (Fig. 4-1):

- algal uptake
- nitrification from ammonium
- denitrification to nitrogen gas
- sediment-water exchange for the bottom layer only
- external loads

The kinetic equation describing these processes is:

$$\frac{\partial NO3}{\partial t} = - \sum_{x=c,d,g,m} (1 - PN_x) P_x \cdot ANC_x \cdot B_x + Nit \cdot NH4 - ANDC \cdot Denit \cdot DOC$$

$$+ \frac{BFNO3}{\Delta z} + \frac{WNO3}{V} \qquad (4\text{-}52)$$

ANDC = mass of nitrate nitrogen reduced per mass of dissolved organic carbon oxidized (0.933 g N per g C from Eq. 4-33)

BFNO3 = sediment-water exchange flux of nitrate (g N m^{-2} day^{-1}), applied to the bottom layer only

WNO3 = external loads of nitrate (g N day^{-1}).

The remainder of this section explains each term in Equations 4-48 to 4-52, except BFNH4 and BFNO3 which are described in Chapter 5 of this document.

4.6.5 Effect of Algae on Nitrogen

The terms within summation ($\sum$) in Equations 4-48 to 4-52 account for the effects of algae on nitrogen. As in phosphorus, both basal metabolism (respiration and excretion) and predation are considered, and thus formulated, to contribute to organic and ammonium nitrogen. That is, algal nitrogen released by both basal metabolism and predation is represented by distribution coefficients; FNR_x, FNL_x, FND_x, FNI_x, FNRP, FNLP, FNDP and FNIP. The sum of four distribution coefficients for basal metabolism should be unity, and so is that for predation.

Algae take up ammonium and nitrate for growth, and ammonium is preferred from thermodynamic considerations. The preference of algae for ammonium is expressed as:

$$PN_x = NH4\frac{NO3}{(KHN_x + NH4)(KHN_x + NO3)} + NH4\frac{KHN_x}{(NH4 + NO3)(KHN_x + NO3)} \quad (4\text{-}53)$$

This equation forces the preference for ammonium to be unity when nitrate is absent, and to be zero when ammonium is absent.

4.6.6 Mineralization and Hydrolysis

The third term on the RHS of Equations 4-48 and 4-49 represents hydrolysis of particulate organic nitrogen and the last term in Eq. 4-50 represents mineralization of dissolved organic nitrogen. Including a mechanism for accelerated hydrolysis and mineralization during nutrient-limited conditions (Section 4.5.7), the formulations for these processes are:

$$K_{RPON} = (K_{RN} + \frac{KHN}{KHN + NH4 + NO3}K_{RNalg}\sum_{x=c,d,g} B_x)\cdot\exp(KT_{HDR}[T - TR_{HDR}]) \quad (4\text{-}54)$$

$$K_{LPON} = (K_{LN} + \frac{KHN}{KHN + NH4 + NO3}K_{LNalg}\sum_{x=c,d,g} B_x)\cdot\exp(KT_{HDR}[T - TR_{HDR}]) \quad (4\text{-}55)$$

$$K_{DON} = (K_{DN} + \frac{KHN}{KHN + NH4 + NO3}K_{DNalg}\sum_{x=c,d,g} B_x)\cdot\exp(KT_{MNL}[T - TR_{MNL}]) \quad (4\text{-}56)$$

K_{RN} = minimum hydrolysis rate of refractory particulate organic nitrogen (day^{-1})

K_{LN} = minimum hydrolysis rate of labile particulate organic nitrogen (day^{-1})

K_{DN} = minimum mineralization rate of dissolved organic nitrogen (day^{-1})

K_{RNalg} & K_{LNalg} = constants that relate hydrolysis of refractory and labile particulate organic nitrogen, respectively, to algal biomass (day^{-1} per g C m^{-3})

K_{DNalg} = constant that relates mineralization to algal biomass (day^{-1} per g C m^{-3})

KHN = mean half-saturation constant for algal nitrogen uptake (g N m^{-3})

$$= \frac{1}{3}\sum_{x=c,d,g} KHN_x \tag{4-57}$$

Equations 4-54 to 4-56 have exponential functions that relate rates to temperature.

4.6.7 Nitrification

Nitrification is a process mediated by autotrophic nitrifying bacteria that obtain energy through the oxidation of ammonium to nitrite and of nitrite to nitrate. The stoichiometry of complete reaction is (Bowie et al. 1985):

$$NH_4^+ + 2O_2 \rightarrow NO_3^- + H_2O + 2H^+ \tag{4-58}$$

The first term in the second line of Eq. 4-51 and its corresponding term in Eq. 4-52 represent the effect of nitrification on ammonium and nitrate, respectively. The kinetics of complete nitrification process are formulated as a function of available ammonium, dissolved oxygen and temperature:

$$Nit = \frac{DO}{KHNit_{DO} + DO}\frac{NH4}{KHNit_N + NH4} Nit_m \cdot f_{Nit}(T) \tag{4-59}$$

$$\begin{aligned} f_{Nit}(T) &= \exp(-KNit1[T - TNit]^2) \qquad if \quad T \le TNit \\ &= \exp(-KNit2[TNit - T]^2) \qquad if \quad T > TNit \end{aligned} \tag{4-60}$$

$KHNit_{DO}$ = nitrification half-saturation constant for dissolved oxygen (g O_2 m^{-3})
$KHNit_N$ = nitrification half-saturation constant for ammonium (g N m^{-3})
Nit_m = maximum nitrification rate at TNit (g N m^{-3} day^{-1})
TNit = optimum temperature for nitrification (°C)
KNit1 = effect of temperature below TNit on nitrification rate ($°C^{-2}$)
KNit2 = effect of temperature above TNit on nitrification rate ($°C^{-2}$).

The Monod function of dissolved oxygen in Eq. 4-59 indicates the inhibition of nitrification at low oxygen level. The Monod function of ammonium indicates that when ammonium is abundant, the nitrification rate is limited by the availability of nitrifying bacteria. The effect of suboptimal temperature is represented using Gaussian form.

4.6.8 Denitrification

The effect of denitrification on dissolved organic carbon was described in Section 4.4.5. Denitrification removes nitrate from the system in stoichiometric proportion to carbon removal as determined by Eq. 4-33. The last term in the first line of Eq. 4-52 represents this removal of nitrate.

4.7 Silica

The present model has two state variables for silica: particulate biogenic silica and available silica.

4.7.1 Particulate Biogenic Silica

Sources and sinks for particulate biogenic silica included in the model are (Fig. 4-1):

- diatom basal metabolism and predation
- dissolution to available silica
- settling
- external loads.

The kinetic equation describing these processes is:

$$\frac{\partial SU}{\partial t} = (FSP_d \cdot BM_d + FSPP \cdot PR_d) ASC_d \cdot B_d - K_{SUA} \cdot SU + \frac{\partial}{\partial z}(WS_d \cdot SU) + \frac{WSU}{V} \qquad (4\text{-}61)$$

SU = concentration of particulate biogenic silica (g Si m^{-3})

FSP_d = fraction of metabolized silica by diatoms produced as particulate biogenic silica

FSPP = fraction of predated diatom silica produced as particulate biogenic silica

ASC_d = silica-to-carbon ratio of diatoms (g Si per g C)

K_{SUA} = dissolution rate of particulate biogenic silica (day^{-1})

WSU = external loads of particulate biogenic silica (g Si day^{-1}).

4.7.2 Available Silica

Sources and sinks for available silica included in the model are (Fig. 4-1):

- diatom basal metabolism, predation, and uptake
- settling of sorbed (particulate) available silica
- dissolution from particulate biogenic silica
- sediment-water exchange of dissolved silica for the bottom layer only
- external loads

The kinetic equation describing these processes is:

$$\frac{\partial SA}{\partial t} = (FSI_d \cdot BM_d + FSIP \cdot PR_d - P_d) ASC_d \cdot B_d + K_{SUA} \cdot SU + \frac{\partial}{\partial z}(WS_{TSS} \cdot SAp) + \frac{BFSAd}{\Delta z} + \frac{WSA}{V} \qquad (4\text{-}62)$$

SA = concentration of available silica (g Si m^{-3}) = SAd + SAp (4-63)

SAd = dissolved available silica (g Si m^{-3})

SAp = particulate (sorbed) available silica (g Si m^{-3})

FSI_d = fraction of metabolized silica by diatoms produced as available silica
FSIP = fraction of predated diatom silica produced as available silica
BFSAd = sediment-water exchange flux of available silica (g Si m^{-2} day^{-1}), applied to bottom layer only.
WSA = external loads of available silica (g Si day^{-1}).

In Eq. 4-62, if total active metal is chosen as a measure of sorption site, the settling velocity of total suspended solid, WS_{TSS}, is replaced by that of particulate metal, WS_s (Sections 4.7.3 and 4.10).

4.7.3 Available Silica System

Analysis of Chesapeake Bay monitoring data indicates that silica shows similar behavior as phosphate in the adsorption-desorption process (Cerco & Cole 1994). As in phosphate, therefore, available silica is defined to include both dissolved and sorbed fractions (Eq. 4-63). Treatment of available silica is the same as total phosphate and the same method that is used to partition dissolved and sorbed phosphate is used to partition dissolved and sorbed available silica:

$$SAp = \frac{K_{SAp} \cdot TSS}{1 + K_{SAp} \cdot TSS} SA \quad \text{or} \qquad SAp = \frac{K_{SAp} \cdot TAMp}{1 + K_{SAp} \cdot TAMp} SA \tag{4-64}$$

$$SAd = \frac{1}{1 + K_{SAp} \cdot TSS} SA \quad \text{or} \qquad SAd = \frac{1}{1 + K_{SAp} \cdot TAMp} SA$$

$$= SA - SAp \tag{4-65}$$

K_{SAp} = empirical coefficient relating available silica sorption to total suspended solid (per g m^{-3}) or particulate total active metal (per mol m^{-3}) concentration.

As in K_{PO4p} in Section 4.5.4, K_{SAp} is the ratio of sorbed to dissolved available silica per unit sorption site available.

4.7.4 Effect of Diatoms on Silica

In Equations 4-62 and 4-63, those terms expressed as a function of diatom biomass (B_d) account for the effects of diatoms on silica. As in phosphorus and nitrogen, both basal metabolism (respiration and excretion) and predation are considered, and thus formulated, to contribute to particulate biogenic and available silica. That is, diatom silica released by both basal metabolism and predation are represented by distribution coefficients; FSP_d, FSI_d, FSPP and FSIP. The sum of two distribution coefficients for basal metabolism should be unity, and so is that for predation. Diatoms require silica as well as phosphorus and nitrogen, and diatom uptake of available silica is represented by $(- P_d \cdot ASC_d \cdot B_d)$ in Eq. 4-63.

4.7.5 Dissolution

The term (- K_{SUA}·SU) in Eq. 4-62 and its corresponding term in Eq. 4-63 represent dissolution of particulate biogenic silica to available silica. The dissolution rate is expressed as an exponential function of temperature:

$$K_{SUA} = K_{SU} \cdot \exp(KT_{SUA}[T - TR_{SUA}]) \quad (4\text{-}66)$$

K_{SU} = dissolution rate of particulate biogenic silica at TR_{SUA} (day^{-1})
KT_{SUA} = effect of temperature on dissolution of particulate biogenic silica ($^{\circ}C^{-1}$)
TR_{SUA} = reference temperature for dissolution of particulate biogenic silica ($^{\circ}C$).

4.8 Chemical Oxygen Demand

In the present model, chemical oxygen demand is the concentration of reduced substances that are oxidizable through inorganic means. The source of chemical oxygen demand in saline water is sulfide released from sediments. A cycle occurs in which sulfate is reduced to sulfide in the sediments and reoxidized to sulfate in the water column. In freshwater, methane is released to the water column by the sediment process model. Both sulfide and methane are quantified in units of oxygen demand and are treated with the same kinetic formulation. The kinetic equation including external loads, if any, is:

$$\frac{\partial COD}{\partial t} = -\frac{DO}{KH_{COD} + DO} KCOD \cdot COD + \frac{BFCOD}{\Delta z} + \frac{WCOD}{V} \quad (4\text{-}67)$$

COD = concentration of chemical oxygen demand (g O_2-equivalents m^{-3})
KH_{COD} = half-saturation constant of dissolved oxygen required for oxidation of chemical oxygen demand (g O_2 m^{-3})
KCOD = oxidation rate of chemical oxygen demand (day^{-1})
BFCOD = sediment flux of chemical oxygen demand (g O_2-equivalents m^{-2} day^{-1}), applied to bottom layer only
WCOD = external loads of chemical oxygen demand (g O_2-equivalents day^{-1}).

An exponential function is used to describe the temperature effect on the oxidation rate of chemical oxygen demand:

$$KCOD = K_{CD} \cdot \exp(KT_{COD}[T - TR_{COD}]) \quad (4\text{-}68)$$

K_{CD} = oxidation rate of chemical oxygen demand at TR_{COD} (day^{-1})
KT_{COD} = effect of temperature on oxidation of chemical oxygen demand ($^{\circ}C^{-1}$)
TR_{COD} = reference temperature for oxidation of chemical oxygen demand ($^{\circ}C$).

4.9 Dissolved Oxygen

Sources and sinks of dissolved oxygen in the water column included in the model are (Fig. 4-1):

- algal photosynthesis and respiration
- nitrification
- heterotrophic respiration of dissolved organic carbon
- oxidation of chemical oxygen demand
- surface reaeration for the surface layer only
- sediment oxygen demand for the bottom layer only
- external loads

The kinetic equation describing these processes is:

$$\frac{\partial DO}{\partial t} = \sum_{x=c,d,g,m} \left((1.3 - 0.3 \cdot PN_x) P_x - (1 - FCD_x) \frac{DO}{KHR_x + DO} BM_x \right) AOCR \cdot B_x$$

$$- AONT \cdot Nit \cdot NH4 - AOCR \cdot K_{HR} \cdot DOC - \frac{DO}{KH_{COD} + DO} KCOD \cdot COD$$

$$+ K_r (DO_s - DO) + \frac{SOD}{\Delta z} + \frac{WDO}{V} \qquad (4\text{-}69)$$

AONT = mass of dissolved oxygen consumed per unit mass of ammonium nitrogen nitrified (4.33 g O_2 per g N; see Section 4.9.2)

AOCR = dissolved oxygen-to-carbon ratio in respiration (2.67 g O_2 per g C; see Section 4.9.1)

K_r = reaeration coefficient (day^{-1}): the reaeration term is applied to the surface layer only

DO_s = saturated concentration of dissolved oxygen (g O_2 m^{-3})

SOD = sediment oxygen demand (g O_2 m^{-2} day^{-1}), applied to the bottom layer only; positive is to the water column

WDO = external loads of dissolved oxygen (g O_2 day^{-1}).

The two sink terms in Eq. 4-69, heterotrophic respiration and chemical oxygen demand, are explained in Section 4.4.4 (Eq. 4-29) and Section 4.8 (Eq. 4-67), respectively. The remainder of this section explains the effects of algae, nitrification and surface reaeration.

4.9.1 Effect of Algae on Dissolved Oxygen

The first line on the RHS of Eq. 4-69 accounts for the effects of algae on dissolved oxygen. Algae produce oxygen through photosynthesis and consume oxygen through respiration. The quantity produced depends on the form of nitrogen utilized for growth. Equations describing production of dissolved oxygen are (Morel 1983):

$$106\,CO_2 + 16\,NH_4^+ + H_2PO_4^- + 106\,H_2O \rightarrow protoplasm + 106\,O_2 + 15\,H^+ \quad (4\text{-}70)$$

$$106\,CO_2 + 16\,NO_3^- + H_2PO_4^- + 122\,H_2O + 17\,H^+ \rightarrow protoplasm + 138\,O_2 \quad (4\text{-}71)$$

When ammonium is the nitrogen source, one mole of oxygen is produced per mole of carbon dioxide fixed. When nitrate is the nitrogen source, 1.3 moles of oxygen are produced per mole of carbon dioxide fixed. The quantity, $(1.3 - 0.3 \cdot PN_x)$, in the first term of Eq. 4-69 is the photosynthesis ratio and represents the molar quantity of oxygen produced per mole of carbon dioxide fixed. It approaches unity as the algal preference for ammonium approaches unity.

The last term in the first line of Eq. 4-69 accounts for the oxygen consumption due to algal respiration (Eq. 4-26). A simple representation of respiration process is:

$$CH_2O + O_2 = CO_2 + H_2O \quad (4\text{-}72)$$

from which, AOCR = 2.67 g O_2 per g C.

4.9.2 Effect of Nitrification on Dissolved Oxygen

The stoichiometry of nitrification reaction (Eq. 4-58) indicates that two moles of oxygen are required to nitrify one mole of ammonium into nitrate. However, cell synthesis by nitrifying bacteria is accomplished by the fixation of carbon dioxide so that less than two moles of oxygen are consumed per mole ammonium utilized (Wezernak & Gannon 1968), i.e., AONT = 4.33 g O_2 per g N.

4.9.3 Effect of Surface Reaeration on Dissolved Oxygen

The reaeration rate of dissolved oxygen at the air-water interface is proportional to the oxygen gradient across the interface, $(DO_s - DO)$, when assuming the air is saturated with oxygen. The saturated concentration of dissolved oxygen, which decreases as temperature and salinity increase, is specified using an empirical formula (Genet et al. 1974):

$$DO_s = 14.5532 - 0.38217 \cdot T + 5.4258 \times 10^{-3} \cdot T^2 - CL \cdot (1.665 \times 10^{-4} - 5.866 \times 10^{-6} \cdot T + 9.796 \times 10^{-8} \cdot T^2) \quad (4\text{-}73)$$

CL = chloride concentration (mg/L) = S/1.80655.

The reaeration coefficient includes the effect of turbulence generated by bottom friction (O'Connor & Dobbins 1958) and that by surface wind stress (Banks & Herrera 1977):

$$K_r = \left(K_{ro} \sqrt{\frac{u_{eq}}{h_{eq}}} + W_{rea} \right) \frac{1}{\Delta z} \cdot KT_r^{T-20} \quad (4\text{-}74)$$

K_{ro} = proportionality constant = 3.933 in MKS unit

u_{eq} = weighted velocity over cross-section (m sec^{-1}) = $\sum(u_k V_k)/\sum(V_k)$

h_{eq} = weighted depth over cross-section (m) = $\sum(V_k)/B_\eta$

B_η = width at the free surface (m)

W_{rea} = wind-induced reaeration (m day^{-1})

$$= 0.728 U_w^{½} - 0.317 U_w + 0.0372 U_w^2 \quad (4\text{-}75)$$

U_w = wind speed (m sec^{-1}) at the height of 10 m above surface

KT_r = constant for temperature adjustment of DO reaeration rate.

4.10 Total Active Metal

The present model requires simulation of total active metal for adsorption of phosphate and silica if that option is chosen (Fig. 4-1). The total active metal state variable is the sum of iron and manganese concentrations, both particulate and dissolved. In the model, the origin of total active metal is benthic sediments. Since sediment release of metal is not explicit in the sediment model (Chapter IV of Park et al. 1995), release is specified in the kinetic portion of the water column model. The only other term included is settling of the particulate fraction. Then, the kinetic equation for total active metal including external loads, if any, may be written as:

$$\frac{\partial TAM}{\partial t} = \frac{KHbmf}{KHbmf + DO} \frac{BFTAM}{\Delta z} e^{Ktam(T - Ttam)} + \frac{\partial}{\partial z}(WS_s \cdot TAMp) + \frac{WTAM}{V} \quad (4\text{-}76)$$

TAM = total active metal concentration (mol m^{-3}) = TAMd + TAMp (4-77)

TAMd = dissolved total active metal (mol m^{-3})

TAMp= particulate total active metal (mol m^{-3})

KHbmf = dissolved oxygen concentration at which total active metal release is half the anoxic release rate (g O_2 m^{-3})

BFTAM = anoxic release rate of total active metal (mol m^{-2} day^{-1}), applied to the bottom layer only

Ktam = effect of temperature on sediment release of total active metal ($^\circ C^{-1}$)

Ttam = reference temperature for sediment release of total active metal ($^\circ C$).

WS_s = settling velocity of particulate metal (m day^{-1})

WTAM = external loads of total active metal (mol day^{-1}).

In estuaries, iron and manganese exist in particular and dissolved forms depending on dissolved oxygen concentration. In the oxygenated water, most of the iron and manganese exist as particulate while under anoxic conditions, large fractions are dissolved although solid-phase sulfides and carbonates exist and may predominate. The partitioning between particulate and dissolved phases is expressed using

a concept that total active metal concentration must achieve a minimum level, which is a function of dissolved oxygen, before precipitation occurs:

$$TAMd = minimum\{TAMdmx \cdot \exp(-Kdotam \cdot DO) \ , \ TAM\} \tag{4-78}$$

$$TAMp = TAM - TAMd \tag{4-79}$$

TAMdmx = solubility of total active metal under anoxic conditions (mol m^{-3})
Kdotam = constant that relates total active metal solubility to dissolved oxygen (per g O_2 m^{-3}).

4.11 Fecal Coliform Bacteria

Fecal coliform bacteria are indicative of organisms from the intestinal tract of humans and other animals and can be used as an indicator bacteria as a measure of public health (Thomann & Mueller 1987). In the present model, fecal coliform bacteria have no interaction with other state variables, and have only one sink term, die-off. The kinetic equation including external loads may be written as:

$$\frac{\partial FCB}{\partial t} = - KFCB \cdot TFCB^{T-20} \cdot FCB + \frac{WFCB}{V} \tag{4-80}$$

FCB = bacteria concentration (MPN per 100 ml)
KFCB = first order die-off rate at 20°C (day^{-1})
TFCB = effect of temperature on decay of bacteria ($°C^{-1}$)
WFCB = external loads of fecal coliform bacteria (MPN per 100 ml m^3 day^{-1}).

4.12 Method of Solution

The kinetic equations for the 21 state variables in the EFDC water column water quality model can be expressed in a 21×21 matrix after linearizing some terms, mostly Monod type expressions:

$$\frac{\partial}{\partial t}[C] = [K] \cdot [C] + [R] \tag{4-81}$$

where [C] is in mass $volume^{-1}$, [K] is in $time^{-1}$ and [R] is in mass $volume^{-1}$ $time^{-1}$. Since the settling of particulate matter from the overlying cell acts as an input for a given cell, when Eq. 4-81 is applied to a cell of finite volume, it may be expressed as:

$$\frac{\partial}{\partial t}[C]_k = [K1]_k \cdot [C]_k + \lambda \cdot [K2]_k \cdot [C]_{k+1} + [R]_k \tag{4-82}$$

where the four matrices [C], [K1], [K2] and [R] are defined in Appendix A of Park et al. (1995). The subscript k designates a cell at the k^{th} vertical layer. The layer index k increases upward with KC vertical layers, k = 1 is the bottom layer and k = KC is the surface layer. Then, $\lambda = 0$ for k = KC, otherwise

$\lambda = 1$. The matrix [K2] is a diagonal matrix, and the non-zero elements account for the settling of particulate matter from the overlying cell.

Equation 4-82 is solved using a second-order accurate trapezoidal scheme over a time step of θ, which may be expressed as:

$$[C]_k^N = \left([I] - \frac{\theta}{2}[K1]_k^O \right)^{-1} \cdot \left([C]_k^O + \frac{\theta}{2}\left\{ [K1]_k^O \cdot [C]_k^O + \lambda [K2]_k^O \cdot [C]_{k+1}^A \right\} + \theta [R]_k^O \right) \quad (4\text{-}83)$$

where $\theta = 2 \cdot m \cdot \Delta t$ is the time step for the kinetic equations; [I] is a unit matrix; $[C]^A = [C]^N + [C]^O$; the superscripts O and N designate the variables before and after being adjusted for the relevant kinetic processes. Since Eq. 4-83 is solved from the surface layer downward, the term with $[C]_{k+1}{}^A$ is known for the k^{th} layer and thus placed on the RHS. In Eq. 4-83, inversion of a matrix can be avoided if the 21 state variables are solved in a proper order. The kinetic equations are solved in the order of the variables in the matrix [C] defined in Appendix A of Park et al. (1995).

4.13 Macroalgae (Periphyton) State Variable

The EFDC water quality model was augmented to represent benthic attached algae (often referred to as macroalgae in estuarine waters and periphyton in fresh waters) using the existing framework for phytoplankton growth kinetics. Mathematical relationships based on the impacts of temperature, available light, available nutrients, stream velocity, and density-dependent interactions were incorporated into the algae growth kinetics framework within EFDC. The major difference between modeling techniques for attached and free-floating algae are as follows: (1) attached algae are expressed in terms of areal densities rather than volumetric concentrations; (2) attached algae growth can be limited by the availability of bottom substrate; (3) the availability of nutrients to the macroalgae matrix can be influenced by stream velocity; and (4) macroalgae are not subject to hydrodynamic transport. A good description of periphyton kinetics as it relates to water quality modeling can be found in Warwick et al. (1997) and has been used to develop this section of the report.

A mass balance approach was used to model macroalgae growth with carbon serving as the measure of standing crop size or biomass. For each model grid cell the equation for macroalgae growth is slightly different than the one for free-floating algae (Eq. 4-6):

$$P_m = PM_m \cdot f_1(N) \cdot f_2(I) \cdot f_3(T) \cdot f_4(V) \cdot f_5(D) \quad (4\text{-}84)$$

where

PM_m = maximum growth rate under optimal conditions for macroalgae

$f_1(N)$ = effect of suboptimal nutrient concentration ($0 \le f_1 \le 1$)

$f_2(I)$ = effect of suboptimal light intensity ($0 \le f_2 \le 1$)

$f_3(T)$ = effect of suboptimal temperature ($0 \le f_3 \le 1$)

$f_4(V)$ = velocity limitation factor ($0 \le f_4 \le 1$)

$f_5(D)$ = density dependent growth rate reduction factor ($0 \le f_5 \le 1$).

The basic growth kinetics for macroalgae were developed from those supplied by EFDC and others developed by Runke (1985). The macroalgae population as a whole is characterized by the total biomass present without considering the different species and their associated environmental processes. The optimum growth for the given temperature is adjusted for light, nutrients, velocity, and density-dependent limitations. Each growth limitation factor can vary from 0 to 1. A value of 1 indicates the factor does not limit growth, and a value of 0 means the factor is so severely limiting that growth is stopped entirely (Bowie et al. 1985).

Stream velocity has a twofold effect on periphyton productivity in freshwater streams: velocity increases to a certain level to enhance biomass accrual, but further increases result in substantial scouring (Horner et al. 1990). A benthic algal population is typified as a plant community with an understory and overstory. The entire community is called a matrix. As the matrix develops, the periphyton community is composed of an outer layer of photosynthetically active cells and inner layers of senescent and decomposing cells. Layering can also develop among different species of periphyton. Environmental conditions within the matrix are altered by the physical structure of the periphyton. This influences nutrient uptake and primary production rates of the algae (Sand-Jensen 1983). Above a certain level, current has a simulating effect on periphyton metabolism by mixing the overlying waters with nutrient-poor waters that develop around cells (Whitford and Schumacher 1964). The physical structure of the periphyton community and nutrient uptake by periphyton interfere with nutrient flux through the microbial matrix (Stevenson and Glover 1993).

Current is constantly scouring periphyton from its substrate. At high enough velocities, shear stress can result in substantial biomass reduction. Even at low velocities, sudden increases in velocity raise instantaneous loss rates substantially, but these high rates persist only briefly (Horner et al. 1990). An increase in velocity above that to which benthic algae are accustomed leads to increased loss rates and temporarily reduced biomass. However, recolonization and growth after biomass reduction are usually rapid. The effects of suboptimal velocity upon growth rate are represented in the model by a velocity limitation function. Two options are available in the model for specifying the velocity limitation: (1) a Michaelis-Menton (or Monod) equation (4-85) and (2) a five-parameter logistic function (4-86). The Monod equation limits macroalgae growth due to low velocities whereas the five-parameter logistic function can be configured to limit growth due to either low or high velocities (see Figure 4-2).

Velocity limitation option 1, the Michaelis-Menton equation is written as follows:

$$f_4(V) = \frac{U}{KMV + U} \tag{4-85}$$

where

U = stream velocity (m/sec)
KMV = half-saturation velocity (m/sec)

Velocity limitation option 2, the five-parameter logistic function is as follows:

$$f_4(V) = d + \frac{a - d}{[\ 1 + (\frac{U}{c})^b\ ]^e} \tag{4-86}$$

where

U = stream velocity (m/sec)
a = asymptote at minimum x
b = slope after asymptote a
c = x-translation
d = asymptote at maximum x
e = slope before asymptote d

The half-saturation velocity in Eq. 4-85 is the velocity at which half the maximum growth rate occurs. This effect is analogous to the nutrient limitation because the effect of velocity at suboptimal levels on periphyton growth is due to increasing the exchange of nutrients between the algal matrix and the overlying water (Runke 1985). However, this formula can be too limiting at low velocities. This function does not allow periphyton growth in still waters, but periphyton does grow in still waters such as lakes. Therefore, the function is applied only at velocities above a minimum threshold level (KMVmin). When velocities are at or below this lower level, the limitation function is applied at the minimum level. Above this velocity, the current produces a steeper diffusion gradient around the periphyton (Whitford and Schumacher 1964). A minimum formulation is used to combine the limiting factors for nitrogen, phosphorus, and velocity. The most severely limiting factor alone limits periphyton growth. Note that Eq. 4-86 can be configured so that low velocities are limiting by setting parameter d greater than parameter a, and vice versa to limit growth due to high velocities. In waters that are rich in nutrients, low velocities will not limit growth. However, high velocities may cause scouring and detachment of the macroalgae resulting in a reduction in biomass. The five-parameter logistic function can be configured to approximate this reduction by limiting growth at high velocities.

Macroalgae (periphyton) growth can also be limited by the availability of suitable substrate (Ross 1983). Macroalgae communities reach maximum rates of primary productivity at low levels of

biomass (McIntire 1973; Pfeifer and McDiffett 1975). The relationship between standing crop and production employs the Michaelis-Menton kinetic equation:

$$f_5(D) = \frac{KBP}{KBP + P_m} \tag{4-87}$$

where

KBP = half-saturation biomass level (g C/m^2)
P_m = macroalgae biomass level (g C/m^2).

The half-saturation biomass level (KBP) is the biomass at which half the maximum growth rate occurs. Caupp et al. (1991) used a KBP value of 5.0 g C/m^2 (assuming 50% of ash free dry mass is carbon) for a region of the Truckee River system in California. The function in Eq. 4-87 allows maximum rates of primary productivity at low levels of biomass with decreasing rates of primary productivity as the community matrix expands.

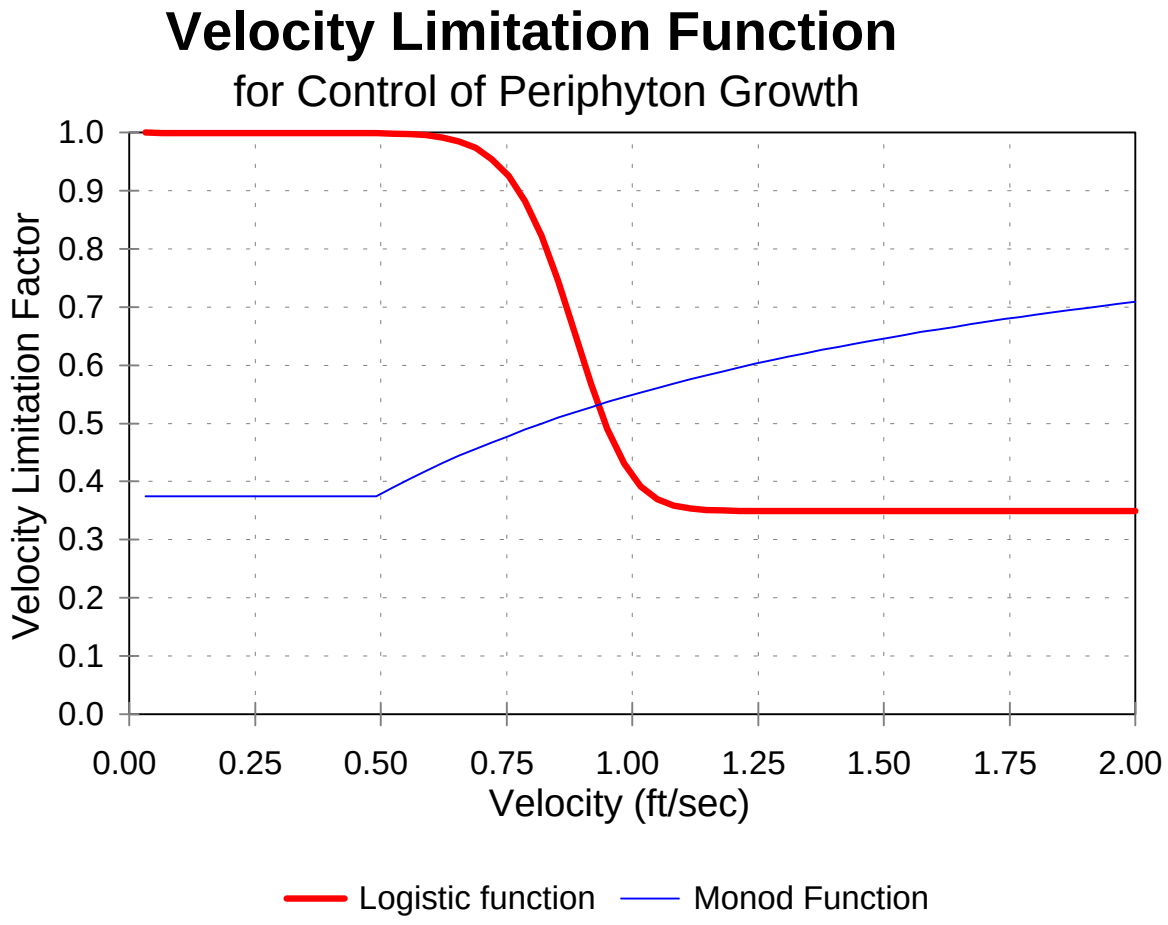

Figure 4-2. Velocity limitation function for (Option 1) the Monod equation where KMV=0.25 m/sec and KMVmin=0.15 m/sec, and (Option 2) the 5-parameter logistic function where a=1.0, b=12.0, c=0.3, d=0.35, and e=3.0 (high velocities are limiting).

Table 4-2. Parameters related to algae in water column.

Parameter	Value[a]	Equation Number[b]
$^{*}PM_c$ (day^{-1})	2.5 (upper Potomac only)	4-6
$^{*}PM_d$ (day^{-1})	2.25	4-6
$^{*}PM_g$ (day^{-1})	2.5	4-6
KHN_x (g N m^{-3})	0.01 (all groups)	4-8
KHP_x (g P m^{-3})	0.001 (all groups)	4-8
KHS (g Si m^{-3})	0.05	4-9
FD	temporally-varying input	4-10
I_o (langleys day^{-1})	temporally-varying input	4-11
$^{*}Ke_b$ (m^{-1})	spatially-varying input	4-13
Ke_{TSS} (m^{-1} per g m^{-3})	NA[c]	4-13
Ke_{Chl} (m^{-1} per mg Chl m^{-3})	0.017	4-13
$CChl_x$ (g C per mg Chl)	0.06 (all groups)	4-13
$(D_{opt})_x$ (m)	1.0 (all groups)	4-14
$(I_s)_{min}$ (langleys day^{-1})	40.0	4-14
CI_a, CI_b & CI_c	0.7, 0.2 & 0.1	4-15
TM_c, TM_d & TM_g (°C)	27.5, 20.0 & 25.0	4-16
$KTG1_c$ & $KTG2_c$ ($°C^{-2}$)	0.005 & 0.004	4-16
$KTG1_d$ & $KTG2_d$ ($°C^{-2}$)	0.004 & 0.006	4-16
$KTG1_g$ & $KTG2_g$ ($°C^{-2}$)	0.008 & 0.01	4-16
STOX (ppt)	1.0	4-17
$^{*}BMR_c$ (day^{-1})	0.04	4-18
$^{*}BMR_d$ (day^{-1})	0.01 0.003 (Jan. - May in saltwater only)	4-18
$^{*}BMR_g$ (day^{-1})	0.01	4-18
TR_x (°C)	20.0 (all groups)	4-18
KTB_x ($°C^{-1}$)	0.069 (all groups)	4-18
$^{*}PRR_c$ (day^{-1})	0.01	4-19
$^{*}PRR_d$ (day^{-1})	0.215 0.065 (Jan. - May in saltwater only)	4-19
$^{*}PRR_g$ (day^{-1})	0.215	4-19
$^{*}WS_c$ (m day^{-1})	0.0	4-5
$^{*}WS_d$ (m day^{-1})	0.35 (January - May) 0.1 (June - December)	4-5
$^{*}WS_g$ (m day^{-1})	0.1	4-5

[a] The evaluation of these values are detailed in Chapter IX of Cerco & Cole (1994).

[b] The equation number where the corresponding parameter is first shown and defined.

[c] Not available in Cerco & Cole (1994) since their formulations do not include these parameters.

[*] The parameters declared as an array in the source code.

Table 4-3. Parameters related to organic carbon in water column.

Parameter	Value[a]	Equation Number[b]
FCRP	0.35	4-20
FCLP	0.55	4-21
FCDP	0.10	4-22
FCD_x	0.0 (all groups)	4-22
$^*WS_{RP}$ (m day^{-1})	1.0	4-20
$^*WS_{LP}$ (m day^{-1})	1.0	4-21
KHR_x (g O_2 m^{-3})	0.5 (all groups)	4-22
$KHOR_{DO}$ (g O_2 m^{-3})	0.5	4-29
K_{RC} (day^{-1})	0.005	4-30
K_{LC} (day^{-1})	0.075	4-31
K_{DC} (day^{-1})	0.01	4-32
K_{RCalg} (day^{-1} per g C m^{-3})	0.0	4-30
K_{LCalg} (day^{-1} per g C m^{-3})	0.0	4-31
K_{DCalg} (day^{-1} per g C m^{-3})	0.0	4-31
TR_{HDR} (°C)	20.0	4-30
TR_{MNL} (°C)	20.0	4-32
KT_{HDR} ($°C^{-1}$)	0.069	4-30
KT_{MNL} ($°C^{-1}$)	0.069	4-31
$KHDN_N$ (g N m^{-3})	0.1	4-34
AANOX	0.5	4-34

[a] The evaluation of these values are detailed in Chapter IX of Cerco & Cole (1994).
[b] The equation number where the corresponding parameter is first shown and defined.
[*] The parameters declared as an array in the source code.

Table 4-4. Parameters related to phosphorus in water column.

Parameter	Value[a]	Equation Number[b]
FPRP	0.1	4-35
FPLP	0.2	4-36
FPDP	0.5	4-37
FPIP	0.2[c]	4-38
FPR_x	0.0 (all groups)	4-35
FPL_x	0.0 (all groups)	4-36
FPD_x	1.0 (all groups)	4-37
FPI_x	0.0[c] (all groups)	4-38
$^*WS_s$ (m day^{-1})	1.0	4-38
K_{PO4p} (per g m^{-3}) for TSS	NA[c]	4-40
K_{PO4p} (per mol m^{-3}) for TAM	6.0	4-40
CP_{prm1} (g C per g P)	42.0	4-43
CP_{prm2} (g C per g P)	85.0	4-43
CP_{prm3} (per g P m^{-3})	200.0	4-43
K_{RP} (day^{-1})	0.005	4-44
K_{LP} (day^{-1})	0.075	4-45
K_{DP} (day^{-1})	0.1	4-46
K_{RPalg} (day^{-1} per g C m^{-3})	0.0	4-44
K_{LPalg} (day^{-1} per g C m^{-3})	0.0	4-45
K_{DPalg} (day^{-1} per g C m^{-3})	0.2	4-46

[a] The evaluation of these values are detailed in Chapter IX of Cerco & Cole (1994).

[b] The equation number where the corresponding parameter is first shown and defined.

[c] Not available in Cerco & Cole (1994) since their formulations do not include these parameters : FPI_x is estimated from $FPR_x+FPL_x+FPD_x+FPI_x = 1$.

[*] The parameters declared as an array in the source code.

Table 4-5. Parameters related to nitrogen in water column.

Parameter	Value[a]	Equation Number[b]
FNRP	0.35	4-48
FNLP	0.55	4-49
FNDP	0.10	4-50
FNIP	0.0	4-51
FNR_x	0.0 (all groups)	4-48
FNL_x	0.0 (all groups)	4-49
FND_x	1.0 (all groups)	4-50
FNI_x	0.0 (all groups)	4-51
ANC_x (g N per g C)	0.167 (all groups)	4-48
ANDC (g N per g C)	0.933	4-52
K_{RN} (day^{-1})	0.005	4-54
K_{LN} (day^{-1})	0.075	4-55
K_{DN} (day^{-1})	0.015	4-56
K_{RNalg} (day^{-1} per g C m^{-3})	0.0	4-54
K_{LNalg} (day^{-1} per g C m^{-3})	0.0	4-55
K_{DNalg} (day^{-1} per g C m^{-3})	0.0	4-56
Nit_m (g N m^{-3} day^{-1})	0.07	4-59
$KHNit_{DO}$ (g O_2 m^{-3})	1.0	4-59
$KHNit_N$ (g N m^{-3})	1.0	4-59
TNit (°C)	27.0	4-60
KNit1 ($°C^{-2}$)	0.0045	4-60
KNit2 ($°C^{-2}$)	0.0045	4-60

[a] The evaluation of these values are detailed in Chapter IX of Cerco & Cole (1994).
[b] The equation number where the corresponding parameter is first shown and defined.

Table 4-6. Parameters related to silica in water column.

Parameter	Value[a]	Equation Number[b]
FSPP	1.0[c]	4-61
FSIP	0.0[c]	4-62
FSP_d	1.0[c]	4-61
FSI_d	0.0[c]	4-62
ASC_d (g Si per g C)	0.5	4-61
K_{SAp} (per g m^{-3}) for TSS	NA[c]	4-64
K_{SAp} (per mol m^{-3}) for TAM	6.0	4-64
K_{SU} (day^{-1})	0.03	4-66
TR_{SUA} ($^{\circ}C$)	20.0	4-66
KT_{SUA} ($^{\circ}C^{-1}$)	0.092	4-66

[a] The evaluation of these values are detailed in Chapter IX of Cerco & Cole (1994).
[b] The equation number where the corresponding parameter is first shown and defined.
[c] Not available in Cerco & Cole (1994) since their formulations do not include these parameters
: FSPP and FSIP are estimated from FSPP+FSIP = 1
: FSP_d and FSI_d are estimated from FSP_d+FSI_d = 1.

Table 4-7. Parameters related to chemical oxygen demand and dissolved oxygen in water column.

Parameter	Value[a]	Equation Number[b]
KH_{COD} (g O_2 m^{-3})	1.5	4-67
K_{CD} (day^{-1})	20.0	4-68
TR_{COD} ($^{\circ}C$)	20.0	4-68
KT_{COD} ($^{\circ}C^{-1}$)	0.041	4-68
AOCR (g O_2 per g C)	2.67	4-69
AONT (g O_2 per g N)	4.33	4-68
K_{ro} (in MKS unit)	3.933[c]	4-69
KT_r	1.024[c] (1.005 - 1.030)	4-74

[a] The evaluation of these values are detailed in Chapter IX of Cerco & Cole (1994).
[b] The equation number where the corresponding parameter is first shown and defined.
[c] Not available in Cerco & Cole (1994) since their formulations do not include these parameters
: K_{ro} is from O'Connor & Dobbins (1958)
: KT_r is from Thomann & Mueller (1987).

Table 4-8. Parameters related to total active metal and fecal coliform bacteria in water column.

Parameter	Value[a]	Equation Number[b]
KHbmf (g O_2 m^{-3})	0.5	4-76
BFTAM (mol m^{-2} day^{-1})	0.01	4-76
Ttam (°C)	20.0	4-76
Ktam (°C^{-1})	0.2	4-76
TAMdmx (mol m^{-3})	0.015	4-77
Kdotam (per g O_2 m^{-3})	1.0	4-77
KFCB (day^{-1})	0.0 - 6.1[c] (seawater)	4-80
TFCB (°C^{-1})	1.07[c]	4-80

[a] The evaluation of these values are detailed in Chapter IX of Cerco & Cole (1994).

[b] The equation number where the corresponding parameter is first shown and defined.

[c] Not available in Cerco & Cole (1994) since their formulations do not include these parameters : KFCB and TFCB are from Thomann & Mueller (1987)

5 - EFDC SEDIMENT PROCESS MODEL

A sediment process model developed by DiToro & Fitzpatrick (1993; hereinafter referred to as D&F) and was coupled with CE-QUAL-ICM for Chesapeake Bay water quality modeling (Cerco & Cole 1994). The sediment process model was slightly modified and incorporated into the EFDC water quality model to simulate the processes in the sediment and at the sediment-water interface. The description of the EFDC sediment process model in this section is from Park et al. (1995). The sediment process model has 27 water quality related state variables and fluxes (Table 5-1).

Table 5-1. EFDC sediment process model state variables and flux terms

1) particulate organic carbon G1 class in layer 2	15) nitrate nitrogen in layer 1
2) particulate organic carbon G2 class in layer 2	16) nitrate nitrogen in layer 2
3) particulate organic carbon G3 class in layer 2	17) phosphate phosphorus in layer 1
4) particulate organic nitrogen G1 class in layer 2	18) phosphate phosphorus in layer 2
5) particulate organic nitrogen G2 class in layer 2	19) available silica in layer 1
6) particulate organic nitrogen G3 class in layer 2	20) available silica in layer 2
7) particulate organic phosphorus G1 class in layer 2	21) ammonia nitrogen flux
8) particulate organic phosphorus G2 class in layer 2	22) nitrate nitrogen flux
9) particulate organic phosphorus G3 class in layer 2	23) phosphate phosphorus flux
10) particulate biogenic silica in layer 2	24) silica flux
11) sulfide/methane in layer 1	25) sediment oxygen demand
12) sulfide/methane in layer 2	26) release of chemical oxygen demand
13) ammonia nitrogen in layer 1	27) sediment temperature
14) ammonia nitrogen in layer 2	

The nitrate state variables, (15), (16) and (22), in the model represent the sum of nitrate and nitrite nitrogen. The three G classes for particulate organic matter (POM) in Layer 2, and the two layers for inorganic substances are described below.

In the sediment model, benthic sediments are represented as two layers (Fig. 5-1). The upper layer (Layer 1) is in contact with the water column and may be oxic or anoxic depending on dissolved oxygen concentration in the overlying water. The lower layer (Layer 2) is permanently anoxic. The upper layer depth, which is determined by the penetration of oxygen into the sediments, is at its maximum only a small fraction of the total depth. Because H_1 (~ 0.1 cm) « H_2,

$$H = H_1 + H_2 \approx H_2 \quad (5\text{-}1)$$

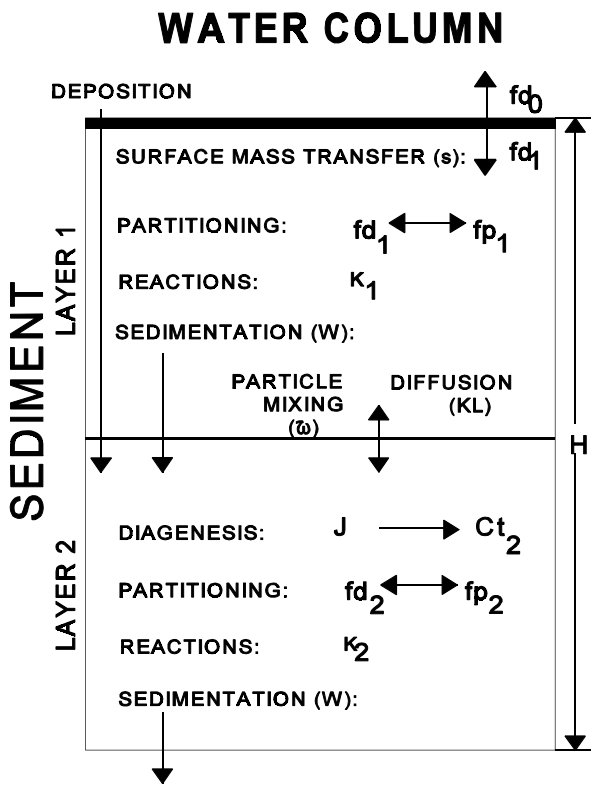

Figure 5-1. Sediment layers and processes included in sediment process model.

where H is the total depth (approximately 10 cm), H_1 is the upper layer depth and H_2 is the lower layer depth.

The model incorporates three basic processes (Fig. 5-2): (1) depositional flux of POM, (2) the diagenesis of POM, and (3) the resulting sediment flux. The sediment model is driven by net settling of particulate organic carbon, nitrogen, phosphorus and silica from the overlying water to the sediments (**depositional flux**). Because of the negligible thickness of the upper layer (Eq. 5-1), deposition proceeds from the water column directly to the lower layer. Within the lower layer, the model simulates the diagenesis (mineralization or decay) of deposited POM, which produces oxygen demand and inorganic nutrients (**diagenesis flux**). The third basic process is the flux of substances produced by diagenesis (**sediment flux**). Oxygen demand, as sulfide (in saltwater) or methane (in freshwater), takes three paths out of the sediments: (1) oxidation at the sediment-water interface as sediment oxygen demand, (2) export to the water column as chemical oxygen demand, or (3) burial to deep, inactive sediments.

Inorganic nutrients produced by diagenesis take two paths out of the sediments: (1) release to the water column or (2) burial to deep, inactive sediments (Fig. 5-2).

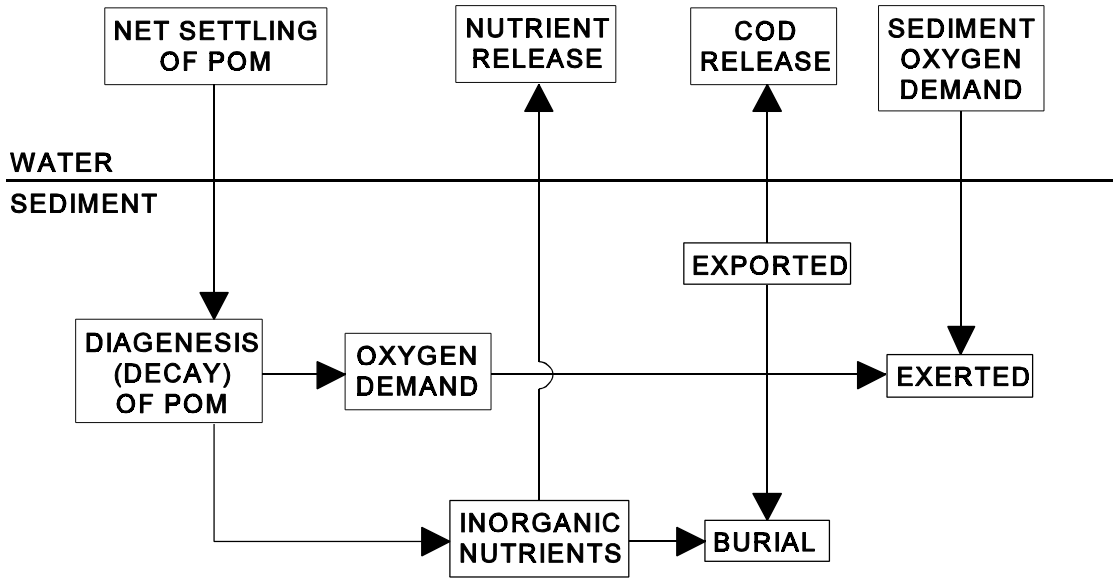

Figure 5-2. Schematic diagram for sediment process model.

This section describes the three basic processes with reactions and sources/sinks for each state variable. The method of solution includes finite difference equations, solution scheme, boundary and initial conditions. Complete model documentation can be found in D&F (1993).

5.1 Depositional Flux

Deposition is one process that couples the water column model with the sediment model. Consequently, deposition is represented in both the water column and sediment models. In the water column model, the governing mass-balance equations for the following state variables contain settling terms, which represent the depositional fluxes.:

- three algal groups, cyanobacteria, diatoms and green algae (Eq. 4-5)
- refractory and labile particulate organic carbon (Equations 4-20 and 4-21)
- refractory and labile particulate organic phosphorus (Equations 4-35 and 4-36) and total phosphate (Eq. 4-38)
- refractory and labile particulate organic nitrogen (Equations 4-48 and 4-49)
- particulate biogenic silica (Eq. 4-61) and available silica (Eq. 4-62)

The sediment model receives these depositional fluxes of particulate organic carbon (POC), particulate organic nitrogen (PON), particulate organic phosphorus (POP) and particulate biogenic silica (PSi). Because of the negligible thickness of the upper layer (Eq. 5-1), deposition is considered to proceed from the water column directly to the lower layer. Since the sediment model has three G classes of POM, G_i (i = 1, 2 or 3), depending on the time scales of reactivity (Section 5.2), the POM fluxes from the water column should be mapped into three G classes based on their reactivity. Then, the depositional fluxes for the i^{th} G class (i = 1, 2 or 3) may be expressed as:

$$J_{POC,i} = FCLP_i \cdot WS_{LP} \cdot LPOC^N + FCRP_i \cdot WS_{RP} \cdot RPOC^N + \sum_{x=c,d,g} FCB_{x,i} \cdot WS_x \cdot B_x^N \quad (5\text{-}2)$$

$$J_{PON,i} = FNLP_i \cdot WS_{LP} \cdot LPON^N + FNRP_i \cdot WS_{RP} \cdot RPON^N + \sum_{x=c,d,g} FNB_{x,i} \cdot ANC_x \cdot WS_x \cdot B_x^N \quad (5\text{-}3)$$

$$J_{POP,i} = FPLP_i \cdot WS_{LP} \cdot LPOP^N + FPRP_i \cdot WS_{RP} \cdot RPOP^N + \sum_{x=c,d,g} FPB_{x,i} \cdot APC \cdot WS_x \cdot B_x^N + \gamma_i \cdot WS_{TSS} \cdot PO4p^N \quad (5\text{-}4)$$

$$J_{PSi} = WS_d \cdot SU^N + ASC_d \cdot WS_d \cdot B_d^N + WS_{TSS} \cdot SAp^N \quad (5\text{-}5)$$

$J_{POM,i}$ = depositional flux of POM (M = C, N or P) routed into the i^{th} G class (g m^{-2} day^{-1})

J_{PSi} = depositional flux of PSi (g Si m^{-2} day^{-1})

$FCLP_i$, $FNLP_i$ & $FPLP_i$ = fraction of water column labile POC, PON and POP, respectively, routed into the i^{th} G class in sediment

$FCRP_i$, $FNRP_i$ & $FPRP_i$ = fraction of water column refractory POC, PON and POP, respectively, routed into the i^{th} G class in sediment

$FCB_{x,i}$, $FNB_{x,i}$ & $FPB_{x,i}$ = fraction of POC, PON and POP, respectively, in the algal group x routed into the i^{th} G class in sediment

γ_i = 1 for i = 1

0 for i = 2 or 3.

In the source code, the sediment process model is solved after the water column water quality model, and the calculated fluxes using the water column conditions at $t = t_n$ are used for the computation of the water quality variables at $t = t_n + \theta$. The superscript N indicates the variables after being updated for the kinetic processes, as defined in Eq. 4-82.

The settling of sorbed phosphate is considered to contribute to the labile G_1 pool in Eq. 5-4, and settling of sorbed silica contributes to J_{PSi} in Eq. 5-5 to avoid creation of additional depositional fluxes

for inorganic particulates. The sum of distribution coefficients should be unity: $\sum_i FCLP_i = \sum_i FNLP_i = \sum_i FPLP_i = \sum_i FCRP_i = \sum_i FNRP_i = \sum_i FPRP_i = \sum_i FCB_{x,i} = \sum_i FNB_{x,i} = \sum_i FPB_{x,i} = 1$. The settling velocities, WS_{LP}, WS_{RP}, WS_x and WS_{TSS}, as defined in the EFDC water column model (Section 4), are net settling velocities. If total active metal is selected as a measure of sorption site, WS_{TSS} is replaced by WS_s in Equations 5-4 and 5-5 (see Sections 4.5 and 4.7).

5.2 Diagenesis Flux

Another coupling point of the sediment model to the water column model is the sediment flux, which is described in Section 5.3. The computation of sediment flux requires that the magnitude of the diagenesis flux be known. The diagenesis flux is explicitly computed using mass-balance equations for deposited POC, PON and POP. (Dissolved silica is produced in the sediments as the result of the dissolution of PSi. Since the dissolution process is different from the bacterial-mediated diagenesis process, it is presented separately in Section 5.4.) In the mass-balance equations, the depositional fluxes of POM are the source terms and the decay of POM in the sediments produces the diagenesis fluxes. The integration of the mass-balance equations for POM provides the diagenesis fluxes that are the inputs for the mass-balance equations for ammonium, nitrate, phosphate and sulfide/methane in the sediments (Section 5.3).

The difference in decay rates of POM is accounted for by assigning a fraction of POM to various decay classes (Westrisch & Berner 1984). POM in the sediments is divided into three G classes, or fractions, representing three scales of reactivity. The G_1 (labile) fraction has a half life of 20 days, and the G_2 (refractory) fraction has a half life of one year. The G_3 (inert) fraction is non-reactive, i.e., it undergoes no significant decay before burial into deep, inactive sediments. The varying reactivity of the G classes controls the time scale over which changes in depositional flux will be reflected in changes in diagenesis flux. If the G_1 class would dominate the POM input into the sediments, then there would be no significant time lag introduced by POM diagenesis and any changes in depositional flux would be readily reflected in diagenesis flux.

Because the upper layer thickness is negligible (Eq. 5-1) and thus depositional flux is considered to proceed directly to the lower layer (Equations 5-2 to 5-5), diagenesis is considered to occur in the lower layer only. The mass-balance equations are similar for POC, PON and POP, and for different G classes. The mass-balance equation in the anoxic lower layer for the i^{th} G class (i = 1, 2 or 3) may be expressed as:

$$H_2 \frac{\partial G_{POM,i}}{\partial t} = - K_{POM,i} \cdot \theta_{POM,i}^{T-20} \cdot G_{POM,i} \cdot H_2 - W \cdot G_{POM,i} + J_{POM,i} \quad (5\text{-}6)$$

$G_{POM,i}$ = concentration of POM (M = C, N or P) in the i^{th} G class in Layer 2 (g m^{-3})

$K_{POM,i}$ = decay rate of the i^{th} G class POM at 20 °C in Layer 2 (day^{-1})

$\theta_{POM,i}$ = constant for temperature adjustment for $K_{POM,i}$

T = sediment temperature (°C)

W = burial rate (m day^{-1}).

Since the G_3 class is inert, $K_{POM,3} = 0$.

Once the mass-balance equations for $G_{POM,1}$ and $G_{POM,2}$ are solved, the diagenesis fluxes are computed from the rate of mineralization of the two reactive G classes:

$$J_M = \sum_{i=1}^{2} K_{POM,i} \cdot \theta_{POM,i}^{T-20} \cdot G_{POM,i} \cdot H_2 \quad (5\text{-}7)$$

J_M = diagenesis flux (g m^{-2} day^{-1}) of carbon (M = C), nitrogen (M = N) or phosphorus (M = P).

5.3 Sediment Flux

The mineralization of POM produces soluble intermediates, which are quantified as diagenesis fluxes in the previous section. The intermediates react in the oxic and anoxic layers, and portions are returned to the overlying water as sediment fluxes. Computation of sediment fluxes requires mass-balance equations for ammonium, nitrate, phosphate, sulfide/methane and available silica. This section describes the flux portion for ammonium, nitrate, phosphate and sulfide/methane of the model. Available silica is described in Section 5.4.

In the upper layer, the processes included in the flux portion are (Fig. 5-1)

- exchange of dissolved fraction between Layer 1 and the overlying water
- exchange of dissolved fraction between Layer 1 and 2 via diffusive transport
- exchange of particulate fraction between Layer 1 and 2 via particle mixing
- loss by burial to the lower layer (Layer 2)
- removal (sink) by reaction
- internal sources.

Since the upper layer is quite thin, $H_1 \sim 0.1$ cm (Eq. 5-1) and the surface mass transfer coefficient (s) is on the order of 0.1 m day^{-1}, then the residence time in the upper layer is: $H_1/s \sim 10^{-2}$ days. Hence, a

steady-state approximation is made in the upper layer. Then the mass-balance equation for ammonium, nitrate, phosphate or sulfide/methane in the upper layer is:

$$H_1 \frac{\partial Ct_1}{\partial t} = 0 = s(fd_0 \cdot Ct_0 - fd_1 \cdot Ct_1) + KL(fd_2 \cdot Ct_2 - fd_1 \cdot Ct_1) + \omega(fp_2 \cdot Ct_2 - fp_1 \cdot Ct_1) - W \cdot Ct_1 - \frac{\kappa_1^2}{s} Ct_1 + J_1 \quad (5\text{-}8)$$

Ct_1 & Ct_2 = total concentrations in Layer 1 and 2, respectively (g m^{-3})

Ct_o = total concentration in the overlying water (g m^{-3})

s = surface mass transfer coefficient (m day^{-1})

KL = diffusion velocity for dissolved fraction between Layer 1 and 2 (m day^{-1})

ω = particle mixing velocity between Layer 1 and 2 (m day^{-1})

fd_o = dissolved fraction of total substance in the overlying water ($0 \le fd_o \le 1$)

fd_1 = dissolved fraction of total substance in Layer 1 ($0 \le fd_1 \le 1$)

fp_1 = particulate fraction of total substance in Layer 1 (= 1 - fd_1)

fd_2 = dissolved fraction of total substance in Layer 2 ($0 \le fd_2 \le 1$)

fp_2 = particulate fraction of total substance in Layer 2 (= 1 - fd_2)

κ_1 = reaction velocity in Layer 1 (m day^{-1})

J_1 = sum of all internal sources in Layer 1 (g m^{-2} day^{-1}).

The first term on the RHS of Eq. 5-8 represents the exchange across sediment-water interface. Then the sediment flux from Layer 1 to the overlying water, which couples the sediment model to the water column model, may be expressed as:

$$J_{aq} = s(fd_1 \cdot Ct_1 - fd_o \cdot Ct_o) \quad (5\text{-}9)$$

J_{aq} = sediment flux of ammonium, nitrate, phosphate or sulfide/methane to the overlying water (g m^{-2} day^{-1}).

The convention used in Eq. 5-9 is that positive flux is from the sediment to the overlying water.

In the lower layer, the processes included in the flux portion are (Fig. 5-1)

- exchange of dissolved fraction between Layer 1 and 2 via diffusive transport
- exchange of particulate fraction between Layer 1 and 2 via particle mixing
- deposition from Layer 1 and burial to the deep inactive sediments
- removal (sink) by reaction
- internal sources including diagenetic source.

The mass-balance equation for ammonium, nitrate, phosphate or sulfide/methane in the lower layer is:

$$H_2 \frac{\partial Ct_2}{\partial t} = - KL(fd_2 \cdot Ct_2 - fd_1 \cdot Ct_1) - \omega(fp_2 \cdot Ct_2 - fp_1 \cdot Ct_1)$$

$$+ W(Ct_1 - Ct_2) - \kappa_2 \cdot Ct_2 + J_2 \qquad (5\text{-}10)$$

κ_2 = reaction velocity in Layer 2 (m day^{-1})

J_2 = sum of all internal sources including diagenesis in Layer 2 (g m^{-2} day^{-1}).

The substances produced by mineralization of POM in sediments may be present in both dissolved and particulate phases. This distribution directly affects the magnitude of the substance that is returned to the overlying water. In Equations 5-8 to 5-10, the distribution of a substance between the dissolved and particulate phases in a sediment is parameterized using a linear partitioning coefficient. The dissolved and particulate fractions are computed from the partitioning equations:

$$fd_1 = \frac{1}{1 + m_1 \cdot \pi_1} \qquad fp_1 = 1 - fd_1 \qquad (5\text{-}11)$$

$$fd_2 = \frac{1}{1 + m_2 \cdot \pi_2} \qquad fp_2 = 1 - fd_2 \qquad (5\text{-}12)$$

m_1 & m_2 = solid concentrations in Layer 1 and 2, respectively (kg L^{-1})

π_1 & π_2 = partition coefficients in Layer 1 and 2, respectively (per kg L^{-1}).

The partition coefficient is the ratio of particulate to dissolved fraction per unit solid concentration (i.e., per unit sorption site available).

All terms, except the last two terms, in Equations 5-8 and 5-10 are common to all state variables and are described in Section 5.3.1. The last two terms represent the reaction and source/sink terms, respectively. These terms, which take different mathematical formulations for different state variables, are described in Sections 5.3.2 to 5.3.5 for ammonium, nitrate, phosphate and sulfide/methane, respectively.

5.3.1 Common Parameters for Sediment Flux

Parameters that are needed for the sediment fluxes are *s*, ω, KL, W, H_2, m_1, m_2, π_1, π_2, κ_1, κ_2, J_1 and J_2 in Equations 5-8 to 5-12. Of these, κ_1, κ_2, J_1 and J_2 are variable-specific. Among the other common parameters, W, H_2, m_1 and m_2, are specified as input. The modeling of the remaining three parameters, *s*, ω, KL, are described in this section.

5.3.1.1 Surface mass transfer coefficient. Owing to the observation that the surface mass transfer coefficient, *s*, can be related to the sediment oxygen demand, SOD (DiToro et al. 1990), *s* can be estimated from the ratio of SOD and overlying water oxygen concentration:

$$s = \frac{D_1}{H_1} = \frac{SOD}{DO_0} \tag{5-13}$$

D_1 = diffusion coefficient in Layer 1 (m^2 day^{-1}).

Knowing *s*, it is possible to estimate the other model parameters.

5.3.1.2 Particulate phase mixing coefficient: The particle mixing velocity between Layer 1 and 2 is parameterized as:

$$\omega = \frac{D_p \cdot \theta_{Dp}^{T-20}}{H_2} \frac{G_{POC,1}}{G_{POC,R}} \frac{DO_0}{KM_{Dp} + DO_0} \tag{5-14}$$

D_p = apparent diffusion coefficient for particle mixing (m^2 day^{-1})

θ_{Dp} = constant for temperature adjustment for D_p

$G_{POC,R}$ = reference concentration for $G_{POC,1}$ (g C m^{-3})

KM_{Dp} = particle mixing half-saturation constant for oxygen (g O_2 m^{-3}).

The enhanced mixing of sediment particles by macrobenthos (bioturbation) is quantified by estimating D_p. The particle mixing appears to be proportional to the benthic biomass (Matisoff 1982), which is correlated to the carbon input to the sediment (Robbins et al. 1989). This is parameterized by assuming that benthic biomass is proportional to the available labile carbon, $G_{POC,1}$, and $G_{POC,R}$ is the reference concentration at which the particle mixing velocity is at its nominal value. The Monod-type oxygen dependency accounts for the oxygen dependency of benthic biomass.

It has been observed that a hysteresis exists in the relationship between the bottom water oxygen and benthic biomass. Benthic biomass increases as the summer progresses. However, the occurrence of anoxia/hypoxia reduces the biomass drastically and also imposes stress on benthic activities. After full overturn, the bottom water oxygen increases but the population does not recover immediately. Hence, the particle mixing velocity, which is proportional to the benthic biomass, does not increase in response to the increased bottom water oxygen. Recovery of benthic biomass following hypoxic events depends on many factors including severity and longevity of hypoxia, constituent species and salinity (Diaz & Rosenberg 1995).

This phenomenon of reduced benthic activities and hysteresis is parameterized based on the idea of stress that low oxygen imposes on the benthic population. It is analogous to the modeling of the toxic effect of chemicals on organisms (Mancini 1983). A first order differential equation is employed, in which the benthic stress 1) accumulates only when overlying oxygen is below KM_{Dp} and 2) is dissipated at a first order rate (Fig. 5-3a):

$$\frac{\partial ST}{\partial t} = - K_{ST} \cdot ST + \left(1 - \frac{DO_0}{KM_{Dp}} \right) \qquad if \quad DO_0 < KM_{Dp}$$

$$\frac{\partial ST}{\partial t} = - K_{ST} \cdot ST \qquad if \quad DO_0 > KM_{Dp} \tag{5-15}$$

ST = accumulated benthic stress (day)

K_{ST} = first order decay rate for ST (day^{-1}).

The behavior of this formulation can be understood by evaluating the steady-state stresses at two extreme conditions of overlying water oxygen, DO_0:

as $DO_0 = 0$	$K_{ST} \cdot ST = 1$	$f(ST) = (1 - K_{ST} \cdot ST) = 0$
as $DO_0 \geq KM_{Dp}$	$K_{ST} \cdot ST = 0$	$f(ST) = (1 - K_{ST} \cdot ST) = 1$

The dimensionless expression, $f(ST) = 1 - K_{ST} \cdot ST$, appears to be the proper variable to quantify the effect of benthic stress on benthic biomass and thus particle mixing (Fig. 5-3b).

The final formulation for the particle mixing velocity including the benthic stress is:

$$\omega = \frac{D_p \cdot \theta_{Dp}^{T-20}}{H_2} \frac{G_{POC,1}}{G_{POC,R}} \frac{DO_0}{KM_{Dp} + DO_0} f(ST) + \frac{Dp_{\min}}{H_2} \tag{5-16}$$

Dp_{min} = minimum diffusion coefficient for particle mixing (m^2 day^{-1}).

The reduction in particle mixing due to the benthic stress, f(ST), is estimated by employing the following procedure. The stress, ST, is normally calculated with Eq. 5-15. Once DO_0 drops below a critical concentration, $DO_{ST,c}$, for $NC_{hypoxia}$ consecutive days or more, the calculated stress is not allowed to decrease until t_{MBS} days of $DO_0 > DO_{ST,c}$. That is, only when hypoxic days are longer than critical hypoxia days ($NC_{hypoxia}$), the maximum stress, or minimum ($1 - K_{ST} \cdot ST$), is retained for a specified period (t_{MBS} days) after DO_0 recovery (Fig. 5-3). No hysteresis occurs if DO_0 does not drop below $DO_{ST,c}$ or if hypoxia lasts less than $NC_{hypoxia}$ days. When applying maximum stress for t_{MBS} days, the subsequent hypoxic days are not included in t_{MBS}. This parameterization of hysteresis essentially assumes seasonal

hypoxia, i.e., one or two major hypoxic events during summer, and might be unsuitable for systems with multiple hypoxic events throughout a year.

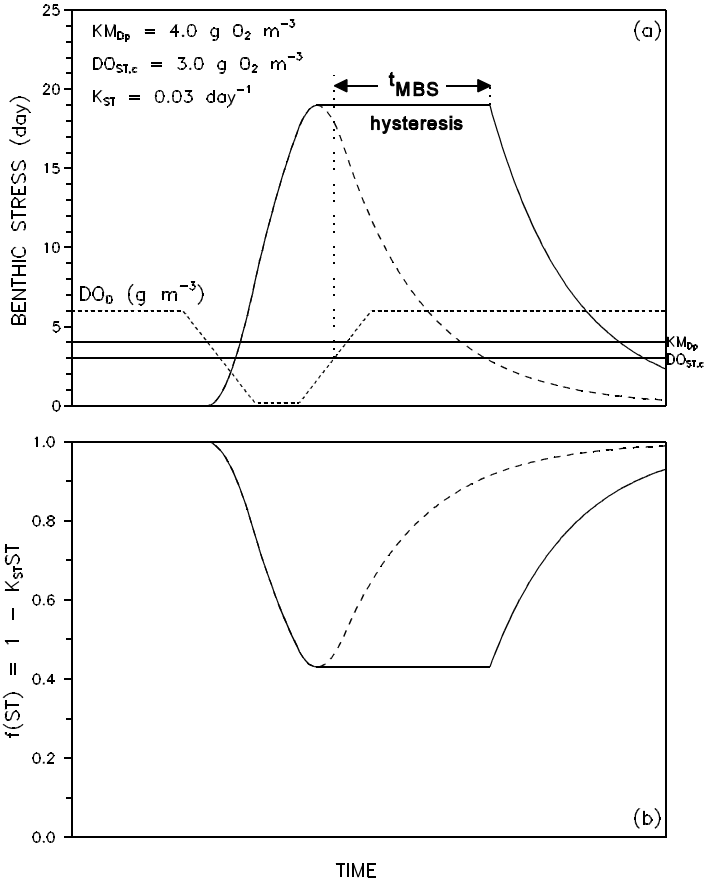

Figure 5-3. Benthic stress (a) and its effect on particle mixing (b) as a function of overlying water column dissolved oxygen concentration.

Three parameters relating to hysteresis, $DO_{ST,c}$, $NC_{hypoxia}$ and t_{MBS}, are functions of many factors including severity and longevity of hypoxia, constituent species and salinity, and thus have site-specific variabilities (Diaz & Rosenberg 1995). The critical overlying oxygen concentration, $DO_{ST,c}$, also depends on the distance from the bottom of the location of $DO_{0.}$ The critical hypoxia days, $NC_{hypoxia}$, depends on tolerance of benthic organisms to hypoxia and thus on benthic community structure (Diaz & Rosenberg 1995). The time lag for the recovery of benthic biomass following hypoxic events, t_{MBS}, tends to be longer for higher salinity. The above three parameters are considered to be spatially constant input parameters.

5.3.1.3 Dissolved phase mixing coefficient. Dissolved phase mixing between Layer 1 and 2 is via passive molecular diffusion, which is enhanced by the mixing activities of the benthic organisms

(bio-irrigation). This is modeled by increasing the diffusion coefficient relative to the molecular diffusion coefficient:

$$KL = \frac{D_d \cdot \theta_{Dd}^{T-20}}{H_2} + R_{BI,BT} \cdot \omega \tag{5-17}$$

D_d = diffusion coefficient in pore water (m^2 day^{-1})

θ_{Dd} = constant for temperature adjustment for D_d

$R_{BI,BT}$ = ratio of bio-irrigation to bioturbation.

The last term in Eq. 5-17 accounts for the enhanced mixing by organism activities.

5.3.2 Ammonia Nitrogen

Diagenesis is assumed not to occur in the upper layer because of its shallow depth, and ammonium is produced by diagenesis in the lower layer:

$$J_{1,NH4} = 0 \qquad J_{2,NH4} = J_N \quad (from\ Eq.\ 5\text{-}7) \tag{5-18}$$

Ammonium is nitrified to nitrate in the presence of oxygen. A Monod-type expression is used for the ammonium and oxygen dependency of the nitrification rate. Then, the oxic layer reaction velocity in Eq. 5-8 for ammonium may be expressed as:

$$\kappa_{1,NH4}^2 = \frac{DO_0}{2 \cdot KM_{NH4,O2} + DO_0} \frac{KM_{NH4}}{KM_{NH4} + NH4_1} \kappa_{NH4}^2 \cdot \theta_{NH4}^{T-20} \tag{5-19}$$

and then the nitrification flux becomes:

$$J_{Nit} = \frac{\kappa_{1,NH4}^2}{s} \cdot NH4_1 \tag{5-20}$$

$KM_{NH4,O2}$ = nitrification half-saturation constant for dissolved oxygen (g O_2 m^{-3})

$NH4_1$ = total ammonium nitrogen concentration in Layer 1 (g N m^{-3})

KM_{NH4} = nitrification half-saturation constant for ammonium (g N m^{-3})

κ_{NH4} = optimal reaction velocity for nitrification at 20°C (m day^{-1})

θ_{NH4} = constant for temperature adjustment for κ_{NH4}

J_{Nit} = nitrification flux (g N m^{-2} day^{-1}).

Nitrification does not occur in the anoxic lower layer:

$$\kappa_{2,NH4} = 0 \tag{5-21}$$

Once Equations 5-8 and 5-10 are solved for $NH4_1$ and $NH4_2$, the sediment flux of ammonium to the overlying water, $J_{aq,NH4}$, can be calculated using Eq. 5-9. Note that it is not $NH4_1$ and $NH4_2$ that determine the magnitude of $J_{aq,NH4}$ (Section X-B-2 in D&F 1993). The magnitude is determined by (1) the diagenesis flux, (2) the fraction that is nitrified, and (3) the surface mass transfer coefficient (*s*) that mixes the remaining portion.

5.3.3 Nitrate Nitrogen

Nitrification flux is the only source of nitrate in the upper layer, and there is no diagenetic source for nitrate in both layers:

$$J_{1,NO3} = J_{Nit} \quad (from\ Eq.\ 5\text{-}19) \qquad J_{2,NO3} = 0 \tag{5-22}$$

Nitrate is present in sediments as dissolved substance, i.e., $\pi_{1,NO3} = \pi_{2,NO3} = 0$, making $fd_{1,NO3} = fd_{2,NO3} = 1$ (Equations 5-11 and 5-12): it also makes $\tilde{\omega}$ meaningless, hence $\tilde{\omega} = 0$. Nitrate is removed by denitrification in both oxic and anoxic layers with the carbon required for denitrification supplied by carbon diagenesis. The reaction velocities in Equations 5-8 and 5-10 for nitrate may be expressed as:

$$\kappa^2_{1,NO3} = \kappa^2_{NO3,1} \cdot \theta^{T-20}_{NO3} \tag{5-23}$$

$$\kappa_{2,NO3} = \kappa_{NO3,2} \cdot \theta^{T-20}_{NO3} \tag{5-24}$$

and the denitrification flux out of sediments as a nitrogen gas becomes:

$$J_{N2(g)} = \frac{\kappa^2_{1,NO3}}{s} NO3_1 + \kappa_{2,NO3} \cdot NO3_2 \tag{5-25}$$

$\kappa_{NO3,1}$ = reaction velocity for denitrification in Layer 1 at 20°C (m day^{-1})
$\kappa_{NO3,2}$ = reaction velocity for denitrification in Layer 2 at 20°C (m day^{-1})
θ_{NO3} = constant for temperature adjustment for $\kappa_{NO3,1}$ and $\kappa_{NO3,2}$
$J_{N2(g)}$ = denitrification flux (g N m^{-2} day^{-1})
$NO3_1$ = total nitrate nitrogen concentration in Layer 1 (g N m^{-3})
$NO3_2$ = total nitrate nitrogen concentration in Layer 2 (g N m^{-3}).

Once Equations 5-8 and 5-10 are solved for $NO3_1$ and $NO3_2$, the sediment flux of nitrate to the overlying water, $J_{aq,NO3}$, can be calculated using Eq. 5-9. The steady-state solution for nitrate showed that the nitrate flux is a linear function of $NO3_0$ (Eq. III-15 in D&F 1993): the intercept quantifies the amount of ammonium in the sediment that is nitrified but not denitrified (thus releases as $J_{aq,NO3}$), and the slope quantifies the extent to which overlying water nitrate is denitrified in the sediment. It also revealed that

if the internal production of nitrate is small relative to the flux of nitrate from the overlying water, the normalized nitrate flux to the sediment, $- J_{aq,NO3}/NO3_0$, is linear in *s* for small *s* and constant for large *s* (Section III-C in D&F 1993). For small *s* (~ 0.01 m day^{-1}), H_1 is large (Eq. 5-13) so that oxic layer denitrification predominates and $J_{aq,NO3}$ is essentially zero independent of $NO3_0$ (Fig. III-4 in D&F 1993).

5.3.4 Phosphate Phosphorus

Phosphate is produced by the diagenetic breakdown of POP in the lower layer:

$$J_{1,PO4} = 0 \qquad J_{2,PO4} = J_P \quad (from\ Eq.\ 5\text{-}7) \tag{5-26}$$

A portion of the liberated phosphate remains in the dissolved form and a portion becomes particulate phosphate, either via precipitation of phosphate-containing minerals (Troup 1974), e.g., vivianite, $Fe_3(PO_4)_2(s)$, or by partitioning to phosphate sorption sites (Lijklema 1980; Barrow 1983; Giordani & Astorri 1986). The extent of particulate formation is determined by the magnitude of the partition coefficients, $\pi_{1,PO4}$ and $\pi_{2,PO4}$, in Equations 5-11 and 5-12. Phosphate flux is strongly affected by DO_0, the overlying water oxygen concentration. As DO_0 approaches zero, the phosphate flux from the sediments increases. This mechanism is incorporated by making $\pi_{1,PO4}$ larger, under oxic conditions, than $\pi_{2,PO4}$. In the model, when DO_0 exceeds a critical concentration, $(DO_0)_{crit,PO4}$, sorption in the upper layer is enhanced by an amount $\Delta\pi_{PO4,1}$:

$$\pi_{1,PO4} = \pi_{2,PO4} \cdot (\Delta\pi_{PO4,1}) \qquad DO_0 > (DO_0)_{crit,PO4} \tag{5-27}$$

When oxygen falls below $(DO_0)_{crit,PO4}$, then:

$$\pi_{1,PO4} = \pi_{2,PO4} \cdot (\Delta\pi_{PO4,1})^{DO_0/(DO_0)_{crit,PO4}} \qquad DO_0 \leq (DO_0)_{crit,PO4} \tag{5-28}$$

which smoothly reduces $\pi_{1,PO4}$ to $\pi_{2,PO4}$ as DO_0 goes to zero. There is no removal reaction for phosphate in both layers:

$$\kappa_{1,PO4} = \kappa_{2,PO4} = 0 \tag{5-29}$$

Once Equations 5-8 and 5-10 are solved for $PO4_1$ and $PO4_2$, the sediment flux of phosphate to the overlying water, $J_{aq,PO4}$, can be calculated using Eq. 5-9.

5.3.5 Sulfide/methane and Oxygen Demand

5.3.5.1 Sulfide. No diagenetic production of sulfide occurs in the upper layer. In the lower layer, sulfide is produced by carbon diagenesis (Eq. 5-7) decremented by the organic carbon consumed by denitrification (Eq. 5-25). Then:

$$J_{1,H2S} = 0 \qquad J_{2,H2S} = a_{O2,C} \cdot J_C - a_{O2,NO3} \cdot J_{N2(g)} \tag{5-30}$$

$a_{O2,C}$ = stoichiometric coefficient for carbon diagenesis consumed by sulfide oxidation (2.6667 g O_2-equivalents per g C)

$a_{O2,NO3}$ = stoichiometric coefficient for carbon diagenesis consumed by denitrification (2.8571 g O_2-equivalents per g N).

A portion of the dissolved sulfide that is produced in the anoxic layer reacts with the iron to form particulate iron monosulfide, FeS(s) (Morse et al. 1987). The particulate fraction is mixed into the oxic layer where it can be oxidized to ferric oxyhydroxide, Fe_2O_3(s). The remaining dissolved fraction also diffuses into the oxic layer where it is oxidized to sulfate. Partitioning between dissolved and particulate sulfide in the model represents the formation of FeS(s), which is parameterized using partition coefficients, $\pi_{1,H2S}$ and $\pi_{2,H2S}$, in Equations 5-11 and 5-12.

The present sediment model has three pathways for sulfide, the reduced end product of carbon diagenesis: (1) sulfide oxidation, (2) aqueous sulfide flux, and (3) burial. The distribution of sulfide among the three pathways is controlled by the partitioning coefficients and the oxidation reaction velocities (Section V-E in D&F 1993). Both dissolved and particulate sulfide are oxidized in the oxic layer, consuming oxygen in the process. In the oxic upper layer, the oxidation rate that is linear in oxygen concentration is used (Cline & Richards 1969; Millero 1986; Boudreau 1991). In the anoxic lower layer, no oxidation can occur. Then, the reaction velocities in Equations 5-8 and 5-10 may be expressed as:

$$\kappa^2_{1,H2S} = \left(\kappa^2_{H2S,d1} \cdot fd_{1,H2S} + \kappa^2_{H2S,p1} \cdot fp_{1,H2S}\right)\theta^{T-20}_{H2S} \frac{DO_0}{2 \cdot KM_{H2S,O2}} \tag{5-31}$$

$$\kappa_{2,H2S} = 0 \tag{5-32}$$

$\kappa_{H2S,d1}$ = reaction velocity for dissolved sulfide oxidation in Layer 1 at 20 °C (m day^{-1})

$\kappa_{H2S,p1}$ = reaction velocity for particulate sulfide oxidation in Layer 1 at 20 °C (m day^{-1})

θ_{H2S} = constant for temperature adjustment for $\kappa_{H2S,d1}$ and $\kappa_{H2S,p1}$

$KM_{H2S,O2}$ = constant to normalize the sulfide oxidation rate for oxygen (g O_2 m^{-3}).

The constant, $KM_{H2S,O2}$, which is included for convenience only, is used to scale the oxygen concentration in the overlying water. At $DO_0 = KM_{H2S,O2}$, the reaction velocity for sulfide oxidation rate is at its nominal value.

The oxidation reactions in the oxic upper layer cause oxygen flux to the sediment, which exerts SOD. By convention, SOD is positive: SOD = $-J_{aq,O2}$. The SOD in the model consists of two components, carbonaceous sediment oxygen demand (CSOD) due to sulfide oxidation and nitrogenous sediment oxygen demand (NSOD) due to nitrification:

$$SOD = CSOD + NSOD = \frac{\kappa_{1,H2S}^2}{s} H2S_1 + a_{O2,NH4} \cdot J_{Nit} \tag{5-33}$$

$H2S_1$ = total sulfide concentration in Layer 1 (g O_2-equivalents m^{-3})

$a_{O2,NH4}$ = stoichiometric coefficient for oxygen consumed by nitrification (4.33 g O_2 per g N).

Equation 4-29 is nonlinear for SOD because the RHS contains *s* (= SOD/DO_0) so that SOD appears on both sides of the equation: note that J_{Nit} (Eq. 5-20) is also a function of *s*. A simple back substitution method is used, as explained in Section 5.6.1.

If the overlying water oxygen is low, then the sulfide that is not completely oxidized in the upper layer can diffuse into the overlying water. This aqueous sulfide flux out of the sediments, which contributes to the chemical oxygen demand in the water column model, is modeled using

$$J_{aq,H2S} = s(fd_{1,H2S} \cdot H2S_1 - COD) \tag{5-34}$$

The sulfide released from the sediment reacts very quickly in the water column when oxygen is available, but can accumulate in the water column under anoxic conditions. The COD, quantified as oxygen equivalents, is entirely supplied by benthic release in the water column model (Eq. 3-16). Since sulfide also is quantified as oxygen equivalents, COD is used as a measure of sulfide in the water column in Eq. 5-34.

5.3.5.2 Methane: When sulfate is used up, methane can be produced by carbon diagenesis and methane oxidation consumes oxygen (DiToro et al. 1990). Owing to the abundant sulfate in the saltwater, only the aforementioned sulfide production and oxidation are considered to occur in the saltwater. Since the sulfate concentration in the freshwater is generally insignificant, methane production is considered to replace sulfide production in the freshwater. In the freshwater, methane is produced by carbon diagenesis in the lower layer decremented by the organic carbon consumed by denitrification, and no diagenetic production of methane occurs in the upper layer (Eq. 5-30):

$$J_{1,CH4} = 0 \qquad J_{2,CH4} = a_{O2,C} \cdot J_C - a_{O2,NO3} \cdot J_{N2(g)} \tag{5-35}$$

The dissolved methane produced takes two pathways: (1) oxidation in the oxic upper layer causing CSOD or (2) escape from the sediment as aqueous flux or as gas flux:

$$J_{2,CH4} = CSOD + J_{aq,CH4} + J_{CH4(g)} \quad (5\text{-}36)$$

$J_{aq,CH4}$ = aqueous methane flux (g O_2-equivalents m^{-2} day^{-1})

$J_{CH4(g)}$ = gaseous methane flux (g O_2-equivalents m^{-2} day^{-1}).

A portion of dissolved methane that is produced in the anoxic layer diffuses into the oxic layer where it is oxidized. This methane oxidation causes CSOD in the freshwater sediment (DiToro et al. 1990):

$$CSOD = CSOD_{\max} \cdot \left(1 - sech[\frac{\kappa_{CH4} \cdot \theta_{CH4}^{T-20}}{s}] \right) \quad (5\text{-}37)$$

$$CSOD_{\max} = minimum\left\{ \sqrt{2 \cdot KL \cdot CH4_{sat} \cdot J_{2,CH4}},\ J_{2,CH4} \right\} \quad (5\text{-}38)$$

$$CH4_{sat} = 100\left(1 + \frac{h + H_2}{10} \right) 1.024^{20-T} \quad (5\text{-}39)$$

$CSOD_{max}$ = maximum CSOD occurring when all the dissolved methane transported to the oxic layer is oxidized

κ_{CH4} = reaction velocity for dissolved methane oxidation in Layer 1 at 20°C (m day^{-1})

θ_{CH4} = constant for temperature adjustment for κ_{CH4}

$CH4_{sat}$ = saturation concentration of methane in the pore water (g O_2-equivalents m^{-3}).

The term, $(h + H_2)/10$ where h and H_2 are in meters, in Eq. 5-39 is the depth from the water surface that corrects for the in situ pressure. Equation 5-39 is accurate to within 3% of the reported methane solubility between 5 and 20°C (Yamamoto et al. 1976).

If the overlying water oxygen is low, the methane that is not completely oxidized can escape the sediment into the overlying water either as aqueous flux or as gas flux. The aqueous methane flux, which contributes to the chemical oxygen demand in the water column model, is modeled using (DiToro et al. 1990):

$$J_{aq,CH4} = CSOD_{\max} \cdot sech[\frac{\kappa_{CH4} \cdot \theta_{CH4}^{T-20}}{s}] = CSOD_{\max} - CSOD \quad (5\text{-}40)$$

Methane is only slightly soluble in water. If its solubility, $CH4_{sat}$ given by Eq. 5-39, is exceeded in the pore water, it forms a gas phase that escapes as bubbles. The loss of methane as bubbles, i.e., the gaseous methane flux, is modeled using Eq. 5-36 with $J_{2,CH4}$ from Eq. 5-35, CSOD from Eq. 5-37 and $J_{aq,CH4}$ from Eq. 5-40 (DiToro et al. 1990).

5.4 Silica

The production of ammonium, nitrate and phosphate in sediments is the result of the mineralization of POM by bacteria. The production of dissolved silica in sediments is the result of the dissolution of particulate biogenic or opaline silica, which is thought to be independent of bacterial processes.

The depositional flux of particulate biogenic silica from the overlying water to the sediments is modeled using Eq. 5-5. With this source, the mass-balance equation for particulate biogenic silica may be written as:

$$H_2 \frac{\partial PSi}{\partial t} = - S_{Si} \cdot H_2 - W \cdot PSi + J_{PSi} + J_{DSi} \quad (5\text{-}41)$$

PSi = concentration of particulate biogenic silica in the sediment (g Si m^{-3})

S_{Si} = dissolution rate of PSi in Layer 2 (g Si m^{-3} day^{-1})

J_{PSi} = depositional flux of PSi (g Si m^{-2} day^{-1}) given by Eq. 5-5

J_{DSi} = detrital flux of PSi (g Si m^{-2} day^{-1}) to account for PSi settling to the sediment that is not associated with the algal flux of biogenic silica.

The processes included in Eq. 5-41 are dissolution (i.e., production of dissolved silica), burial, and depositional and detrital fluxes from the overlying water. Equation 5-41 can be viewed as the analog of the diagenesis equations for POM (Eq. 5-6). The dissolution rate is formulated using a reversible reaction that is first order in silica solubility deficit and follows a Monod-type relationship in particulate silica:

$$S_{Si} = K_{Si} \cdot \theta_{Si}^{T-20} \frac{PSi}{PSi + KM_{PSi}} (Si_{sat} - fd_{2,Si} \cdot Si_2) \quad (5\text{-}42)$$

K_{Si} = first order dissolution rate for PSi at 20°C in Layer 2 (day^{-1})

θ_{Si} = constant for temperature adjustment for K_{Si}

KM_{PSi} = silica dissolution half-saturation constant for PSi (g Si m^{-3})

Si_{sat} = saturation concentration of silica in the pore water (g Si m^{-3}).

The mass-balance equations for mineralized silica can be formulated using the general forms, Equations 5-8 and 5-10. There is no source/sink term and no reaction in the upper layer:

$$J_{1,Si} = \kappa_{1,Si} = 0 \tag{5-43}$$

In the lower layer, silica is produced by the dissolution of particulate biogenic silica, which is modeled using Eq. 5-42. The two terms in Eq. 5-42 correspond to the source term and reaction term in Eq. 5-10:

$$J_{2,Si} = K_{Si} \cdot \theta_{Si}^{T-20} \frac{PSi}{PSi + KM_{PSi}} Si_{sat} \cdot H_2 \tag{5-44}$$

$$\kappa_{2,Si} = K_{Si} \cdot \theta_{Si}^{T-20} \frac{PSi}{PSi + KM_{PSi}} f_{d2,Si} \cdot H_2 \tag{5-45}$$

A portion of silica dissolved from particulate silica sorbs to solids and a portion remains in the dissolved form. Partitioning using the partition coefficients, $\pi_{1,Si}$ and $\pi_{2,Si}$, in Equations 5-11 and 5-12 controls the extent to which dissolved silica sorbs to solids. Since silica shows similar behavior as phosphate in the adsorption-desorption process, the same partitioning method as applied to phosphate (Section 5.3.4) is used for silica. That is, when DO_0 exceeds a critical concentration, $(DO_0)_{crit,Si}$, sorption in the upper layer is enhanced by an amount $\Delta\pi_{Si,1}$:

$$\pi_{1,Si} = \pi_{2,Si} \cdot (\Delta\pi_{Si,1}) \qquad DO_0 > (DO_0)_{crit,Si} \tag{5-46}$$

When oxygen falls below $(DO_0)_{crit,Si}$, then:

$$\pi_{1,Si} = \pi_{2,Si} \cdot (\Delta\pi_{Si,1})^{DO_0/(DO_0)_{crit,Si}} \qquad DO_0 \leq (DO_0)_{crit,Si} \tag{5-47}$$

which smoothly reduces $\pi_{1,Si}$ to $\pi_{2,Si}$ as DO_0 goes to zero.

Once Equations 5-8 and 5-10 are solved for Si_1 and Si_2, the sediment flux of silica to the overlying water, $J_{aq,Si}$, can be calculated using Eq. 5-9.

5.5 Sediment Temperature

All rate coefficients in the aforementioned mass-balance equations are expressed as a function of sediment temperature, T. The sediment temperature is modeled based on the diffusion of heat between the water column and sediment:

$$\frac{\partial T}{\partial t} = \frac{D_T}{H^2}(T_W - T) \tag{5-48}$$

D_T = heat diffusion coefficient between the water column and sediment (m^2 sec^{-1})

T_W = temperature in the overlying water column (°C) calculated by Eq. 4-82.

The model application in D&F and Cerco & Cole (1994) used $D_T = 1.8 \times 10^{-7}$ m^2 sec^{-1}.

5.6 Method of Solution

5.6.1 Finite-Difference Equations and Solution Scheme

An implicit integration scheme is used to solve the governing mass-balance equations. The finite difference form of Eq. 5-8 may be expressed as:

$$0 = s(fd_0 \cdot Ct_0' - fd_1 \cdot Ct_1') + KL(fd_2 \cdot Ct_2' - fd_1 \cdot Ct_1') + \omega(fp_2 \cdot Ct_2' - fp_1 \cdot Ct_1') - W \cdot Ct_1' - \frac{\kappa_1^2}{s} Ct_1' + J_1' \quad (5\text{-}49)$$

where the primed variables designate the values evaluated at $t+\theta$ and the unprimed variables are those at t, where θ is defined in Eq. 4-82. The finite difference form of Eq. 5-10 may be expressed as:

$$0 = -KL(fd_2 \cdot Ct_2' - fd_1 \cdot Ct_1') - \omega(fp_2 \cdot Ct_2' - fp_1 \cdot Ct_1') + W(Ct_1' - Ct_2') - (\kappa_2 + \frac{H_2}{\theta}) Ct_2' + \left(J_2' + \frac{H_2}{\theta} Ct_2 \right) \quad (5\text{-}50)$$

The two terms, - $(H_2/\theta)Ct_2'$ and $(H_2/\theta)Ct_2$, are from the derivative term, $H_2(\partial Ct_2/\partial t)$ in Eq. 5-10, each of which simply adds to the Layer 2 removal rate and the forcing function, respectively. Setting these two terms equal to zero results in the steady-state model. The two unknowns, Ct_1' and Ct_2', can be calculated at every time step using:

$$\begin{pmatrix} s \cdot fd_1 + a_1 + \frac{\kappa_1^2}{s} & -a_2 \\ -a_1 & a_2 + W + \kappa_2 + \frac{H_2}{\theta} \end{pmatrix} \begin{pmatrix} Ct_1' \\ Ct_2' \end{pmatrix} = \begin{pmatrix} J_1' + s \cdot fd_0 \cdot Ct_0' \\ J_2' + \frac{H_2}{\theta} Ct_2 \end{pmatrix} \quad (5\text{-}51)$$

$$a_1 = KL \cdot fd_1 + \omega \cdot fp_1 + W \qquad a_2 = KL \cdot fd_2 + \omega \cdot fp_2 \quad (5\text{-}52)$$

The solution of Eq. 5-51 requires an iterative method since the surface mass transfer coefficient, s, is a function of the SOD (Eq. 5-13), which is also a function of s (Eq. 5-33). A simple back substitution method is used:

(1) Start with an initial estimate of SOD: for example, SOD = $a_{O2,C} \cdot J_C$ or the previous time step SOD.

(2) Solve Eq. 5-51 for ammonium, nitrate, and sulfide/methane.

(3) Compute the SOD using Eq. 5-33.

(4) Refine the estimate of SOD: a root finding method (Brent's method in Press et al. 1986) is used to make the new estimate.

(5) Go to (2) if no convergence.

(6) Solve Eq. 5-51 for phosphate and silica.

For the sake of symmetry, the equations for diagenesis, particulate biogenic silica and sediment temperature are also solved in implicit form. The finite difference form of the diagenesis equation (Eq. 5-6) may be expressed as:

$$G'_{POM,i} = \left(G_{POM,i} + \frac{\theta}{H_2} J_{POM,I} \right) \left(1 + \theta \cdot K_{POM,i} \cdot \theta_{POM,i}^{T-20} + \frac{\theta}{H_2} W \right)^{-1} \tag{5-53}$$

The finite difference form of the PSi equation (Eq. 5-41) may be expressed as:

$$PSi' = \left(PSi + \frac{\theta}{H_2} (J_{PSi} + J_{DSi}) \right) \left(1 + \theta \cdot K_{Si} \cdot \theta_{Si}^{T-20} \frac{Si_{sat} - f_{d2,Si} \cdot Si_2}{PSi + KM_{PSi}} + \frac{\theta}{H_2} W \right)^{-1} \tag{5-54}$$

using Eq. 5-36 for the dissolution term, in which PSi in the Monod-type term has been kept at time level *t* to simplify the solution. The finite difference form of the sediment temperature equation (Eq. 5-48) may be expressed as:

$$T' = \left(T + \frac{\theta}{H^2} D_T \cdot T_W \right) \left(1 + \frac{\theta}{H^2} D_T \right)^{-1} \tag{5-55}$$

5.6.2 Boundary and Initial Conditions

The above finite difference equations constitute an initial boundary-value problem. The boundary conditions are the depositional fluxes ($J_{POM,i}$ and J_{PSi}) and the overlying water conditions (Ct_0 and T_W) as a function of time, which are provided from the water column water quality model. The initial conditions are the concentrations at $t = 0$, $G_{POM,i}(0)$, PSi(0), $Ct_1(0)$, $Ct_2(0)$ and T(0), to start the computations. Strictly speaking, these initial conditions should reflect the past history of the overlying water conditions and depositional fluxes, which is often impractical because of lack of field data for these earlier years.

Table 5-2. Assignment of water column particulate organic matter (POM) to sediment G classes used in Cerco & Cole (1994).

WCM Variable	Carbon & Phosphorus			Nitrogen		
	G_1	G_2	G_3	G_1	G_2	G_3
A. "stand alone" model	0.65	0.20	0.15	0.65	0.25	0.10
B. coupled model						
Labile Particulate	1.0	0.0	0.0	1.0	0.0	0.0
Refractory Particulate[a]						
: Bay and Tributary Zones 1	0.0	0.11	0.89	0.0	0.26	0.74
: Bay Zones 2 and 10	0.0	0.43	0.57	0.0	0.54	0.46
: All Other Zones	0.0	0.73	0.27	0.0	0.82	0.18
Algae	0.65	0.255	0.095	0.65	0.28	0.07

[a] See Figure 10-6 in Cerco & Cole (1994) for the definition of Zones.

Table 5-3. Sediment burial rates (W) used in Cerco & Cole (1994).

Bay Zones[a]	Rate (cm yr^{-1})	Tributary Zones[a]	Rate (cm yr^{-1})
1, 2, 10	0.50	1	0.50
3, 6, 9	0.25	2, 3	0.25
7, 8	0.37		

[a] See Figure 10-6 in Cerco & Cole (1994) for the definition of Zones.

6 - COMMENTS

The Virginia Institute of Marine Science's three-dimensional Hydrodynamic-Eutrophication Model (HEM-3D) consists of the hydrodynamic model, the water column water quality model and the sediment process model. The hydrodynamic model is the EFDC described in Hamrick (1992). Application of the hydrodynamic model involves grid generation, data analysis for initial and boundary conditions, model calibration/verification, and interpretation of model results. The application of the hydrodynamic model to the Indian River Lagoon/Turkey Creek region is described in Tetra Tech (1993).

The model formulations and their method of solution for the water column water quality model and sediment process model are described in this report. Application of the water quality and sediment process models involves data analysis for initial and boundary conditions, evaluation of external loadings, model calibration/verification, and interpretation of model results. The application of the water quality and sediment process models to an idealized, hypothetical system will be described in another report. Description of input data files is given in Appendix B of this report, which is provided in a disk.

References

Aller, R.C. 1982. The effects of macrobenthos on chemical properties of marine sediment and overlying water, pp. 53-102. In: P.L. McCall & M.J.S. Tevesz (eds.), Animal-Sediment Relations: The Biogenic Alteration of Sediments, Plenum Press, NY.

Ambrose, Jr., R.B., Wool, T.A., Connolly, J.P. & Schanz, R.W. 1988. WASP4, a hydrodynamic and water quality model: model theory, user's manual and programmer's guide. EPA/600/3-87/039, Environmental Research Lab., US EPA, 297 pp.

Banks, R.B. & Herrera, F.F. 1977. Effect of wind and rain on surface reaeration. J. of the Environmental Engineering Division, ASCE, 103(EE3): 489-504.

Barrow, N.J. 1983. A mechanistic model for describing the sorption and desorption of phosphate by soil. J. of Soil Science, 34: 733-750.

Boni, L., Carpené, E., Wynne, D., & Reti, M. 1989. Alkaline phosphatase activity in *Protogonyaulax tamarensis*. J. of Plankton Research, 11(5): 879-885.

Boudreau, B.P. 1991. Modelling the sulfide-oxygen reaction and associated pH gradients in porewaters. Geochimica et Cosmochimica Acta, 55: 145-159.

Bowie, G.L., Mills, W.B., Porcella, D.B., Campbell, C.L., Pagenkopf, J.R., Rupp, G.L., Johnson, K.M., Chan, P.W.H., Gherini, S.A. & Chamberlin, C.E. 1985. Rates, constants and kinetics formulations in surface water quality modeling (second edition). EPA/600/3-85/040, Environmental Research Lab., US EPA, 455 pp.

Brush, G.S. 1984. Patterns of recent sediment accumulation in Chesapeake Bay (Virginia-Maryland, U.S.A.) tributaries. Chemical Geology, 44: 227-242.

Carritt, D.E. & Goodgal, S. 1954. Sorption reactions and some ecological implications. Deep-Sea Research, 1: 224-243.

Cerco, C.F. & Cole, T.M. 1994. Three-dimensional eutrophication model of Chesapeake Bay: Volume 1, main report. Technical Report EL-94-4, US Army Engineer Waterways Experiment Station, Vicksburg, MS.

Chróst, R.J. & Overbek, J. 1987. Kinetics of alkaline phosphatase activity and phosphorus availability for phytoplankton and bacterioplankton in Lake Plußsee (North German eutrophic lake). Microbial Ecology, 13: 229-248.

Cline, J.D. & Richards, F.A. 1969. Oxygenation of hydrogen sulfide in seawater at constant salinity, temperature and pH. Environmental Science & Technology, 3(9): 838-843.

Diaz, R.J. & Rosenberg, R. 1995. Marine benthic hypoxia: a review of its ecological effects and the behavioural responses of benthic macrofauna. Oceanography and Marine Biology: an Annual Review, 33: 245-303.

DiToro, D.M. 1980. Applicability of cellular equilibrium and Monod theory to phytoplankton growth kinetics. Ecological Modelling, 8: 201-218.

DiToro, D.M., Paquin, P.R., Subburamu, K. & Gruber, D.A. 1990. Sediment oxygen demand model: methane and ammonia oxidation. J. of Environmental Engineering, ASCE, 116(5): 945-986.

DiToro, D.M. & Fitzpatrick, J.J. 1993. Chesapeake bay sediment flux model. Contract Report EL-93-2, US Army Engineer Waterways Experiment Station, Vicksburg, MS, 316 pp.

Froelich, P.N. 1988. Kinetic control of dissolved phosphate in natural rivers and estuaries: a primer on the phosphate buffer mechanism. Limnology and Oceanography, 33(4, part 2): 649-668.

Gardner, W.S., Seitzinger, S.P. & Malczyk, J.M. 1991. The effects of sea salts on the forms of nitrogen released from estuarine and freshwater sediments: does ion pairing affect ammonium flux? Estuaries, 14(2): 157-166.

Genet, L.A., Smith, D.J. & Sonnen, M.B. 1974. Computer program documentation for the dynamic estuary model. Prepared for US EPA, Systems Development Branch, Washington, D.C.

Giordani, P. & Astorri, M. 1986. Phosphate analysis of marine sediments. Chemistry in Ecology, 2: 103-112.

Hamrick, J. M., 1992a: A Three-Dimensional Environmental Fluid Dynamics Computer Code: Theoretical and Computational Aspects. The College of William and Mary, Virginia Institute of Marine Science. Special Report 317, 63 pp.

Hamrick, J. M., 1992b: Estuarine environmental impact assessment using a three-dimensional circulation and transport model. Estuarine and Coastal Modeling, Proceedings of the 2nd International Conference, M. L. Spaulding et al, Eds., American Society of Civil Engineers, New York, 292-303.

Hamrick, J. M., 1994: Linking hydrodynamic and biogeochemcial transport models for estuarine and coastal waters. Estuarine and Coastal Modeling, Proceedings of the 3rd International Conference, M. L. Spaulding et al, Eds., American Society of Civil Engineers, New York, 591-608.

Hamrick, J. M., 1996: A User's Manual for the Environmental Fluid Dynamics Computer Code (EFDC). The College of William and Mary, Virginia Institute of Marine Science, Special Report 331, 234 pp.

Hamrick, J. M., and T. S. Wu, 1996: Computational design and optimization of the EFDC/HEM3D surface water hydrodynamic and eutrophication models. Computational Methods for Next Generation Environmental Models, G. Delich, Ed., Society of Industrial and Applied Mathematics, Philadelphia, in press.

Kremer, J.N. & Nixon, S.W. 1978. A coastal marine ecosystem: simulation and analysis. Ecological Studies 24, Springer-Verlag, New York, 217 pp.

Kuo, A.Y., Neilson, B.J. & Park, K. 1991. A modeling study of the water quality of the upper tidal Rappahannock River. Special Report in Applied Marine Science and Ocean Eng. (SRAMSOE) #314, School of Marine Science (SMS)/Virginia Institute of Marine Science (VIMS), The College of William and Mary, VA, 164 pp.

Kuo, A.Y. & Park, K. 1994. A PC-based tidal prism water quality model for small coastal basins and tidal creeks. SRAMSOE #324, SMS/VIMS, The College of William and Mary, VA, 119 pp.

Lebo, M.E. 1991. Particle-bound phosphorus along an urbanized coastal plain estuary. Marine Chemistry, 34: 225-246.

Lijklema, L. 1980. Interaction of ortho-phosphate with iron (III) and aluminum hydroxides. Environmental Science & Technology, 14(5): 537-541.

Llansó, R.J. 1992. Effects of hypoxia on estuarine benthos: the lower Rappahannock River (Chesapeake Bay), a case study. Estuarine, Coastal and Shelf Science, 35: 491-515.

Mackin, J.E. & Aller, R.C. 1984. Ammonium adsorption in marine sediments. Limnology and oceanography, 29(2): 250-257.

Mancini, J.L. 1983. A method for calculating effects, on aquatic organisms, of time varying cocnentrations. Water Research, 17(10): 1355-1362.

Matisoff, G. 1982. Mathematical models of bioturbation, pp. 289-330. In: P.L. McCall & M.J.S. Tevesz (eds.), Animal-Sediment Relations: The Biogenic Alteration of Sediments, Plenum Press, NY.

Millero, F.J. 1986. The thermodynamics and kinetics of the hydrogen sulfide system in natural waters. Marine Chemistry, 18: 121-147.

Morel, F. 1983. Principles of Aquatic Chemistry. John Wiley & Sons, New York, NY, 446 pp.

Morse, J.W., Millero, F.J., Cornwell, J.C. & Rickard, D. 1987. The chemistry of the hydrogen sulfide and iron sulfide systems in natural waters. Earth-Science Reviews, 24: 1-42.

O'Connor, D.J. & Dobbins, W.E. 1958. Mechanism of reaeration in natural streams. Transactions of the Americal Society of Civil Engineers, 123(2934): 641-684.

Odum, E.P. 1971. Fundamentals of ecology (third edition). W.B. Saunders Co., Philadelphia, PA, 574pp.

Officer, C.B., Lynch, D.R., Setlock, G.H. & Helz, G.R. 1984. Recent sedimentation rates in Chesapeake Bay, pp. 131-157. In: V.S. Kennedy (ed.), The Estuary as a Filter, Academic Press.

Park, K. & Kuo, A.Y. 1993. A vertical two-dimensional model of hydrodynamics and water quality in estuaries. SRAMSOE #321, SMS/VIMS, The College of William and Mary, VA, 47 pp.

Park, K. & Kuo, A.Y. submitted. An accurate solution scheme for mass-balance equations of non-conservative substances: multi-step computation decoupling kinetic processes from physical transport. Submitted to Water Research.

Parsons, T.R., Takahashi, M. & Hargrave, B. 1984. Biological oceanographic processes (third edition). Pergamon Press, 330 pp.

Press, W.H., Flannery, B.P., Teukolsky, S.A. & Vetterling, W.T. 1986. Numerical recipes: the art of scientific computing. Cambridge University Press, 818 pp.

Redfield, A.C., Ketchum, B.H. & Richards, F.A. 1963. The influence of organisms on the composition of sea-water (Chapter 2) pp 26-77. In: M.N. Hill (ed.), The Sea - Ideas and Observations on Progress in the Study of the Seas: Vol. 2, Composition of Sea Water, Comparative and Descriptive Oceanography, Interscience Publishers.

Robbins, J.A., Keilty, T., White, D.S. & Edgington, D.N. 1989. Relationships among tubificid abundances, sediment composition and accumulation rates in Lake Erie. Canadian J. of Fisheries & Aquatic Sciences, 46(2): 223-231.

Rosenberg, R. 1980. Effect of oxygen deficiency on benthic macrofauna in fjords, pp. 499-514. In: H.J. Freeland, D.M. Farmer & C.D. Levings (eds.), Fjord Oceanography, Plenum Press, NY.

Sørensen, J. & Revsbech, N.P. 1990. Denitrification in stream biofilm and sediment: in situ variation and control factors, pp. 277-289. In: N.P. Revsbech & J. Sørensen (eds.), Denitrification in Soil and Sediment, FEMS Symposium No. 56, Plenum Press, NY.

Steele, J.H. 1962. Environmental control of photosynthesis in the sea. Limnology and Oceanography, 7(2): 137-150.

Stumm, W. & Morgan, J.J. 1981. Aquatic chemistry, an introduction emphasizing chemical equilibria in natural waters (second edition). John Wiley & Sons, Inc., 780 pp.

Tetra Tech. 1993. User's guide for the IRL/TC three-dimensional hydrodynamic and salinity model. Tetra Tech, Inc., Prepared for Florida Institute of Technology and St. Johns River Water Management District, Florida.

Thomann, R.V. & Fitzpatrick, J.J. 1982. Calibration and verification of a mathematical model of the eutrophication of the Potomac Estuary. HydroQual, Inc., Final Report to Department of Environmental Services, Washington, D.C., 500 pp.

Thomann, R.V., Jaworski, N.J., Nixon, S.W., Paerl, H.W. & Taft, J. 1985. The 1983 algal bloom in the Potomac Estuary. The Algal Bloom Expert Panel, Pepared for the Potomac Strategy State/EPA Management Committee, US EPA Region III, Philadelphia, PA.

Thomann, R.V. & Mueller, J.A. 1987. Principles of surface water quality modeling and control. Harper & Row, Publishers, Inc., 644 pp.

Troup, R. 1974. The interaction of iron with phosphate, carbonate and sulfide in Chesapeake Bay interstitial waters: a thermodynamic interpretation. Ph.D. Dissertation, Johns Hopkins University, MD, 114 p.

Westrich, J.T. & Berner, R.A. 1984. The role of sedimentary organic matter in bacterial sulfate reduction: the G model tested. Limnology and Oceanography, 29(2): 236-249.

Wezernak, C.T. & Gannon, J.J. 1968. Evaluation of nitrification in streams. J. of the Sanitary Engineering Division, ASCE, 94(SA5): 883-895.

Yamamoto, S., Alcauskas, J.B. & Crozler, T.E. 1976. Solubility of methane in distilled water and seawater. J. of Chemical and Engineering Data, 21(1): 78-80.

Appendix A. Final Solutions of Kinetic Equations

The matrices in Eq. 4-82, $[C]_k$ in mass volume^{-1}, $[K1]_k$ and $[K2]_k$ in time^{-1} and $[R]_k$ in mass volume^{-1} time^{-1}, are defined below. For the diagonal matrix $[K2]_k$, which accounts for the settling of particulate matter from the overlying cell, only the diagonal terms are shown. In the matrix $[C]_k$, the LHS of the equal sign lists the names of the state variables used in this report, while the RHS lists the names used in the source code.

$$[C]_k = \begin{pmatrix} B_c = WQV_1 \\ B_d = WQV_2 \\ B_g = WQV_3 \\ RPOC = WQV_4 \\ LPOC = WQV_5 \\ DOC = WQV_6 \\ RPOP = WQV_7 \\ LPOP = WQV_8 \\ DOP = WQV_9 \\ PO4t = WQV_{10} \\ RPON = WQV_{11} \\ LPON = WQV_{12} \\ DON = WQV_{13} \\ NH4 = WQV_{14} \\ NO3 = WQV_{15} \\ SU = WQV_{16} \\ SA = WQV_{17} \\ COD = WQV_{18} \\ DO = WQV_{19} \\ TAM = WQV_{20} \\ FCB = WQV_{21} \end{pmatrix}_k \qquad ent_{ii}\left([K2]_k\right) = \begin{pmatrix} t_{1,c} \\ t_{2,d} \\ t_{3,g} \\ t_4 \\ t_5 \\ 0 \\ t_7 \\ t_8 \\ 0 \\ t_{10} \\ t_{11} \\ t_{12} \\ 0 \\ 0 \\ 0 \\ t_{16} \\ t_{17} \\ 0 \\ 0 \\ t_{20} \\ 0 \end{pmatrix}_k \qquad [R]_k = \begin{pmatrix} r_{1,c} \\ r_{2,d} \\ r_{3,g} \\ r_4 \\ r_5 \\ r_6 \\ r_7 \\ r_8 \\ r_9 \\ r_{10} \\ r_{11} \\ r_{12} \\ r_{13} \\ r_{14} \\ r_{15} \\ r_{16} \\ r_{17} \\ r_{18} \\ r_{19} \\ r_{20} \\ r_{21} \end{pmatrix}_k$$

$$[K1]_k = \begin{pmatrix}
a_{1,c} & 0 & 0 & 0 & 0 & 0 & 0 & 0 & 0 & 0 & 0 & 0 & 0 & 0 & 0 & 0 & 0 & 0 & 0 \\
0 & a_{2,d} & 0 & 0 & 0 & 0 & 0 & 0 & 0 & 0 & 0 & 0 & 0 & 0 & 0 & 0 & 0 & 0 & 0 \\
0 & 0 & a_{3,g} & 0 & 0 & 0 & 0 & 0 & 0 & 0 & 0 & 0 & 0 & 0 & 0 & 0 & 0 & 0 & 0 \\
a_{4,c} & a_{4,d} & a_{4,g} & b_4 & 0 & 0 & 0 & 0 & 0 & 0 & 0 & 0 & 0 & 0 & 0 & 0 & 0 & 0 & 0 \\
a_{5,c} & a_{5,d} & a_{5,g} & 0 & c_5 & 0 & 0 & 0 & 0 & 0 & 0 & 0 & 0 & 0 & 0 & 0 & 0 & 0 & 0 \\
a_{6,c} & a_{6,d} & a_{6,g} & b_6 & c_6 & d_6 & 0 & 0 & 0 & 0 & 0 & 0 & 0 & 0 & 0 & 0 & 0 & 0 & 0 \\
a_{7,c} & a_{7,d} & a_{7,g} & 0 & 0 & 0 & e_7 & 0 & 0 & 0 & 0 & 0 & 0 & 0 & 0 & 0 & 0 & 0 & 0 \\
a_{8,c} & a_{8,d} & a_{8,g} & 0 & 0 & 0 & 0 & f_8 & 0 & 0 & 0 & 0 & 0 & 0 & 0 & 0 & 0 & 0 & 0 \\
a_{9,c} & a_{9,d} & a_{9,g} & 0 & 0 & 0 & e_9 & f_9 & g_9 & 0 & 0 & 0 & 0 & 0 & 0 & 0 & 0 & 0 & 0 \\
a_{10,c} & a_{10,d} & a_{10,g} & 0 & 0 & 0 & 0 & 0 & g_{10} & h_{10} & 0 & 0 & 0 & 0 & 0 & 0 & 0 & 0 & 0 \\
a_{11,c} & a_{11,d} & a_{11,g} & 0 & 0 & 0 & 0 & 0 & 0 & 0 & i_{11} & 0 & 0 & 0 & 0 & 0 & 0 & 0 & 0 \\
a_{12,c} & a_{12,d} & a_{12,g} & 0 & 0 & 0 & 0 & 0 & 0 & 0 & 0 & j_{12} & 0 & 0 & 0 & 0 & 0 & 0 & 0 \\
a_{13,c} & a_{13,d} & a_{13,g} & 0 & 0 & 0 & 0 & 0 & 0 & 0 & i_{13} & j_{13} & k_{13} & 0 & 0 & 0 & 0 & 0 & 0 \\
a_{14,c} & a_{14,d} & a_{14,g} & 0 & 0 & 0 & 0 & 0 & 0 & 0 & 0 & 0 & k_{14} & l_{14} & 0 & 0 & 0 & 0 & 0 \\
a_{15,c} & a_{15,d} & a_{15,g} & 0 & 0 & d_{15} & 0 & 0 & 0 & 0 & 0 & 0 & 0 & l_{15} & 0 & 0 & 0 & 0 & 0 \\
0 & a_{16,d} & 0 & 0 & 0 & 0 & 0 & 0 & 0 & 0 & 0 & 0 & 0 & 0 & 0 & m_{16} & 0 & 0 & 0 \\
0 & a_{17,d} & 0 & 0 & 0 & 0 & 0 & 0 & 0 & 0 & 0 & 0 & 0 & 0 & 0 & m_{17} & n_{17} & 0 & 0 \\
0 & 0 & 0 & 0 & 0 & 0 & 0 & 0 & 0 & 0 & 0 & 0 & 0 & 0 & 0 & 0 & 0 & o_{18} & 0 \\
a_{19,c} & a_{19,d} & a_{19,g} & 0 & 0 & d_{19} & 0 & 0 & 0 & 0 & 0 & 0 & 0 & l_{19} & 0 & 0 & 0 & o_{19} & p_{19} \\
0 & 0 & 0 & 0 & 0 & 0 & 0 & 0 & 0 & 0 & 0 & 0 & 0 & 0 & 0 & 0 & 0 & 0 & 0 \\
0 & 0 & 0 & 0 & 0 & 0 & 0 & 0 & 0 & 0 & 0 & 0 & 0 & 0 & 0 & 0 & 0 & 0 & 0
\end{pmatrix} q$$

The non-zero elements in $[K1]_k$, $[K2]_k$ and $[R]_k$ are given below. As explained in Section 4-12, the layer index k increases upward: k = 1 is the bottom layer and k = KC is the surface layer. Hereinafter the subscript k to designate the kth layer is omitted.

$$a_{1,c} = P_c^{\,O} - BM_c^{\,O} - PR_c^{\,O} - \frac{WS_c^{\,O}}{\Delta z^{\,O}} \qquad t_{1,c} = \frac{(WS_c^{\,O})_{k+1}}{\Delta z^{\,O}} \qquad r_{1,c} = \frac{WB_c^{\,O}}{V^{\,O}}$$

$$a_{2,d} = P_d^O - BM_d^O - PR_d^O - \frac{WS_d^O}{\Delta z^O} \qquad t_{2,d} = \frac{(WS_d^O)_{k+1}}{\Delta z^O} \qquad r_{2,d} = \frac{WB_d^O}{V^O}$$

$$a_{3,g} = P_g^O - BM_g^O - PR_g^O - \frac{WS_g^O}{\Delta z^O} \qquad t_{3,g} = \frac{(WS_g^O)_{k+1}}{\Delta z^O} \qquad r_{3,g} = \frac{WB_g^O}{V^O}$$

$$a_{4,x} = FCRP \cdot PR_x^O \qquad b_4 = -b_6 - \frac{WS_{RP}^O}{\Delta z^O}$$

$$t_4 = \frac{(WS_{RP}^O)_{k+1}}{\Delta z^O} \qquad r_4 = \frac{WRPOC^O}{V^O}$$

$$a_{5,x} = FCLP \cdot PR_x^O \qquad c_5 = -c_6 - \frac{WS_{LP}^O}{\Delta z^O}$$

$$t_5 = \frac{(WS_{LP}^O)_{k+1}}{\Delta z^O} \qquad r_5 = \frac{WLPOC^O}{V^O}$$

$$a_{6,x} = \left(FCD_x + (1 - FCD_x) \frac{KHR_x}{KHR_x + DO^O} \right) BM_x^O + FCDP \cdot PR_x^O$$

$$b_6 = K_{RPOC}^O \qquad c_6 = K_{LPOC}^O$$

$$d_6 = -K_{HR}^O - Denit^O \qquad r_6 = \frac{WDOC^O}{V^O}$$

$$a_{7,x} = (FPR_x \cdot BM_x^O + FPRP \cdot PR_x^O) APC^O \qquad e_7 = -e_9 - \frac{WS_{RP}^O}{\Delta z^O}$$

$$t_7 = t_4 \qquad r_7 = \frac{WRPOP^O}{V^O}$$

$$a_{8,x} = (FPL_x \cdot BM_x^O + FPLP \cdot PR_x^O) APC^O \qquad f_8 = -f_9 - \frac{WS_{LP}^O}{\Delta z^O}$$

$$t_8 = t_5 \qquad r_8 = \frac{WLPOP^{O}}{V^{O}}$$

$$a_{9,x} = (FPD_x \cdot BM_x^{O} + FPDP \cdot PR_x^{O}) APC^{O} \qquad e_9 = K_{RPOP}^{O}$$

$$f_9 = K_{LPOP}^{O} \qquad g_9 = -\, g_{10}$$

$$r_9 = \frac{WDOP^{O}}{V^{O}}$$

$$a_{10,x} = (FPI_x \cdot BM_x^{O} + FPIP \cdot PR_x^{O} - P_x^{O}) APC^{O} \qquad g_{10} = K_{DOP}^{O}$$

$$h_{10} = -\frac{WS_{TSS}^{O}}{\Delta z^{O}} \frac{K_{PO4p} \cdot TSS^{O}}{1 + K_{PO4p} \cdot TSS^{O}}$$

$$t_{10} = \frac{(WS_{TSS}^{O})_{k+1}}{\Delta z^{O}} \frac{K_{PO4p} \cdot TSS_{k+1}^{O}}{1 + K_{PO4p} \cdot TSS_{k+1}^{O}}$$

$$r_{10} = \frac{BFPO4^{O}}{\Delta z^{O}} + \frac{WPO4t^{O}}{V^{O}}$$

$$a_{11,x} = (FNR_x \cdot BM_x^{O} + FNRP \cdot PR_x^{O}) ANC_x \qquad i_{11} = -\, i_{13} - \frac{WS_{RP}^{O}}{\Delta z^{O}}$$

$$t_{11} = t_4 \qquad r_{11} = \frac{WRPON^{O}}{V^{O}}$$

$$a_{12,x} = (FNL_x \cdot BM_x^{O} + FNLP \cdot PR_x^{O}) ANC_x \qquad j_{12} = -\, j_{13} - \frac{WS_{LP}^{O}}{\Delta z^{O}}$$

$$t_{12} = t_5 \qquad r_{12} = \frac{WLPON^{O}}{V^{O}}$$

$$a_{13,x} = (FND_x \cdot BM_x^{O} + FNDP \cdot PR_x^{O}) ANC_x \qquad i_{13} = K_{RPON}^{O}$$

$$j_{13} = K_{LPON}^{O} \qquad k_{13} = -\, k_{14}$$

$$r_{13} = \frac{WDON^{O}}{V^{O}}$$

$$a_{14,x} = (FNI_x \cdot BM_x^{O} + FNIP \cdot PR_x^{O} - PN_x^{O} \cdot P_x^{O}) ANC_x \qquad k_{14} = K_{DON}^{O}$$

$$l_{14} = -Nit^{O} \qquad r_{14} = \frac{BFNH4^{O}}{\Delta z^{O}} + \frac{WNH4^{O}}{V^{O}}$$

$$a_{15,x} = -(1 - PN_x^{O}) P_x^{O} \cdot ANC_x \qquad d_{15} = -ANDC \cdot Denit^{O}$$

$$l_{15} = Nit^{O} \qquad r_{15} = \frac{BFNO3^{O}}{\Delta z^{O}} + \frac{WNO3^{O}}{V^{O}}$$

$$a_{16,d} = (FSP_d \cdot BM_d^{O} + FSPP \cdot PR_d^{O}) ASC_d \qquad m_{16} = -m_{17} - \frac{WS_d^{O}}{\Delta z^{O}}$$

$$t_{16} = \frac{(WS_d^{O})_{k+1}}{\Delta z^{O}} \qquad r_{16} = \frac{WSU^{O}}{V^{O}}$$

$$a_{17,d} = (FSI_d \cdot BM_d^{O} + FSIP \cdot PR_d^{O} - P_d^{O}) ASC_d \qquad m_{17} = K_{SUA}^{O}$$

$$n_{17} = -\frac{WS_{TSS}^{O}}{\Delta z^{O}} \frac{K_{SAp} \cdot TSS^{O}}{1 + K_{SAp} \cdot TSS^{O}}$$

$$t_{17} = \frac{(WS_{TSS}^{O})_{k+1}}{\Delta z^{O}} \frac{K_{SAp} \cdot TSS_{k+1}^{O}}{1 + K_{SAp} \cdot TSS_{k+1}^{O}} \qquad r_{17} = \frac{BFSA^{O}}{\Delta z^{O}} + \frac{WSA^{O}}{V^{O}}$$

$$o_{18} = -\frac{DO^{O}}{KH_{COD} + DO^{O}} KCOD^{O}$$

$$r_{18} = \frac{BFCOD^{O}}{\Delta z^{O}} + \frac{WCOD^{O}}{V^{O}}$$

$$a_{19,x} = \left((1.3 - 0.3 \cdot PN_x^{O}) P_x^{O} - (1 - FCD_x) \frac{DO^{O}}{KHR_x + DO^{O}} BM_x^{O} \right) AOCR$$

$$d_{19} = -AOCR \cdot K_{HR}^{O} \qquad l_{19} = -AONT \cdot Nit^{O}$$

$$o_{19} = o_{18} \qquad p_{19} = -K_r^{O}$$

$$r_{19} = K_r^{O} \cdot DO_s^{O} + \frac{SOD^{O}}{\Delta z^{O}} + \frac{WDO^{O}}{V^{O}}$$

$$q_{20} = -\frac{WS_s^{O}}{\Delta z^{O}}$$

$$t_{20} = \frac{(WS_s^{O})_{k+1}}{\Delta z^{O}}$$

$$r_{20} = \frac{KHbmf}{KHbmf + DO^{O}} \frac{BFTAM}{\Delta z^{O}} e^{Ktam(T^{O} - Ttam)} - \frac{(WS_s^{O})_{k+1} \cdot TAMd_{k+1}^{O}}{\Delta z^{O}} + \frac{WS_s^{O} \cdot TAMd^{O}}{\Delta z^{O}} + \frac{WT}{V}$$

$$s_{21} = -KFCB \cdot TFCB^{T^{O} - 20} \qquad r_{21} = \frac{WFCB^{O}}{V^{O}}$$

The diagonal matrix $[K2]_k$ is applied only when $k \neq KC$, as indicated by λ in Eq. 4-82, and so is the second term on the RHS of r_{20}. The sediment-water exchange terms in the matrix $[R]_k$ are applied only when k = 1 (bottom layer), and the terms for dissolved oxygen reaeration in p_{19} and r_{19} are applied only when k = KC (surface layer).

Equation 4-82 is solved using a second-order accurate trapezoidal scheme over a time step of θ (Eq. 4-83). To avoid inversion of a matrix in Eq. 4-83, the kinetic equations are solved in the order of the variables in the matrix [C]. The final forms of Eq. 4-83 for each of the state variables are:

$$B_c^{N} = \left(B_c^{O} + \frac{\theta}{2}\left\{a_{1,c} \cdot B_c^{O} + \lambda \cdot t_{1,c} \cdot (B_c)_{k+1}^{A}\right\} + \theta \cdot r_{1,c}\right)\left(1 - \frac{\theta}{2} a_{1,c}\right)^{-1}$$

$$B_d^{N} = \left(B_d^{O} + \frac{\theta}{2}\left\{a_{2,d} \cdot B_d^{O} + \lambda \cdot t_{2,d} \cdot (B_d)_{k+1}^{A}\right\} + \theta \cdot r_{2,d}\right)\left(1 - \frac{\theta}{2} a_{2,d}\right)^{-1}$$

$$B_g^{N} = \left(B_g^{O} + \frac{\theta}{2}\left\{a_{3,g} \cdot B_g^{O} + \lambda \cdot t_{3,g} \cdot (B_g)_{k+1}^{A}\right\} + \theta \cdot r_{3,g}\right)\left(1 - \frac{\theta}{2} a_{3,g}\right)^{-1}$$

$$RPOC^{N} = \left(RPOC^{O} + \frac{\theta}{2} \cdot TT_{RPOC} + \theta \cdot r_4 \right) \left(1 - \frac{\theta}{2} b_4 \right)^{-1}$$

$$TT_{RPOC} = \sum_{x=c,d,g} a_{4,x} \cdot B_x^{A} + b_4 \cdot RPOC^{O} + \lambda \cdot t_4 \cdot RPOC_{k+1}^{A}$$

$$LPOC^{N} = \left(LPOC^{O} + \frac{\theta}{2} \cdot TT_{LPOC} + \theta \cdot r_5 \right) \left(1 - \frac{\theta}{2} c_5 \right)^{-1}$$

$$TT_{LPOC} = \sum_{x=c,d,g} a_{5,x} \cdot B_x^{A} + c_5 \cdot LPOC^{O} + \lambda \cdot t_5 \cdot LPOC_{k+1}^{A}$$

$$DOC^{N} = \left(DOC^{O} + \frac{\theta}{2} \cdot TT_{DOC} + \theta \cdot r_6 \right) \left(1 - \frac{\theta}{2} d_6 \right)^{-1}$$

$$TT_{DOC} = \sum_{x=c,d,g} a_{6,x} \cdot B_x^{A} + b_6 \cdot RPOC^{A} + c_6 \cdot LPOC^{A} + d_6 \cdot DOC^{O}$$

$$RPOP^{N} = \left(RPOP^{O} + \frac{\theta}{2} \cdot TT_{RPOP} + \theta \cdot r_7 \right) \left(1 - \frac{\theta}{2} e_7 \right)^{-1}$$

$$TT_{RPOP} = \sum_{x=c,d,g} a_{7,x} \cdot B_x^{A} + e_7 \cdot RPOP^{O} + \lambda \cdot t_7 \cdot RPOP_{k+1}^{A}$$

$$LPOP^{N} = \left(LPOP^{O} + \frac{\theta}{2} \cdot TT_{LPOP} + \theta \cdot r_8 \right) \left(1 - \frac{\theta}{2} f_8 \right)^{-1}$$

$$TT_{LPOP} = \sum_{x=c,d,g} a_{8,x} \cdot B_x^{A} + f_8 \cdot LPOP^{O} + \lambda \cdot t_8 \cdot LPOP_{k+1}^{A}$$

$$DOP^{N} = \left(DOP^{O} + \frac{\theta}{2} \cdot TT_{DOP} + \theta \cdot r_9 \right) \left(1 - \frac{\theta}{2} g_9 \right)^{-1}$$

$$TT_{DOP} = \sum_{x=c,d,g} a_{9,x} \cdot B_x^{A} + e_9 \cdot RPOP^{A} + f_9 \cdot LPOC^{A} + g_9 \cdot DOP^{O}$$

$$PO4t^{N} = \left(PO4t^{O} + \frac{\theta}{2} \cdot TT_{PO4t} + \theta \cdot r_{10} \right) \left(1 - \frac{\theta}{2} h_{10} \right)^{-1}$$

$$TT_{PO4t} = \sum_{x=c,d,g} a_{10,x} \cdot B_x^{A} + g_{10} \cdot DOP^{A} + h_{10} \cdot PO4t^{O} + \lambda \cdot t_{10} \cdot PO4t_{k+1}^{A}$$

$$RPON^{N} = \left(RPON^{O} + \frac{\theta}{2} \cdot TT_{RPON} + \theta \cdot r_{11} \right) \left(1 - \frac{\theta}{2} i_{11} \right)^{-1}$$

$$TT_{RPON} = \sum_{x=c,d,g} a_{11,x} \cdot B_x^{A} + i_{11} \cdot RPON^{O} + \lambda \cdot t_{11} \cdot RPON_{k+1}^{A}$$

$$LPON^{N} = \left(LPON^{O} + \frac{\theta}{2} \cdot TT_{LPON} + \theta \cdot r_{12} \right) \left(1 - \frac{\theta}{2} j_{12} \right)^{-1}$$

$$TT_{LPON} = \sum_{x=c,d,g} a_{12,x} \cdot B_x^{A} + j_{12} \cdot LPON^{O} + \lambda \cdot t_{12} \cdot LPON_{k+1}^{A}$$

$$DON^{N} = \left(DON^{O} + \frac{\theta}{2} \cdot TT_{DON} + \theta \cdot r_{13} \right) \left(1 - \frac{\theta}{2} k_{13} \right)^{-1}$$

$$TT_{DON} = \sum_{x=c,d,g} a_{13,x} \cdot B_x^{A} + i_{13} \cdot RPON^{A} + j_{13} \cdot LPON^{A} + k_{13} \cdot DON^{O}$$

$$NH4^{N} = \left(NH4^{O} + \frac{\theta}{2} \left\{ \sum_{x=c,d,g} a_{14,x} \cdot B_x^{A} + k_{14} \cdot DON^{A} + l_{14} \cdot NH4^{O} \right\} + \theta \cdot r_{14} \right) \left(1 - \frac{\theta}{2} l_{14} \right)^{-1}$$

$$NO3^{N} = NO3^{O} + \frac{\theta}{2} \left\{ \sum_{x=c,d,g} a_{15,x} \cdot B_x^{A} + d_{15} \cdot DOC^{A} + l_{15} \cdot NH4^{A} \right\} + \theta \cdot r_{15}$$

$$SU^{N} = \left(SU^{O} + \frac{\theta}{2} \left\{ a_{16,d} \cdot B_d^{A} + m_{16} \cdot SU^{O} + \lambda \cdot t_{16} \cdot SU_{k+1}^{A} \right\} + \theta \cdot r_{16} \right) \left(1 - \frac{\theta}{2} m_{16} \right)^{-1}$$

$$SA^{N} = \left(SA^{O} + \frac{\theta}{2} \left\{ a_{17,d} \cdot B_d^{A} + m_{17} \cdot SU^{A} + n_{17} \cdot SA^{O} + \lambda \cdot t_{17} \cdot SA_{k+1}^{A} \right\} + \theta \cdot r_{17} \right) \left(1 - \frac{\theta}{2} n_{17} \right.$$

$$COD^{N} = \left(COD^{O} + \frac{\theta}{2} \cdot o_{18} \cdot COD^{O} + \theta \cdot r_{18} \right) \left(1 - \frac{\theta}{2} o_{18} \right)^{-1}$$

$$DO^{N} = \left(DO^{O} + \frac{\theta}{2} \cdot TT_{DO} + \theta \cdot r_{19} \right) \left(1 - \frac{\theta}{2} p_{19} \right)^{-1}$$

$$TT_{DO} = \sum_{x=c,d,g} a_{19,x} \cdot B_x^{A} + d_{19} \cdot DOC^{A} + l_{19} \cdot NH4^{A} + o_{19} \cdot COD^{A} + p_{19} \cdot DO^{O}$$

$$TAM^{N} = \left(TAM^{O} + \frac{\theta}{2} \left\{ q_{20} \cdot TAM^{O} + \lambda \cdot t_{20} \cdot TAM_{k+1}^{A} \right\} + \theta \cdot r_{20} \right) \left(1 - \frac{\theta}{2} q_{20} \right)^{-1}$$

$$FCB^{N} = \left(FCB^{O} + \frac{\theta}{2} \cdot s_{21} \cdot FCB^{O} + \theta \cdot r_{21} \right) \left(1 - \frac{\theta}{2} s_{21} \right)^{-1}$$

where $C^{A} = C^{N} + C^{O}$.

Appendix B. Program Organization for Input and Output Files

Program input and output require several data files, each of which is specified in the program by a logical unit number. Tables B-1 and B-2 list the logical unit numbers for water quality and sediment process models, respectively. Since the information of physical transport processes is provided by the hydrodynamic model, the water quality model should be run with the hydrodynamic model. The sediment process model should be run with the water quality model since the water quality model provides the depositional fluxes to the sediment process model. This appendix describes input and output file organization for water quality and sediment process models.

In the source code, twenty-one state variables are identified by assigning a serial number from 1 to 21 in the order of the variables defined in the matrix [C] (Appendix A): cyanobacteria (Bc), diatoms (Bd), green algae (Bg), refractory particulate organic carbon (RPOC), labile particulate organic carbon (LPOC), dissolved organic carbon (DOC), refractory particulate organic phosphorus (RPOP), labile particulate organic phosphorus (LPOP), dissolved organic phosphorus (DOP), total phosphate (PO4t), refractory particulate organic nitrogen (RPON), labile particulate organic nitrogen (LPON), dissolved organic nitrogen (DON), ammonium nitrogen (NH4), nitrate nitrogen (NO3), particulate biogenic silica (SU), available silica (SA), chemical oxygen demand (COD), dissolved oxygen (DO), total active metal (TAM) and fecal coliform bacteria (FCB). The units are g m^{-3} except TAM in mol m^{-3} and FCB in MPN per 100 mL.

The parameters that have been defined in Chapters III and IV are not defined again in this appendix. Instead, the equation number where the corresponding parameters is first appeared and defined is given.

B-1. Input Data Description for Water Quality Model

This section explains line-by-line the input data files for water quality model. Each data group and each line are preceded by text titles for identification purpose. Some of these text titles, which do not affect the model run, are not described, and omitted using FORMAT descriptor slash (/), in this section.

Once the model starts, it opens the unit numbers **8** and **9** (Table B-1). Then, control passes to the subroutine RWQC1, where input parameters are read in from the unit number **8**.

B-1-1. Logical unit **8** (WQ3D-CON.IN)

The unit number **8** contains the program control parameters and constant parameters for rate coefficients, initial conditions, boundary conditions, and files names for spatially and/or temporally varying conditions.

TITLE(M), M=1,3 (A79)

: three-line text to identify a simulation.

TITLE(1) (/, A79)

: one blank line and one-line text to identify the following data group.

IWQDT, IWQM, IWQBEN, IWQSI, IWQFCB, IWQSRP, IWQSTOX (/, 7I8)

: IWQDT = m in Fig. 2-1, i.e., the kinetic equations are solved every $2 \cdot m \cdot \Delta t$ where $2 \cdot \Delta t$ is the time step for advection.

: IWQM = 1 activates the full version water quality model with twenty-one state variables, and IWQM = 2 activates the simplified version with nine state variables (Chapter V). Otherwise an error will be issued and the program be stopped.

: IWQBEN = 1 activates the sediment process model. When IWQBEN = 1, IWQM = 1 activates the full version sediment process model with twenty-seven state variables and IWQM = 2 activates the simplified version with twenty-three state variables (Chapter V). If IWQBEN = 0, spatially and temporally constant benthic fluxes are read in from the unit number **8**. If IWQBEN = 2, the subroutine RWQBEN reads in spatially and/or temporally varying benthic fluxes from the unit **25**. Otherwise an error will be issued and the program be stopped.

: IWQSI = 1 simulates silica state variables, SU and SA. Otherwise no silica simulation.

: IWQFCB = 1 simulates FCB. Otherwise no FCB simulation.

: IWQSRP = 1 if TAM is simulated to account for the sorption of PO4t and SA. If IWQSRP = 2, TAM is not modeled and total suspended sediment (SED), which is provided by the hydrodynamic model, is used to account for the sorption of PO4t and SA: an error will be issued and the program be stopped if IWQSRP =2 and SED is not modeled, i.e., ISTRAN(4) $\neq$ 1.

Otherwise no sorption of PO4t and SA is simulated.

: IWQSTOX = 1 if salinity toxicity is applied to cyanobacteria, i.e., freshwater species (Eq. 3-1b). Otherwise no salinity toxicity to cyanobacteria, i.e., saltwater species.

IWQZ, IWQNC, IWQRST (/, 3I8)

: IWQZ = number of zones for spatially varying water quality parameters. The parameters that may vary spatially are defined in the source code as an array with the dimension of NWQZ. Then, each cell is mapped using an array IWQZMAP(L,K) to designate the zone for that cell (Appendix B-1-2). An error will be issued and the program be stopped if IWQZ > NWQZ.

: IWQNC = 1 opens the unit number **30** and writes the diagnostic information for negative concentration. Otherwise no output to unit **30**.

: IWQRST = 1 opens the unit number **31** and writes the spatial distributions for all state variables at the end of simulation, which may be used as a restart file for the later model run. Otherwise no output to unit **31**.

IWQICI, IWQAGR, IWQSTL, IWQSUN, IWQPSL, IWQNPL (/, 6I8)

: If IWQICI = 1, the subroutine RWQICI reads in spatially and/or temporally varying conditions for water column state variables from the unit number INWQICI (**21**). These conditions may be used to specify a spatial pattern at any time as well as to specify initial conditions. If IWQICI = 2, the subroutine RWQRST reads spatially varying initial conditions from a restart file (unit number INWQRST). Otherwise constant initial conditions are read in from the unit **8**.

: If IWQAGR = 1, the subroutine RWQAGR reads in spatially and/or temporally varying algal growth, respiration and predation rates, and base light extinction coefficient from the unit number **22**. Otherwise constant coefficients are read in from the unit **8**.

: If IWQSTL = 1, the subroutine RWQSTL reads in spatially and/or temporally varying settling velocities for algae, refractory particulate matter, labile particulate matter and particulate metal from the unit number **23**. Otherwise constant coefficients are read in from the unit **8**.

: If IWQSUN = 1, the subroutine RWQSUN reads in temporally varying parameters for light

intensity (daily light intensity and fractional daylength) from the unit number **24**. Otherwise constant inputs are read in from the unit **8**.

: If IWQPSL = 1, the subroutine RWQPSL reads in temporally varying point source discharges and loadings from the unit number **26**. Otherwise constant inputs are read in from the unit **8**.

: If IWQNPL = 1, the subroutine RWQNPL reads in spatially and/or temporally varying nonpoint source discharges and loadings from the unit number **27**. Otherwise constant inputs are read in from the unit **8**.

```
IWQTS, TWQTSB, TWQTSE, WQTSDT  (/, I8, 3F8.4)
TITLE (M), M=1,3  (A79)
DO M=1,IWQTS
   IWQTSI(M), IWQTSJ(M), (ICWQTS(NW,M),NW=1,NTSWQV)  (2I5,13I5,/,10X,8I5)
END DO
```

: IWQTS = number of cells for time-series output. Time-series output is written every TWQTSDT hours, from TWQTSB days till TWQTSE days (after the model start). The present model implementation allows time-series output at maximum of 30 horizontal cells (IWQTS ≤ NWQTS = 30).

: ICWQTS(NW,M) = 1 generates time-series output for the variable NW at all vertical layers in the cell (IWQTSI(M),IWQTSJ(M)). Otherwise no time series output. The present model implementation allows time-series output for 20 (NTSWQV) variables. They are identified by a serial number from 1 to 20: chlorophyll 'a' (CHL), particulate organic carbon (POC), DOC, particulate organic phosphorus (POP), DOP, PO4t, dissolved phosphate (PO4d, Eq. 3-8c), APC (Eq. 3-8e), particulate organic nitrogen (PON), DON, NH4, NO3, SU, SA, dissolved silica (SAd, Eq. 3-15c), COD, DO, TAM, particulate total active metal (TAMp, Eq. 3-18b) and FCB. Some of non-state variables are computed using:

$$CHL = \sum_{x=c,d,g} \frac{B_x}{CChl_x} \qquad POC = RPOC + LPOC$$

$$POP = RPOP + LPOP \qquad PON = RPON + LPON$$

Note that the variables, POC, POP and PON, do not include the portion in the algal biomass, which can be estimated from CHL.

TITLE(1) (/, A79)

: one blank line and one-line text to identify the following data group (algae).

WQKHNC,WQKHND,WQKHNG,WQKHPC,WQKHPD,WQKHPG,WQKHS,WQSTOX (/, 8F8.4)
WQKETSS,WQKECHL,WQCHLC,WQCHLD,WQCHLG,WQDOPC,WQDOPD,WQDOPG (/, 8F8.4)
WQI0,WQISMIN,WQFD,WQCIA,WQCIB,WQCIC (/, 6F8.4)
WQTMC,WQTMD,WQTMG,WQKG1C,WQKG2C,WQKG1D,WQKG2D,WQKG1G,WQKG2G (/, 9F8.4)
WQTRC,WQTRD,WQTRG,WQKTBC,WQKTBD,WQKTBG (/, 6F8.4)

: WQKHNx, WQKHPx = KHN_x and KHP_x, respectively, in Eq. 3-1c.

: WQKHS = KHS in Eq. 3-1d.

: WQSTOX = STOX in Eq. 3-1l, applied to cyanobacteria only when IWQSTOX = 1.

: WQKETSS, WQKECHL = Ke_{TSS} and Ke_{Chl}, respectively, in Eq. 3-1h.

: WQCHLx = $CChl_x$ in Eq. 3-1h.

: WQDOPx = $(D_{opt})_x$ in Eq. 3-1i.

: WQI0 = initial daily light intensity at water surface (langleys day^{-1}).

: WQISMIN = $(I_s)_{min}$ in Eq. 3-1i.

: WQFD = FD in Eq. 3-1e, which is used only when IWQSUN $\neq$ 1.

: WQCIA, WQCIB, WQCIC = CI_a, CI_b and CI_c, respectively, in Eq. 3-1j.

: WQTMx = TM_x in Eq. 3-1k.

: WQKG1x, WQKG2x = $KTG1_x$ and $KTG1_x$, respectively, in Eq. 3-1k.

: WQTRx, WQKTBx = TR_x and KTB_x, respectively, in Eq. 3-1m.

TITLE(1) (/, A79)

: one blank line and one-line text to identify the following data group (carbon).

WQFCRP,WQFCLP,WQFCDP,WQFCDC,WQFCDD,WQFCDG,WQKHRC,WQKHRD,WQKHRG (/, 9F8.4)
WQKRC,WQKLC,WQKDC,WQKRCALG,WQKLCALG,WQKDCALG (/, 6F8.4)
WQTRHDR,WQTRMNL,WQKTHDR,WQKTMNL,WQKHORDO,WQKHDNN,WQAANOX (/, 7F8.4)

: WQFCRP, WQFCLP, WQFCDP = FCRP (Eq. 3-2), FCLP (Eq. 3-3) and FCDP (Eq. 3-4), respectively.

: WQFCDx, WQKHRx = FCD_x and KHR_x, respectively, in Eq. 3-4.

: WQKRC, WQKRCALG = K_{RC} and K_{RCalg}, respectively, in Eq. 3-4h.

: WQKLC, WQKLCALG = K_{LC} and K_{LCalg}, respectively, in Eq. 3-4i.

: WQKDC, WQKDCALG = K_{DC} and K_{DCalg}, respectively, in Eq. 3-4j.

: WQTRHDR, WQKTHDR = TR_{HDR} and KT_{HDR}, respectively, in Eq. 3-4h.

: WQTRMNL, WQKTMNL = TR_{MNL} and KT_{MNL}, respectively, in Eq. 3-4j.

: WQKHORDO = $KHOR_{DO}$ in Eq. 3-4g.

: WQKHDNN, WQAANOX = $KHDN_{N}$ and AANOX, respectively, in Eq. 3-4l.

TITLE(1) (/, A79)

: one blank line and one-line text to identify the following data group (phosphorus).

WQFPRP,WQFPLP,WQFPDP,
WQFPIP,WQFPRC,WQFPRD,WQFPRG,WQFPLC,WQFPLD,WQFPLG (/, 10F8.4)
WQFPDC,WQFPDD,WQFPDG,WQFPIC,WQFPID,WQFPIG,WQKPO4P (/, 7F8.4)
WQKRP,WQKLP,WQKDP,
WQKRPALG,WQKLPALG,WQKDPALG,WQCP1PRM,WQCP2PRM,WQCP3PRM (/, 9F8.4)

: WQFPRP, WQFPLP, WQFPDP, WQFPIP = FPRP (Eq. 3-5), FPLP (Eq. 3-6), FPDP (Eq. 3-7) and FPIP (Eq. 3-8), respectively.

: WQFPRx, WQFPLx, WQFPDx, WQFPIx = FPR_x (Eq. 3-5), FPL_x (Eq. 3-6), FPD_x (Eq. 3-7) and FPI_x (Eq. 3-8), respectively.

: WQKPO4P = coefficient relating PO4t sorption to SED (per g m^{-3}) if IWQSRP = 2 or TAM (per mol m^{-3}) if IWQSRP = 1.

: WQKRP, WQKRPALG = K_{RP} and K_{RPalg}, respectively, in Eq. 3-8f.

: WQKLP, WQKLPALG = K_{LP} and K_{LPalg}, respectively, in Eq. 3-8g.

: WQKDP, WQKDPALG = K_{DP} and K_{DPalg}, respectively, in Eq. 3-8h.

: WQCP1PRM, WQCP2PRM, WQCP3PRM = CP_{prm1}, CP_{prm2} and CP_{prm3}, respectively, in Eq. 3-8e.

TITLE(1) (/, A79)

: one blank line and one-line text to identify the following data group (nitrogen).

WQFNRP,WQFNLP,WQFNDP,
WQFNIP,WQFNRC,WQFNRD,WQFNRG,WQFNLC,WQFNLD,WQFNLG (/, 10F8.4)
WQFNDC,WQFNDD,WQFNDG,WQFNIC,WQFNID,WQFNIG,WQANCC,WQANCD,WQANCG (/, 9F8.4)
WQANDC,WQNITM,WQKHNDO,WQKHNN,WQTNIT,WQKN1,WQKN2 (/, 7F8.4)
WQKRN,WQKLN,WQKDN,WQKRNALG,WQKLNALG,WQKDNALG (/, 6F8.4)

: WQFNRP, WQFNLP, WQFNDP, WQFNIP = FNRP (Eq. 3-9), FNLP (Eq. 3-10), FNDP (Eq. 3-11) and FNIP (Eq. 3-12), respectively.

: WQFNRx, WQFNLx, WQFNDx, WQFNIx = FNR_x (Eq. 3-9), FNL_x (Eq. 3-10), FND_x (Eq. 3-11) and FNI_x (Eq. 3-11), respectively.

: WQANCx, WQANDC = ANC_x (Eq. 3-9) and ANDC (Eq. 3-13), respectively.

: WQNITM = Nit_m in Eq. 3-13g.

: WQKHNDO, WQKHNN = $KHNit_{DO}$ and $KHNit_N$, respectively, in Eq. 3-13g.

: WQTNIT, WQKN1, WQKN2 = TNit, $KNit_1$ and $KNit_2$, respectively, in Eq. 3-13g.

: WQKRN, WQKRNALG = K_{RN} and K_{RNalg}, respectively, in Eq. 3-13b.

: WQKLN, WQKLNALG = K_{LN} and K_{LNalg}, respectively, in Eq. 3-13c.

: WQKDN, WQKDNALG = K_{DN} and K_{DNalg}, respectively, in Eq. 3-13d.

TITLE(1) (/, A79)

: one blank line and one-line text to identify the following data group (silica).

WQFSPP,WQFSIP,WQFSPD,WQFSID,WQASCD,WQKSAP,WQKSU,WQTRSUA,WQKTSUA (/, 9F8.4)

: WQFSPP, WQFSIP = FSPP (Eq. 3-14) and FSIP (Eq. 3-15), respectively.

: WQFSPd, WQFSId = FSP_d (Eq. 3-14) and FSI_d (Eq. 3-15), respectively.

: WQASCD = ASC_d in Eq. 3-14.

: WQKSAP = coefficient relating SA sorption to SED (per g m^{-3}) if IWQSRP = 2 or TAM (per mol m^{-3}) if IWQSRP = 1.

: WQKSU, WQTRSUA, WQKTSUA = K_{SUA}, TR_{SUA} and KT_{SUA}, respectively, in Eq. 3-15d.

TITLE(1) (/, A79)

: one blank line and one-line text to identify the following data group (COD and DO).

WQAOCR,WQAONT,WQKRO,WQKTR,WQKHCOD,WQKCD,WQTRCOD,WQKTCOD (/, 8F8.4)

: WQAOCR, WQAONT = AOCR and AONT, respectively, in Eq. 3-17.

: WQKRO, WQKTR = K_{ro} and KT_r, respectively, in Eq. 3-17e.

: WQKHCOD = KH_{COD} in Eq. 3-16.

: WQKCD, WQTRCOD, WQKTCOD = K_{CD}, TR_{COD} and KT_{COD}, respectively, in Eq. 3-16a.

TITLE(1) (/, A79)

: one blank line and one-line text to identify the following data group (TAM and FCB)

WQKHBMF,WQBFTAM,WQTTAM,WQKTAM,WQTAMDMX,WQKDOTAM,WQKFCB,WQTFCB (/, 8F8.4)

: WQKHBMF, WQBFTAM, WQTTAM, WQKTAM = KHbmf, BFTAM, Ttam and Ktam, respectively, in Eq. 3-18.

: WQTAMDMX, WQKDOTAM = TAMdmx and Kdotam, respectively, in Eq. 3-18b.

: WQKFCB, WQTFCB = KFCB and TFCB, respectively, in Eq. 3-19.

At this point, control passes to the main program and hence to the subroutine RWQC2.

TITLE (/, A79)

: one blank line and one-line text to identify the following data group.

NWQOBS, NWQOBW, NWQOBE, NWQOBN (/, 4I8)

: number of open boundary cells on south, west, east and north boundaries, respectively. These should be the same as the corresponding variables in the hydrodynamic model, i.e., NWQOBS = NCBS, NWQOBW = NCBW, NWQOBE = NCBE and NWQOBN = NCBN. These also should not be larger than the their defined array size: NWQOBS ≤ NBBSM, NWQOBW ≤ NBBWM, NWQOBE ≤ NBBEM and NWQOBN ≤ NBBNM. The variables that do not include "WQ" in their names are defined in the hydrodynamic model.

TITLE (/, A79)

: one blank line and one-line text to identify the following data group (south boundary).

```
IF NWQOBS > 0
   TITLE(M), M=1,3  (A79)
   DO M=1,NWQOBS
      IWQCBS(M),JWQCBS(M),(IWQOBS(M,NW),NW=1,NWQV)  (2I5,13I5,/,10X,8I5)
   END DO
   TITLE(M), M=1,5  (A79)
   DO M=1,NWQOBS
      IWQCBS(M),JWQCBS(M),(WQOBCS(M,1,NW),NW=1,NWQV)
         (2I5,6F8.3,/,10X,7F8.3,/,10X,8F8,3)
   END DO
   TITLE(M), M=1,5  (A79)
   DO M=1,NWQOBS
      IWQCBS(M),JWQCBS(M),(WQOBCS(M,2,NW),NW=1,NWQV)
         (2I5,6F8.3,/,10X,7F8.3,/,10X,8F8.3)
   END DO
END IF
```

: TITLE(M) = text variable to identify the parameters that follow.

: IWQCBS(M), JWQCBS(m) = (i,j) cell index on south open boundary. These should be the

same as the corresponding variables in the hydrodynamic model: IWQCBS = ICBS and JWQCBS = JCBS.

: The subroutine 'XXXX' reads in IWQOBS(M,NW) lines of time-series records at the open boundary cell (IWQCBS(M), JWQCBS(m)) for the state variable NW, and the open boundary conditions are constructed by linear interpolation. If IWQOBS(M,NW) = 0, temporally constant open boundary conditions are constructed using WQOBCS(M,1,NW), WQOBCS(M,2,NW) and NTSCRS.

: WQOBCS(M,1,NW), WQOBCS(M,2,NW) = temporally constant, ultimate inflowing bottom and surface layer, respectively, concentrations

: NTSCRS = number of time steps to recover ultimate concentrations on flow reversal from outflow to inflow.

TITLE (/, A79)

: one blank line and one-line text to identify the following data group (west boundary).

```
IF NWQOBW > 0
   TITLE(M), M=1,3  (A79)
   DO M=1,NWQOBW
      IWQCBW(M),JWQCBW(M),(IWQOBW(M,NW),NW=1,NWQV)  (2I5,13I5,/,10X,8I5)
   END DO
   TITLE(M), M=1,5  (A79)
   DO M=1,NWQOBW
      IWQCBW(M),JWQCBW(M),(WQOBCW(M,1,NW),NW=1,NWQV)
         (2I5,6F8.3,/,10X,7F8.3,/,10X,8F8,3)
   END DO
   TITLE(M), M=1,5  (A79)
   DO M=1,NWQOBW
      IWQCBW(M),JWQCBW(M),(WQOBCW(M,2,NW),NW=1,NWQV)
         (2I5,6F8.3,/,10X,7F8.3,/,10X,8F8.3)
   END DO
END IF
```

: see above for south boundary.

TITLE (/, A79)

: one blank line and one-line text to identify the following data group (east boundary).

```
IF NWQOBE > 0
   TITLE(M), M=1,3  (A79)
   DO M=1,NWQOBE
      IWQCBE(M),JWQCBE(M),(IWQOBE(M,NW),NW=1,NWQV)  (2I5,13I5,/,10X,8I5)
   END DO
```

```
    TITLE(M), M=1,5  (A79)
    DO M=1,NWQOBE
        IWQCBE(M),JWQCBE(M),(WQOBCE(M,1,NW),NW=1,NWQV)
            (2I5,6F8.3,/,10X,7F8.3,/,10X,8F8,3)
    END DO
    TITLE(M), M=1,5  (A79)
    DO M=1,NWQOBE
        IWQCBE(M),JWQCBE(M),(WQOBCE(M,2,NW),NW=1,NWQV)
            (2I5,6F8.3,/,10X,7F8.3,/,10X,8F8.3)
    END DO
END IF
```

: see above for south boundary.

```
TITLE  (/, A79)
```

: one blank line and one-line text to identify the following data group (north boundary).

```
IF NWQOBN > 0
    TITLE(M), M=1,3  (A79)
    DO M=1,NWQOBN
        IWQCBN(M),JWQCBN(M),(IWQOBN(M,NW),NW=1,NWQV)  (2I5,13I5,/,10X,8I5)
    END DO
    TITLE(M), M=1,5  (A79)
    DO M=1,NWQOBN
        IWQCBN(M),JWQCBN(M),(WQOBCN(M,1,NW),NW=1,NWQV)
            (2I5,6F8.3,/,10X,7F8.3,/,10X,8F8,3)
    END DO
    TITLE(M), M=1,5  (A79)
    DO M=1,NWQOBN
        IWQCBN(M),JWQCBN(M),(WQOBCN(M,2,NW),NW=1,NWQV)
            (2I5,6F8.3,/,10X,7F8.3,/,10X,8F8.3)
    END DO
END IF
```

: see above for south boundary.

```
TITLE  (/, A79, ///)
```

: one blank line and four-line text to identify the following data group.

```
WQV(2,1,NW), NW=1,NWQV  (6F8.4, /, 7F8.4, /, 8F8.4)
```

: spatially constant initial conditions for NW = 1 to 21 (NWQV), see the matrix [C] in Appendix A for the definition of variables. The units are g m^{-3} except TAM in mol m^{-3} (NW = 20) and FCB in MPN per 100 mL (NW = 21). These values are used only when IWQICI ≠ 1.

```
TITLE  (/, A79)
```

: one blank line and one-line text to identify the following data group.

WQPMC(1),WQPMD(1),WQPMG(1),WQBMRC(1),
WQBMRD(1),WQBMRG(1),WQPRRC(1),WQPRRD(1),WQPRRG(1),WQKEB(1) (/, 10F8.4)

: spatially and temporally constant WQPMx (PM_x in Eq. 3-1a), WQBMRx (BMR_x in Eq. 3-1m), WQPRRx (PRR_x in Eq. 3-1n), and WQKEB (Ke_b in Eq. 3-1h). These values are used only when IWQAGR ≠ 1.

TITLE (/, A79)

: one blank line and one-line text to identify the following data group.

WQWSC(1),WQWSD(1),WQWSG(1),WQWSRP(1),WQWSLP(1),WQWSS(1) (/, 6F8.4)

: spatially and temporally constant settling velocities (m day^{-1}), WQWSx (WS_x in Eq. 3-1), WQWSRP (WS_{RP} in Eq. 3-2), WQWSLP (WS_{LP} in Eq. 3-3) and WQWSS (WS_s in Eq. 3-18). These values are used only when IWQSTL ≠ 1.

TITLE (/, A79)

: one blank line and one-line text to identify the following data group.

WQBFPO4D(1),WQBFNH4(1),
WQBFNO3(1),WQBFSAD(1),WQBFCOD(1),WQBFO2(1) (/, 6F8.4)

: spatially and temporally constant benthic fluxes (g m^{-2} day^{-1}), WQBFPO4D (BFPO4d in Eq. 3-8), WQBFNH4 (BFNH4 in Eq. 3-12), WQBFNO3 (BFNO3 in Eq. 3-13), WQBFSAD (BFSAd in Eq. 3-15), WQBFCOD (BFCOD in Eq. 3-16) and WQBFO2 (SOD in Eq. 3-17). These values are used only when IWQBEN = 0.

TITLE (/, A79)

: one blank line and one-line text to identify the following data group (spatially and temporally constant point source discharge and loadings). All values under this title are used only when IWQPSL ≠ 1.

IWQPS (/, I8, ///)

: number of cells into which point source input discharges.

DO M=1,IWQPS
I,J,K, XPSQ,(XPSL(NW),NW=1,NWQV) (3I5,1X,7F8.3,/,16X,7F8.3,/,16X,8F8.3)
END DO

: (I,J,K) = cell index for point source input

: XPSQ = point source discharge (m^3 sec^{-1}).

: XPSL(NW) = point source loadings (kg day^{-1}) for the state variables NW = 1 to 18.

: XPSL(19) = DO concentration in point source discharge (g m^{-3}).

: XPSL(20) = point source loading of TAM (kmol day^{-1}).

: XPSL(21) = FCB concentration in point source discharge (MPN per 100 mL).

TITLE (/, A79, ///)

: one blank line and four-line text to identify the following data group.

XDSQ, (XDSL(NW), NW=1,NWQV) (7F8.4, /, 7F8.4, /, 8F8.4)

: spatially and temporally constant nonpoint source discharge and loadings into all cells.

: XDSQ = nonpoint source discharge (m sec^{-1}).

: The definition and unit of XDSL(NW) are the same as those of XPSL(NW).

: These values are used only when IWQNPL ≠ 1.

TITLE (/, A79)

: one blank line and one-line text to identify the following data group.

RSTOFN (44X, A50)

: output file name for the spatial distributions for all water column state variables at the end of simulation, which may be used as a restart file for the later model run. If IWQRST = 1, RSTOFN is opened with the unit number **31**. If IWQRST ≠ 1, then RSTOFN must be 'none', otherwise an error will be issued and the program be stopped.

ICIFN (44X, A50)

: input file name for spatially and/or temporally varying initial conditions for water column state variables. If IWQICI = 1, ICIFN is opened with the unit number **21**. If IWQICI ≠ 1, then ICIFN must be 'none', otherwise an error will be issued and the program be stopped.

AGRFN (44X, A50)

: input file name for spatially and/or temporally varying algal growth, respiration and predation rates, and base light extinction coefficient. If IWQAGR = 1, AGRFN is opened with the unit number **22**. If IWQAGR ≠ 1, then AGRFN must be 'none', otherwise an error will be issued and the program be stopped.

STLFN (44X, A50)

: input file name for spatially and/or temporally varying settling velocities. If IWQSTL = 1,

STLFN is opened with the unit number **23**. If IWQSTL ≠ 1, then STLFN must be 'none', otherwise an error will be issued and the program be stopped.

SUNFN (44X, A50)

: input file name for temporally varying parameters for light intensity and temperature. If IWQSUN = 1, SUNFN is opened with the unit number **24**. If IWQSUN ≠ 1, then SUNFN must be 'none', otherwise an error will be issued and the program be stopped.

BENFN (44X, A50)

: input file name for spatially and/or temporally varying benthic fluxes. If IWQBEN = 2, BENFN is opened with the unit number **25**. If IWQBEN ≠ 2, then BENFN must be 'none', otherwise an error will be issued and the program be stopped.

PSLFN (44X, A50)

: input file name for temporally varying point source discharges and loadings. If IWQPSL = 1, PSLFN is opened with the unit number **26**. If IWQPSL ≠ 1, then PSLFN must be 'none', otherwise an error will be issued and the program be stopped.

NPLFN (44X, A50)

: input file name for spatially and/or temporally varying nonpoint source discharges and loadings. If IWQNPL = 1, NPLFN is opened with the unit number **27**. If IWQNPL ≠ 1, then NPLFN must be 'none', otherwise an error will be issued and the program be stopped.

NCOFN (44X, A50)

: output file name for diagnostic information for negative concentration. If IWQNC = 1, NCOFN is opened with the unit number **30**. If IWQNC ≠ 1, then NCOFN must be 'none', otherwise an error will be issued and the program be stopped.

At this point, the unit number **8** is closed and control passes to the main program and hence to the subroutine RWQMAP.

B-1-2. Logical unit **7** (WQ3D-MAP.IN)

The parameters that may vary spatially are defined in the source code as an array with the dimension of NWQZ. Then, each cell is mapped using an array IWQZMAP(L,K) to designate the zone number for each cell. The subroutine RWQMAP reads in IWQZMAP(L,K) from the unit number **7**. The present model implementation allows maximum 20 zones

(NWQZ = 20).

TITLE(M), M=1,3 (/, 3(A79), //)

: three-line text to describe the unit number **7**.

I, J, K, IWQZX, M=1,IC×JC×KC (4I5)

: IWQZX = IWQZMAP(LIJ(I,J),K) = cell mapping index (from 1 to NWQZ) for spatially varying parameters for the cell (I,J,K). Note that all active water cells should be mapped with IWQZMAP(L,K), otherwise an error will be issued and the program be stopped.

At this point, the unit number **7** is closed and control passes to the main program. If IWQICI = 2, control passes to the subroutine RWQRST.

B-1-3. Logical unit **21** (if IWQICI = 2)

If IWQICI = 2, the subroutine RWQRST reads in spatially varying initial conditions from a restart file.

DO M=1,(LA-1)×KC
L, K, (WQV(L,K,NW), NW=1,NWQV) (2I5, 21E12.4)
END DO

: spatially varying initial conditions for NW = 1 to 21 (NWQV), which are the spatial distributions at the end of previous run. The units are g m^{-3} except TAM in mol m^{-3} (NW = 20) and FCB in MPN per 100 mL (NW = 21).

At this point, the unit number **21** is closed and control passes to the main program. If IWQBEN = 1, control passes to the subroutines SMRIN1, SMRIN2 and RSMMAP. These three subroutines read in input parameters for sediment process model from the unit numbers **11** and **7**, which are described in Appendix B-2. After this point, depending on the values of control parameters, various subroutines read in spatially and/or temporally varying input parameters for water quality variables, which are described in the remaining of this section.

B-1-4. Logical unit **21** (if IWQICI = 1)

If IWQICI = 1, the subroutine RWQICI reads in spatially and/or temporally varying conditions from the unit number **21**.

TITLE(M), M=1,3 (A79)

: three-line text to identify the input file. These lines are read in only once at the first reading, i.e., they are needed only when IWQTICI = 0.

TITLE(1) (/, A79)

: one blank line and one-line text to identify the following data group.

DO M=2,LA
I, J, K, (XWQV(NW),NW=1,NWQV) (3I5, 21E12.4)
END DO

: spatially varying conditions.

IWQTICI, ICICONT (I7, 1X, A3)

: ICICONT = 'END' indicates no more reading from the unit number **21**. Otherwise, the subroutine RWQICI will read temporally varying conditions at IWQTICI days.

B-1-5. Logical unit **22** (if IWQAGR = 1)

If IWQAGR = 1, the subroutine RWQAGR reads in spatially and/or temporally varying parameters for algal growth, base metabolism and predation rates, and base light extinction coefficient from the unit number **22**.

TITLE(M), M=1,3 (A79)

: three-line text to identify the input file. These lines are read in only once at the first reading, i.e., they are needed only when IWQTAGR = 0.

TITLE(1) (/, A79)

: one blank line and one-line text to identify the following data group.

J, WQPMC(I),WQPMD(I),WQPMG(I),WQBMRC(I),WQBMRD(I),
WQBMRG(I),WQPRRC(I),WQPRRD(I),WQPRRG(I),WQKEB(I), I=1,IWQZ (I8, 10F8.3)

: spatially varying parameters for algal dynamics (see Appendix B-1-1 for definition of variables).

IWQTAGR, AGRCONT (I7, 1X, A3)

: AGRCONT = 'END' indicates no more reading from the unit number **22**. Otherwise, the subroutine RWQAGR will read temporally varying parameters at IWQTAGR days.

B-1-6. Logical unit **23** (if IWQSTL = 1)

If IWQSTL = 1, the subroutine RWQSTL reads in spatially and/or temporally varying settling velocities from the unit number **23**.

TITLE(M), M=1,3 (A79)

: three-line text to identify the input file. These lines are read in only once at the first reading, i.e., they are needed only when IWQTSTL = 0.

TITLE(1) (/, A79)

: one blank line and one-line text to identify the following data group.

J, WQWSC(I),WQWSD(I),
WQWSG(I),WQWSRP(I),WQWSLP(I),WQWSS(I), I=1,IWQZ (I8, 6F8.3)

: spatially varying parameters for settling velocities (see Appendix B-1-1 for definition of variables).

IWQTSTL, STLCONT (I7, 1X, A3)

: STLCONT = 'END' indicates no more reading from the unit number **23**. Otherwise, the subroutine RWQSTL will read temporally varying parameters at IWQTSTL days.

B-1-7. Logical unit **24** (if IWQSUN = 1)

If IWQSUN = 1, the subroutine RWQSUN reads in temporally varying parameters for light intensity from the unit number **24**.

TITLE(M), M=1,3 (A79)

: three-line text to identify the input file. These lines are read in only once at the first reading, i.e., they are needed only when IWQTSUN = 0.

TITLE(1) (/, A79)

: one blank line and one-line text to identify the following data group.

WQI0, FD (2F8.3)

: temporally varying parameters (see Appendix B-1-1 for definition of variables).

IWQTSUN, SUNCONT (I7, 1X, A3)

: SUNCONT = 'END' indicates no more reading from the unit number **24**. Otherwise, the subroutine RWQSUN will read temporally varying parameters at IWQTSUN days.

B-1-8. Logical unit **25** (if IWQBEN = 2)

If IWQBEN = 2, the subroutine RWQBEN reads in spatially and/or temporally varying benthic fluxes from the unit number **25**.

TITLE(M), M=1,3 (A79)

: three-line text to identify the input file. These lines are read in only once at the first reading, i.e., they are needed only when IWQTBEN = 0.

TITLE(1) (/, A79)

: one blank line and one-line text to identify the following data group.

J, XBFPO4D(I),XBFNH4(I),
XBFNO3(I),XBFSAD(I),XBFCOD(I),XBFO2(I), I=1,IWQZ (I8, 6F8.3)

: spatially varying benthic fluxes (see Appendix B-1-1 for definition of variables).

IWQTBEN, BENCONT (I7, 1X, A3)

: BENCONT = 'END' indicates no more reading from the unit number **25**. Otherwise, the subroutine RWQBEN will read temporally varying parameters at IWQTBEN days.

B-1-9. Logical unit **26** (if IWQPSL = 1)

If IWQPSL = 1, the subroutine RWQPSL reads in temporally varying point source discharges and loadings from the unit number **26**.

TITLE(M), M=1,3 (A79)

: three-line text to identify the input file.

IWQPS (/, I5)

: number of cells into which point source input discharges.

The above three-line text and one integer variable are read in only once at the first reading, i.e., they are needed only when IWQTPSL = 0.

TITLE(1) (/, A79)

: one blank line and one-line text to identify the following data group.

```
DO M=1,IWQPS
   I, J, K, WQPSQ(M),(WQWPSL(M,NW),NW=1,NWQV)
        (3I5,1X,7F8.3,/,16X,7F8.3,/,16X,8F8.3)
END DO
```

: temporally varying point source discharges and loadings (see Appendix B-1-1 for

definition of variables).

IWQTPSL, PSLCONT (I7, 1X, A3)

: PSLCONT = 'END' indicates no more reading from the unit number **26**. Otherwise, the subroutine RWQPSL will read temporally varying parameters at IWQTPSL days.

B-1-10. Logical unit **27** (if IWQNPL = 1) XXXXX

If IWQNPL = 1, the subroutine RWQNPL reads in spatially and/or temporally varying nonpoint source discharges and loadings from the unit number **27**.

TITLE(M), M=1,3 (A79)

: three-line text to identify the input file. These lines are read in only once at the first reading, i.e., they are needed only when IWQTNPL = 0.

TITLE (/, A79)

: one blank line and one-line text to identify the following data group.

```
DO L=2,LA
   I, J, WQDSQ(M),(WQWNPL(M,NW),NW=1,NWQV)
      (3I5,1X,7F8.3,/,16X,7F8.3,/,16X,8F8.3)
END DO
```

: spatially and temporally varying nonpoint source discharge and loadings (see Appendix B-1-1 for definition of variables).

IWQTNPL, NPLCONT (I7, 1X, A3)

: NPLCONT = 'END' indicates no more reading from the unit number **27**. Otherwise, the subroutine RWQNPL will read temporally varying parameters at IWQTNPL days.

B-2. Input Data Description for Sediment Process Model

As explained at the end of Appendix B-1-3, if IWQBEN = 1, three subroutines SMRIN1, SMRIN2 and RSMMAP read in input parameters for sediment process model from the unit numbers **11** and **7** (Table B-2). This section explains line-by-line the input data files for sediment process model. Each data group and each line are proceeded by text titles for identification purpose. Some of these text titles, which do not affect the model run, are not described, and omitted using FORMAT descriptor slash (/), in this section.

B-2-1. Logical unit **11** (WQ3D-SM.IN)

TITLE(M), M=1,3 (A79)

: three-line text to identify a simulation of sediment process model.

TITLE(1) (/, A79)

: one blank line and one-line text to identify the following data group.

ISMZ, ISMICI, ISMRST, ISMHYST, ISMZB (/, 5I8)

: ISMZ = number of zones for spatially varying sediment parameters. The parameters that may vary spatially are defined in the source code as an array with the dimension of NSMZ. Then, each sediment cell is mapped using an array ISMZMAP(L) to designate the zone for that cell (Appendix B-2-2). An error will be issued and the program be stopped if ISMZ > NSMZ.

: If ISMICI = 1, the subroutine RWQICI reads in spatially and/or temporally varying conditions for sediment state variables from the unit number INSMICI (**40**). These conditions may be used to specify a spatial pattern at any time as well as to specify initial conditions. If ISMICI = 2, the subroutine RSMRST reads spatially varying initial conditions from a restart file (unit number INSMRST). Otherwise constant initial conditions are read in from the unit **11**.

: ISMRST = 1 opens the unit number **45** and writes the spatial distributions for all sediment state variables at the end of simulation, which may be used as a restart file for the later model run. Otherwise no output to unit **45**.

: ISMHYST = 1 activates the hysteresis in benthic mixing described in Section IV-3-1B. Otherwise, no hysteresis in benthic mixing due to low oxygen conditions.

: ISZB = 1 opens the unit number **46** and writes the diagnostic information for the function ZBRENT. Two kinds of error message will be recorded in the unit **46**, 1) when the function ZBRENT exceeds the specified maximum iteration and still cannot converge and 2) the root is not bracketed for the function ZBRENT. If ISZB ≠ 1, no output to unit **46**.

ISMTS, TSMTSB, TSMTSE, SMTSDT (/, I8, 3F8.4)
TITLE (1) (A79)
DO M=1,ISMTS
ISMTSI(M), ISMTSJ(M), (ICSMTS(NW,M),NW=1,NTSSMV) (2I8, 3I8)
END DO

: ISMTS = number of cells for sediment time-series output. Time-series output is written every TSMTSDT hours, from TSMTSB days till TSMTSE days (after the model start). The

present model implementation allows time-series output at maximum of 30 horizontal cells (ISMTS $\leq$ NSMTS = 30).

: ICSMTS(NW,M) = 1 generates time-series output for the sediment variable NW at the horizontal cell (ISMTSI(M),ISMTSJ(M)). Otherwise no time series output. The present model implementation allows time-series output for 3 (NTSSMV) groups of sediment variables. They are identified by a serial number from 1 to 3: particulate organic matter (POM), inorganic matter (IM) and benthic fluxes (BF). The group POM includes 10 state variables, (1) to (10) in Chapter IV. The group IM includes 10 variables, (11) to (20) in Chapter IV. The group BF includes 7 variables, (21) to (27) in Chapter IV.

DifT (/, F8.3)

: D_T in Eq. 4-40.

TITLE(1) (/, A79)

: one blank line and one-line text to identify the following data group.

SMFNBC(1),SMFNBC(2),SMFNBC(3),
SMFNBD(1),SMFNBD(2),SMFNBD(3),SMFNBG(1),SMFNBG(2),SMFNBG(3) (/, 9F8.3)
SMFPBC(1),SMFPBC(2),SMFPBC(3),
SMFPBD(1),SMFPBD(2),SMFPBD(3),SMFPBG(1),SMFPBG(2),SMFPBG(3) (/, 9F8.3)
SMFCBC(1),SMFCBC(2),SMFCBC(3),
SMFCBD(1),SMFCBD(2),SMFCBD(3),SMFCBG(1),SMFCBG(2),SMFCBG(3) (/, 9F8.3)

: SMFNBx(I), SMFPBx(I), SMFCBx(I) = $FNB_{x,i}$ (Eq. 4-2), $FNB_{x,i}$ (Eq. 4-3) and $FNB_{x,i}$ (Eq. 4-4), respectively.

TITLE(1) (/, A79)

: one blank line and one-line text to identify the following data group.

SMKPON(1),SMKPON(2),SMKPON(3),
SMKPOP(1),SMKPOP(2),SMKPOP(3),SMKPOC(1),SMKPOC(2),SMKPOC(3) (/, 9F8.3)
SMTHKN(1),SMTHKN(2),SMTHKN(3),
SMTHKP(1),SMTHKP(2),SMTHKP(3),SMTHKC(1),SMTHKC(2),SMTHKC(3) (/, 9F8.3)

: SMKPON(I), SMKPOP(I), SMKPOC(I) = $K_{PON,i}$, $K_{POP,i}$ and $K_{POC,i}$, respectively, in Eq. 4-6.

: SMTHKN(I), SMTHKP(I), SMTHKC(I) = $\theta_{PON,i}$, $\theta_{PON,i}$ and $\theta_{PON,i}$, respectively, in Eq. 4-6.

TITLE(1) (/, A79)

: one blank line and one-line text to identify the following data group.

SMM1,SMM2,SMTHDD,SMTHDP,SMPOCR,SMKMDP,SMKBST,XSMDPMIN,SMRBIBT (/, 9F8.3)
SMO2BS,SMTDMBS,SMTCMBS (/, 3F8.3)

: SMM1, SMM2 = m_1 and m_2, respectively, in Eq. 4-11.

: SMTHDD, SMTHDP = θ_{Dd} (Eq. 4-16) and θ_{Dp} (Eq. 4-13), respectively.

: SMPOCR, SMKMDp = $G_{POC,R}$ and KM_{Dp}, respectively, in Eq. 4-13.

: SMKBST, SMDPMIN, SMRBIBT = K_{ST} (Eq. 4-14), Dp_{min} (Eq. 4-15) and $R_{BI,BT}$ (Eq. 4-16), respectively.

: SMO2BS, SMTDMBS, SMTCMBS = $DO_{ST,c}$, t_{MBS} and $NC_{hypoxia}$, respectively, in Section IV-3-1B.

TITLE(1) (/, A79)

: one blank line and one-line text to identify the following data group.

SMP1NH4,SMP2NH4,SMKMNH4,SMKMO2N,SMTHNH4,SMTHNO3,SMP2PO4,SMCO2PO4
(/,8F8.3)

: P1NH4, P2NH4 = $\pi_{1,NH4}$ and $\pi_{2,NH4}$, respectively, in Section IV-3-2.

: SMKMNH4, SMKMO2N, SMTHNH4 = KM_{NH4}, $KM_{NH4,O2}$ and θ_{NH4}, respectively, in Eq. 4-18.

: SMTHNO3 = θ_{NO3} in Eq. 4-22.

: SMP2PO4, SMCO2PO4 = $\pi_{2,PO4}$ and $(DO_0)_{crit,PO4}$, respectively, in Eq. 4-25.

TITLE(1) (/, A79)

: one blank line and one-line text to identify the following data group.

SMP1H2S,SMP2H2S,SMKD1HS,
SMKP1HS,SMTHH2S,SMKMH2S,SMKCH4,SMTHCH4,SMCSHSCH (/, 9F8.3)
SMO2C,SMO2NO3,SMO2NH4 (/, 3F8.3)

: P1H2S, P2H2S = $\pi_{1,H2S}$ and $\pi_{2,H2S}$, respectively, in Section IV-3-5.

: SMKD1HS, SMKP1HS = $\kappa_{H2S,d1}$ and $\kappa_{H2S,p1}$, respectively, in Eq. 4-28-1.

: SMTHH2S, SMKMH2S = θ_{H2S} and $KM_{H2S,O2}$, respectively, in Eq. 4-28-1.

: SMKCH4, SMTHCH4 = κ_{CH4} and θ_{CH4}, respectively, in Eq. 4-33.

: SMCSHSCH = critical salinity (ppt) to divide sulfide and methane oxidation (Section IV-3-5B).

: SMO2C, aO2NO3 = $a_{O2,C}$ and $a_{O2,NO3}$, respectively, in Eq. 4-27.

: SMO2NH4 = $a_{O2,NH4}$ in Eq. 4-29.

TITLE(1) (/, A79)

: one blank line and one-line text to identify the following data group.

SMKSI,SMTHSI,SMKMPSI,SMSISAT,SMP2SI,SMDP1SI,SMCO2SI,SMJDSI (/, 8F8.3)

: SMKSI, SMTHSI = K_{Si} and θ_{Si}, respectively, in Eq. 4-36.

: SMKMPSI, SMSISAT = KM_{PSi} and Si_{sat}, respectively, in Eq. 4-36.

: SMP2SI, SMDP1SI, SMCO2SI = $\pi_{2,Si}$, $\Delta\pi_{Si,1}$ and $(DO_0)_{crit,Si}$, respectively, in Eq. 4-39.

: SMJDSI = $J_{D,Si}$ in Eq. 4-35.

At this point, control passes to the main program and hence to the subroutine SMRIN2.

TITLE(M), M=1,2 (/, 2(A79))

: one blank line and two-line text to identify the following data group.

SMPON(1,1),SMPON(1,2),SMPON(1,3),SMPOP(1,1),
SMPOP(1,2),SMPOP(1,3),SMPOC(1,1),SMPOC(1,2),SMPOC(1,3) (9F8.4)

: spatially constant initial conditions for particulate organic matter (g m^{-3}).

: SMPOM(1,i) = i^{th} G class (i = 1, 2, 3) particulate organic matter (M = N, P or C).

TITLE(1) (A79)

: one-line text to identify the following data group.

SM1NH4(1),SM2NH4(1),SM2NO3(1),
SM2PO4(1),SM2H2S(1),SMPSI(1),SM2SI(1),SMBST(1),SMT(1) (9F8.4)

: spatially constant initial conditions for inorganic matter and silica (g m^{-3}).

: SM1NH4(1), SM2NH4(1) = ammonium concentrations in sediment Layers 1 and 2, respectively.

: SM2NO3(1), SM2PO4(1), SM2H2S(1) = nitrate, phosphate and hydrogen sulfide (methane in freshwater, see Section IV-3-5) concentrations, respectively, in sediment Layer 2.

: SMPSI(1), SM2SI(1) = particulate biogenic silica and available silica concentrations, respectively, in sediment Layer 2.

: SMBST(1) = accumulated benthic stress (day), see Eq. 4-14.

: SMT(1) = sediment temperature (°C).

Note that the solution of the mass-balance equation for Layer 1, because of the steady-state assumption made for this layer, does not require the Layer 1 variables at an old time step, and thus the initial conditions for Layer 1. The only exception is SM1NH4(1), which is used to

calculate nitrification in Layer 1.

TITLE(M), M=1,2 (/, 2(A79))

: one blank line and two-line text to identify the following data group (spatially varying parameters, grouped as ISMZ number of zones).

J, SMHSED(I),SMW2(I),SMDD(I),SMDP(I), SMKNH4(I),SMK1NO3(I),SMK2NO3(I),SMDP1PO4(I), I=1,ISMZ (I8, 8F8.4)

: SMHSED(I) = $H \approx H_2$ in Eq. 4-1.

: SMW2(I) = W in Eq. 4-6.

: SMDD(I), SMDP(I) = D_d (Eq. 4-16) and D_p (Eq. 4-13), respectively.

: SMKNH4(I) = κ_{NH4} in Eq. 4-18.

: SMK1NO3(I), SMK2NO3(I) = $\kappa_{NO3,1}$ and $\kappa_{NO3,2}$, respectively, in Eq. 4-22.

: SMDP1PO4(I) = $\Delta\pi_{PO4,1}$ in Eq. 4-25.

TITLE(M), M=1,2 (/, 2(A79))

: one blank line and two-line text to identify the following data group (spatially varying parameters, grouped as ISMZ number of zones).

J, SMFNR(N,1),SMFNR(N,2),SMFNR(N,3),SMFPR(N,1),SMFPR(N,2), SMFPR(N,3),SMFCR(N,1),SMFCR(N,2),SMFCR(N,3), N=1,ISMZ (I8, 9F8.4)

: SMFNR(N,i), SMFPR(N,i), SMFCR(N,i) = $FNRP_i$, $FPRP_i$ and $FCRP_i$, respectively, in the N^{th} zone (Equations 4-2 to 4-4).

Note that 100% of water column labile POM is routed to the 1st G class in sediment.

At this point, the unit number **11** is closed and control passes to the main program and hence to the subroutine RSMMAP.

B-2-2. Logical unit **7** (SM-MAP.IN)

As in the water column water quality mode, the sediment parameters that may vary spatially are defined in the source code as an array with the dimension of NSMZ. Then, each sediment cell is mapped using an array ISMZMAP(L) to designate the zone number for each cell. The subroutine RSMMAP reads in ISMZMAP(L) from the unit number **7**. The present model implementation allows maximum 20 zones (NSMZ = 20).

TITLE(M), M=1,3 (/, 3(A79), //)

: three-line text to describe the unit number **7**.

I, J, ISMZX, M=1,IC×JC (3I5)

: ISMZX = ISMZMAP(LIJ(I,J)) = cell mapping index (from 1 to NSMZ) for spatially varying sediment parameters for the cell (I,J). Note that all active sediment cells should be mapped with ISMZMAP(L), otherwise an error will be issued and the program be stopped.

At this point, the unit number **7** is closed and control passes to the main program. If ISMICI = 2, control passes to the subroutine RSMRST.

B-2-3. Logical unit **40** (if ISMICI = 2)

If ISMICI = 2, the subroutine RSMRST reads in spatially varying initial conditions for sediment variables from a restart file.

```
DO M=2,LA
  L, (SMPON(L,NW),NW=1,NSMG),(SMPOP(L,NW),NW=1,NSMG),
     (SMPOC(L,NW),NW=1,NSMG),SM1NH4(L),SM2NH4(L),SM2NO3(L),
     SM2PO4(L),SM2H2S(L),SMPSI(L),SM2SI(L),SMBST(L),SMT(L)  (I5, 18E12.4)
END DO
```

: spatially varying initial conditions, which are the spatial distributions at the end of previous run. The units are g m^{-3}.

At this point, the unit number **40** is closed and control passes to the main program. After this point, if ISMICI = 1, control passes to the subroutine RSMICI.

B-2-4. Logical unit **40** (if ISMICI = 1)

If ISMICI = 1, the subroutine RSMICI reads in spatially and/or temporally varying conditions for sediment variables from the unit number **40**.

TITLE(M), M=1,3 (A79)

: three-line text to identify the input file. These lines are read in only once at the first reading, i.e., they are needed only when ISMTICI = 0.

TITLE(1) (/, A79)

: one blank line and one-line text to identify the following data group.

```
DO M=2,LA
   I,J, (XSMPON(NW),NW=1,NSMG),(XSMPOP(NW),NW=1,NSMG),
        (XSMPOC(NW),NW=1,NSMG),XSM1NH4,XSM2NH4,XSM2NO3,
        XSM2PO4,XSM2H2S,XSMPSI,XSM2SI,XSMBST,XSMT  (I5, 18E12.4)
END DO
```

: spatially varying conditions.

ISMTICI, ICICONT (I7, 1X, A3)

: ICICONT = 'END' indicates no more reading from the unit number **40**. Otherwise, the subroutine RSMICI will read temporally varying conditions at ISMTICI days.

Table B-1. Data file organization for water quality model[*].

UNIT NO	READ or WRITE	EXAMPLE	DESCRIPTION
8	read	WQ3D-CON.IN[a]	program control parameters, constant coefficients, and time-varying input and output file names
9	read	WQ3D.OUT[a]	general model output listing read-in parameters
7	read	WQ3D-MAP.IN[a]	mapping information for all active water cells for spatially varying parameters
21	read	WQ3D-ICI.IN[b]	spatially/temporally varying conditions
21	read	WQ3D-RST.IN[b]	spatially varying initial conditions (restart file)
22	read	WQ3D-AGR.IN[b]	spatially and/or temporally varying coefficients for algal dynamics
23	read	WQ3D-STL.IN[b]	spatially and/or temporally varying settling velocities
24	read	WQ3D-SUN.IN[b]	temporally varying coefficients for light intensity
25	read	WQ3D-BEN.IN[b]	spatially and/or temporally varying benthic fluxes
26	read	WQ3D-PSL.IN[b]	temporally varying point source inputs
27	read	WQ3D-NPL.IN[b]	spatially and/or temporally varying nonpoint source inputs
30	write	WQ3D-NC.LOG[b]	diagnostic output for negative concentrations
31	write	WQ3D-RST.OUT[b]	spatial distributions at the end model run (restart file)

[*] Time-series output for water quality variables is generated using a generic subroutine in the hydrodynamic model.

[a] These file names are fixed in the source code.

[b] Optional units depending on control parameters.

Table B-2. Data file organization for sediment process model[*,a].

UNIT NO	READ or WRITE	EXAMPLE	DESCRIPTION
11	read	WQ3D-SM.IN[b]	input coefficients for sediment process model
7	read	SM-MAP.IN[b,c]	mapping information for all active sediment cells for spatially varying parameters
40	read	SM-ICI.IN[b,c]	spatially/temporally varying conditions
40	read	SM-RST.IN[b,c]	spatially varying initial conditions (restart file)
45	write	SM-RST.OUT[b,c]	spatial distributions at the end model run (restart file)
46	write	ZBRENT.LOG[b,c]	diagnostic output for function ZBRENT

[*] Time-series output for sediment variables is generated using a generic subroutine in the hydrodynamic model.

[a] All input and output units for sediment process model are optional.

[b] These files are not optional once the sediment process model is activated.

[c] These file names are fixed in the source code.

Water Quality Model Parameters (listed in order of appearance)

B_x = algal biomass of algal group x (g C m^{-3})

t = time (day)

P_x = production rate of algal group x (day^{-1})

BM_x = basal metabolism rate of algal group x (day^{-1})

PR_x = predation rate of algal group x (day^{-1})

WS_x = settling velocity of algal group x (m day^{-1})

WB_x = external loads of algal group x (g C day^{-1})

V = cell volume (m^3).

PM_x = maximum growth rate under optimal conditions for algal group x (day^{-1})

$f_1(N)$ = effect of suboptimal nutrient concentration ($0 \le f_1 \le 1$)

$f_2(I)$ = effect of suboptimal light intensity ($0 \le f_2 \le 1$)

$f_3(T)$ = effect of suboptimal temperature ($0 \le f_3 \le 1$).

$f_4(S)$ = effect of salinity on cyanobacteria growth ($0 \le f_4 \le 1$)

NH4 = ammonium nitrogen concentration (g N m^{-3})

NO3 = nitrate nitrogen concentration (g N m^{-3})

KHN_x = half-saturation constant for nitrogen uptake for algal group x (g N m^{-3})

PO4d = dissolved phosphate phosphorus concentration (g P m^{-3})

KHP_x = half-saturation constant for phosphorus uptake for algal group x (g P m^{-3}).

SAd = concentration of dissolved available silica (g Si m^{-3})

KHS = half-saturation constant for silica uptake for diatoms (g Si m^{-3}).

FD = fractional daylength ($0 \le FD \le 1$)

Kess = total light extinction coefficient (m^{-1})

Δz = layer thickness (m)

I_o = daily total light intensity at water surface (langleys day^{-1})

$(I_s)_x$ = optimal light intensity for algal group x (langleys day^{-1})

H_T = depth from the free surface to the top of the layer (m).

Ke_b = background light extinction (m^{-1})

Ke_{TSS} = light extinction coefficient for total suspended solid (m^{-1} per g m^{-3})

TSS = total suspended solid concentration (g m^{-3}) provided from the hydrodynamic model

Ke_{Chl} = light extinction coefficient for chlorophyll 'a' (m^{-1} per mg Chl m^{-3})

$CChl_x$ = carbon-to-chlorophyll ratio in algal group x (g C per mg Chl).

$(D_{opt})_x$ = depth of maximum algal growth for algal group x (m)

$(I_o)_{avg}$ = adjusted surface light intensity (langleys day^{-1}).

I_1 = daily light intensity one day preceding model day (langleys day^{-1})

I_2 = daily light intensity two days preceding model day (langleys day^{-1})

T = temperature (°C) provided from the hydrodynamic model

TM_x = optimal temperature for algal growth for algal group x (°C)

$KTG1_x$ = effect of temperature below TM_x on growth for algal group x ($°C^{-2}$)

$KTG2_x$ = effect of temperature above TM_x on growth for algal group x ($°C^{-2}$).

STOX = salinity at which Microcystis growth is halved (ppt)

S = salinity in water column (ppt) provided from the hydrodynamic model.

BMR_x = basal metabolism rate at TR_x for algal group x (day^{-1})

KTB_x = effect of temperature on metabolism for algal group x ($°C^{-1}$)

TR_x = reference temperature for basal metabolism for algal group x (°C).

PRR_x = predation rate at TR_x for algal group x (day^{-1}).

RPOC = concentration of refractory particulate organic carbon (g C m^{-3})

LPOC = concentration of labile particulate organic carbon (g C m^{-3})

FCRP = fraction of predated carbon produced as refractory particulate organic carbon

FCLP = fraction of predated carbon produced as labile particulate organic carbon

K_{RPOC} = dissolution rate of refractory particulate organic carbon (day^{-1})

K_{LPOC} = dissolution rate of labile particulate organic carbon (day^{-1})

WS_{RP} = settling velocity of refractory particulate organic matter (m day^{-1})

WS_{LP} = settling velocity of labile particulate organic matter (m day^{-1})

WRPOC = external loads of refractory particulate organic carbon (g C day^{-1})

WLPOC = external loads of labile particulate organic carbon (g C day^{-1}).

DOC = concentration of dissolved organic carbon (g C m^{-3})

FCD_x = fraction of basal metabolism exuded as dissolved organic carbon at infinite dissolved oxygen (group x)

KHR_x = half-saturation constant of dissolved oxygen for algal DOC excretion for group x (g O_2 m^{-3})

DO = dissolved oxygen concentration (g O_2 m^{-3})

FCDP = fraction of predated carbon produced as dissolved organic carbon

K_{HR} = heterotrophic respiration rate of dissolved organic carbon (day^{-1})

Denit = denitrification rate (day^{-1}) given in Eq. 4-34

WDOC = external loads of dissolved organic carbon (g C day^{-1}).

K_{RC} = minimum dissolution rate of refractory particulate organic carbon (day^{-1})

K_{LC} = minimum dissolution rate of labile particulate organic carbon (day^{-1})

K_{DC} = minimum respiration rate of dissolved organic carbon (day^{-1})

K_{RCalg} =constants related dissolution of refractory POC to algal biomass (day^{-1} per g C m^{-3})

K_{LCalg} =constants related dissolution of labile POC, to algal biomass (day^{-1} per g C m^{-3})

K_{DCalg} = constant that relates respiration to algal biomass (day^{-1} per g C m^{-3})

KT_{HDR} = effect of temperature on hydrolysis of particulate organic matter ($°C^{-1}$)

TR_{HDR} = reference temperature for hydrolysis of particulate organic matter (°C)

KT_{MNL} = effect of temperature on mineralization of dissolved organic matter ($°C^{-1}$)

TR_{MNL} = reference temperature for mineralization of dissolved organic matter (°C)

$KHDN_N$ = denitrification half-saturation constant for nitrate (g N m^{-3})

AANOX = ratio of denitrification rate to oxic dissolved organic carbon respiration rate

RPOP = concentration of refractory particulate organic phosphorus (g P m^{-3})

LPOP = concentration of labile particulate organic phosphorus (g P m^{-3})

FPR_x = fraction of metabolized phosphorus by algal group x produced as refractory POP.

FPL_x = fraction of metabolized phosphorus by algal group x produced as labile POP.

FPRP = fraction of predated phosphorus produced as refractory particulate organic phosphorus

FPLP = fraction of predated phosphorus produced as labile particulate organic phosphorus

APC = mean phosphorus-to-carbon ratio in all algal groups (g P per g C)

K_{RPOP} = hydrolysis rate of refractory particulate organic phosphorus (day^{-1})

K_{LPOP} = hydrolysis rate of labile particulate organic phosphorus (day-1)

WRPOP = external loads of refractory particulate organic phosphorus (g P day^{-1})

WLPOP = external loads of labile particulate organic phosphorus (g P day^{-1})

DOP = concentration of dissolved organic phosphorus (g P m^{-3})

FPD_x = fraction of metabolized phosphorus by algal group x produced as dissolved organic phosphorus

FPDP = fraction of predated phosphorus produced as dissolved organic phosphorus

K_{DOP} = mineralization rate of dissolved organic phosphorus (day^{-1})

WDOP = external loads of dissolved organic phosphorus (g P day^{-1})

PO4t = total phosphate (g P m^{-3}) = PO4d + PO4p

PO4d = dissolved phosphate (g P m^{-3})

PO4p = particulate (sorbed) phosphate (g P m^{-3})

FPI_x = fraction of metabolized phosphorus by algal group x produced as inorganic phosphorus

FPIP = fraction of predated phosphorus produced as inorganic phosphorus

WS_{TSS} = settling velocity of suspended solid (m day^{-1}), provided by the hydrodynamic model

BFPO4d = sediment-water exchange flux of phosphate (g P m^{-2} day^{-1}), applied to the bottom layer only

WPO4t = external loads of total phosphate (g P day^{-1})

CP_{prm1} = minimum carbon-to-phosphorus ratio (g C per g P)

CP_{prm2} = difference between minimum and maximum carbon-to-phosphorus ratio (g C per g P)

CP_{prm3} = effect of dissolved phosphate concentration on carbon-to-phosphorus ratio (per g P m^{-3})

K_{RP} = minimum hydrolysis rate of refractory particulate organic phosphorus (day^{-1})

K_{LP} = minimum hydrolysis rate of labile particulate organic phosphorus (day^{-1})

K_{DP} = minimum mineralization rate of dissolved organic phosphorus (day^{-1})

K_{RPalg} = constants that relate hydrolysis of refractory POP to algal biomass (day^{-1} per g C m^{-3})

K_{LPalg} = constants that relate hydrolysis of labile POP to algal biomass (day^{-1} per g C m^{-3})

K_{DPalg} = constant that relates mineralization to algal biomass (day^{-1} per g C m^{-3})

KHP = mean half-saturation constant for algal phosphorus uptake (g P m^{-3})

RPON = concentration of refractory particulate organic nitrogen (g N m^{-3})

LPON = concentration of labile particulate organic nitrogen (g N m^{-3})

FNR_x = fraction of metabolized nitrogen by algal group x produced as refractory particulate organic nitrogen

FNL_x = fraction of metabolized nitrogen by algal group x produced as labile particulate organic nitrogen

FNRP = fraction of predated nitrogen produced as refractory particulate organic nitrogen

FNLP = fraction of predated nitrogen produced as labile particulate organic nitrogen

ANC_x = nitrogen-to-carbon ratio in algal group x (g N per g C)

K_{RPON} = hydrolysis rate of refractory particulate organic nitrogen (day^{-1})

K_{LPON} = hydrolysis rate of labile particulate organic nitrogen (day^{-1})

WRPON = external loads of refractory particulate organic nitrogen (g N day^{-1})

WLPON = external loads of labile particulate organic nitrogen (g N day^{-1})

DON = concentration of dissolved organic nitrogen (g N m^{-3})

FND_x = fraction of metabolized nitrogen by algal group x produced as dissolved organic nitrogen

FNDP = fraction of predated nitrogen produced as dissolved organic nitrogen

K_{DON} = mineralization rate of dissolved organic nitrogen (day^{-1})

WDON = external loads of dissolved organic nitrogen (g N day^{-1})

FNI_x = fraction of metabolized nitrogen by algal group x produced as inorganic nitrogen

FNIP = fraction of predated nitrogen produced as inorganic nitrogen

PN_x = preference for ammonium uptake by algal group x ($0 \le PN_x \le 1$)

Nit = nitrification rate (day^{-1}) given in Eq. 4-59

BFNH4 = sediment-water exchange flux of ammonium (g N m^{-2} day^{-1}), applied to the bottom layer only.

WNH4 = external loads of ammonium (g N day^{-1})

ANDC = mass of nitrate nitrogen reduced per mass of DOC oxidized (0.933 g N per g C from Eq. 4-33)

BFNO3 = sediment-water exchange flux of nitrate (g N m^{-2} day^{-1}), applied to the bottom layer only

WNO3 = external loads of nitrate (g N day^{-1})

K_{RN} = minimum hydrolysis rate of refractory particulate organic nitrogen (day^{-1})

K_{LN} = minimum hydrolysis rate of labile particulate organic nitrogen (day^{-1})

K_{DN} = minimum mineralization rate of dissolved organic nitrogen (day^{-1})

K_{RNalg} = constants that relate hydrolysis of refractory PON to algal biomass (day^{-1} per g C m^{-3})

K_{LNalg} = constants that relate hydrolysis of labile PON to algal biomass (day^{-1} per g C m^{-3})

K_{DNalg} = constant that relates mineralization to algal biomass (day^{-1} per g C m^{-3})

KHN = mean half-saturation constant for algal nitrogen uptake (g N m^{-3})

$KHNit_{DO}$ = nitrification half-saturation constant for dissolved oxygen (g O_2 m^{-3})

$KHNit_N$ = nitrification half-saturation constant for ammonium (g N m^{-3})

Nit_m = maximum nitrification rate at TNit (g N m^{-3} day^{-1})

TNit = optimum temperature for nitrification (°C)

KNit1 = effect of temperature below TNit on nitrification rate ($°C^{-2}$)

KNit2 = effect of temperature above TNit on nitrification rate ($°C^{-2}$)

SU = concentration of particulate biogenic silica (g Si m^{-3})

FSP_d = fraction of metabolized silica by diatoms produced as particulate biogenic silica

FSPP = fraction of predated diatom silica produced as particulate biogenic silica

ASC_d = silica-to-carbon ratio of diatoms (g Si per g C)

K_{SUA} = dissolution rate of particulate biogenic silica (day^{-1})

WSU = external loads of particulate biogenic silica (g Si day^{-1})

SA = concentration of available silica (g Si m^{-3}) = Sad + SAp

SAd = dissolved available silica (g Si m^{-3})

SAp = particulate (sorbed) available silica (g Si m^{-3})

FSI_d = fraction of metabolized silica by diatoms produced as available silica

FSIP = fraction of predated diatom silica produced as available silica

BFSAd = sediment-water exchange flux of available silica (g Si m^{-2} day^{-1}), applied to the bottom layer only.

WSA = external loads of available silica (g Si day^{-1})

K_{SAp} = empirical coefficient relating available silica sorption to total suspended solid (per g m^{-3})

K_{SAp} = or particulate total active metal (per mol m^{-3}) concentration

K_{SU} = dissolution rate of particulate biogenic silica at TR_{SUA} (day^{-1})

KT_{SUA} = effect of temperature on dissolution of particulate biogenic silica ($^{\circ}C^{-1}$)

TR_{SUA} = reference temperature for dissolution of particulate biogenic silica ($^{\circ}C$)

COD = concentration of chemical oxygen demand (g O_2-equivalents m^{-3})

KH_{COD} = half-saturation constant of dissolved oxygen required for oxidation of COD (g O_2 m^{-3})

KCOD = oxidation rate of chemical oxygen demand (day^{-1})

BFCOD = sediment flux of COD (g O_2-equivalents m^{-2} day^{-1}), applied to the bottom layer only

WCOD = external loads of chemical oxygen demand (g O_2-equivalents day^{-1})

K_{CD} = oxidation rate of chemical oxygen demand at TR_{COD} (day^{-1})

KT_{COD} = effect of temperature on oxidation of chemical oxygen demand ($^{\circ}C^{-1}$)

TR_{COD} = reference temperature for oxidation of chemical oxygen demand ($^{\circ}C$)

AONT = mass of dissolved oxygen consumed per unit mass of ammonium nitrogen

AONT = nitrified (4.33 g O_2 per g N)

AOCR = dissolved oxygen-to-carbon ratio in respiration (2.67 g O_2 per g C)

K_r = reaeration coefficient (day^{-1}): the reaeration term is applied to the surface layer only

DO_s = saturated concentration of dissolved oxygen (g O_2 m^{-3})

SOD =sediment oxygen demand (g O_2 m^{-2} day^{-1}), applied to the bottom layer only

WDO = external loads of dissolved oxygen (g O_2 day^{-1})

AONT = 4.33 g O_2 per g N.

K_{ro} = proportionality constant = 3.933 in MKS unit

u_{eq} = weighted velocity over cross-section (m sec^{-1}) = $\sum(u_k V_k)/\sum(V_k)$

h_{eq} = weighted depth over cross-section (m) = $\sum(V_k)/B_\eta$

B_η = width at the free surface (m)

W_{rea} = wind-induced reaeration (m day^{-1}) $= 0.728\,U_w^{½} - 0.317\,U_w + 0.0372\,U_w^2$

U_w = wind speed (m sec^{-1}) at the height of 10 m above surface

KT_r = constant for temperature adjustment of DO reaeration rate

TAM = total active metal concentration (mol m^{-3}) = TAMd + TAMp

TAMd = dissolved total active metal (mol m^{-3})

TAMp = particulate total active metal (mol m^{-3})

KHbmf = dissolved oxygen concentration at which total active metal release is half the anoxic

KHbmf = release rate (g O_2 m^{-3})

BFTAM = anoxic release rate of total active metal (mol m^{-2} day^{-1}), applied to the bottom layer only

Ktam = effect of temperature on sediment release of total active metal ($^{\circ}C^{-1}$)

Ttam = reference temperature for sediment release of total active metal ($^{\circ}C$).

WS_s = settling velocity of particulate metal (m day^{-1})

WTAM = external loads of total active metal (mol day^{-1})

TAMdmx = solubility of total active metal under anoxic conditions (mol m^{-3})

Kdotam = constant that relates total active metal solubility to dissolved oxygen concentration (per g O_2 m^{-3})

FCB = bacteria concentration (MPN per 100 ml)

KFCB = first order die-off rate at 20 $^{\circ}C$ (day^{-1})

TFCB = effect of temperature on decay of bacteria ($^{\circ}C^{-1}$)

WFCB = external loads of fecal coliform bacteria (MPN per 100 ml m^3 day^{-1})

Water Quality Model Parameters (sorted in alphabetical order)

AANOX = ratio of denitrification rate to oxic dissolved organic carbon respiration rate

ANC_x = nitrogen-to-carbon ratio in algal group x (g N per g C)

ANDC = mass of nitrate nitrogen reduced per mass of DOC oxidized (0.933 g N per g C)

AOCR = dissolved oxygen-to-carbon ratio in respiration (2.67 g O_2 per g C)

AONT = 4.33 g O_2 per g N

AONT = mass of dissolved oxygen consumed per unit mass of ammonium nitrogen

AONT = nitrified (4.33 g O_2 per g N)

APC = mean phosphorus-to-carbon ratio in all algal groups (g P per g C)

ASC_d = silica-to-carbon ratio of diatoms (g Si per g C)

B_η = width at the free surface (m)

BFCOD = sediment flux of COD (g O_2-equivalents m^{-2} day^{-1}), applied to the bottom layer only

BFNH4 = sediment-water exchange flux of ammonium (g N m^{-2} day^{-1}), applied to the bottom layer only.

BFNO3 = sediment-water exchange flux of nitrate (g N m^{-2} day^{-1}), applied to the bottom layer only

BFPO4d = sediment-water exchange flux of phosphate (g P m^{-2} day^{-1}), applied to the bottom layer only

BFSAd = sediment-water exchange flux of available silica (g Si m^{-2} day^{-1}), applied to the bottom layer only.

BFTAM = anoxic release rate of total active metal (mol m^{-2} day^{-1}), applied to the bottom layer only

BMR_x = basal metabolism rate at TR_x for algal group x (day^{-1})

BM_x = basal metabolism rate of algal group x (day^{-1})

B_x = algal biomass of algal group x (g C m^{-3})

$CChl_x$ = carbon-to-chlorophyll ratio in algal group x (g C per mg Chl)

COD = concentration of chemical oxygen demand (g O_2-equivalents m^{-3})

CP_{prm1} = minimum carbon-to-phosphorus ratio (g C per g P)

CP_{prm2} = difference between minimum and maximum carbon-to-phosphorus ratio (g C per g P)

CP_{prm3} = effect of dissolved phosphate concentration on carbon-to-phosphorus ratio (per g P m^{-3})

Denit = denitrification rate (day^{-1})

$(D_{opt})_x$ = depth of maximum algal growth for algal group x (m)

DO = dissolved oxygen concentration (g O_2 m^{-3})

DOC = concentration of dissolved organic carbon (g C m^{-3})

DON = concentration of dissolved organic nitrogen (g N m^{-3})

DOP = concentration of dissolved organic phosphorus (g P m^{-3})

DO_s = saturated concentration of dissolved oxygen (g O_2 m^{-3})

$f_1(N)$ = effect of suboptimal nutrient concentration ($0 \le f_1 \le 1$)

$f_2(I)$ = effect of suboptimal light intensity ($0 \le f_2 \le 1$)

$f_3(T)$ = effect of suboptimal temperature ($0 \le f_3 \le 1$)

$f_4(S)$ = effect of salinity on cyanobacteria growth ($0 \le f_4 \le 1$)

FCB = bacteria concentration (MPN per 100 ml)

FCDP = fraction of predated carbon produced as dissolved organic carbon

FCD_x = fraction of basal metabolism exuded as dissolved organic carbon at infinite dissolved oxygen (group x)

FCLP = fraction of predated carbon produced as labile particulate organic carbon

FCRP = fraction of predated carbon produced as refractory particulate organic carbon

FD = fractional daylength ($0 \le FD \le 1$)

FNDP = fraction of predated nitrogen produced as dissolved organic nitrogen

FND_x = fraction of metabolized nitrogen by algal group x produced as dissolved organic nitrogen

FNIP = fraction of predated nitrogen produced as inorganic nitrogen

FNI_x = fraction of metabolized nitrogen by algal group x produced as inorganic nitrogen

FNLP = fraction of predated nitrogen produced as labile particulate organic nitrogen

FNL_x = fraction of metabolized nitrogen by algal group x produced as labile particulate organic nitrogen

FNRP = fraction of predated nitrogen produced as refractory particulate organic nitrogen

FNR_x = fraction of metabolized nitrogen by algal group x produced as refractory particulate organic nitrogen

FPDP = fraction of predated phosphorus produced as dissolved organic phosphorus

FPD_x = fraction of metabolized phosphorus by algal group x produced as dissolved organic phosphorus

FPIP = fraction of predated phosphorus produced as inorganic phosphorus

FPI_x = fraction of metabolized phosphorus by algal group x produced as inorganic phosphorus

FPLP = fraction of predated phosphorus produced as labile particulate organic phosphorus

FPL_x = fraction of metabolized phosphorus by algal group x produced as labile POP.

FPRP = fraction of predated phosphorus produced as refractory particulate organic phosphorus

FPR_x = fraction of metabolized phosphorus by algal group x produced as refractory POP.

FSI_d = fraction of metabolized silica by diatoms produced as available silica

FSIP = fraction of predated diatom silica produced as available silica

FSP_d = fraction of metabolized silica by diatoms produced as particulate biogenic silica

FSPP = fraction of predated diatom silica produced as particulate biogenic silica

h_{eq} = weighted depth over cross-section (m) = $\sum(V_k)/B_\eta$

H_T = depth from the free surface to the top of the layer (m)

I_1 = daily light intensity one day preceding model day (langleys day^{-1})

I_2 = daily light intensity two days preceding model day (langleys day^{-1})

I_o = daily total light intensity at water surface (langleys day^{-1})

$(I_o)_{avg}$ = adjusted surface light intensity (langleys day^{-1})

$(I_s)_x$ = optimal light intensity for algal group x (langleys day^{-1})

K_{CD} = oxidation rate of chemical oxygen demand at TR_{COD} (day^{-1})

KCOD = oxidation rate of chemical oxygen demand (day^{-1})

K_{DC} = minimum respiration rate of dissolved organic carbon (day^{-1})

K_{DCalg} = constant that relates respiration to algal biomass (day^{-1} per g C m^{-3})

K_{DN} = minimum mineralization rate of dissolved organic nitrogen (day^{-1})

K_{DNalg} = constant that relates mineralization to algal biomass (day^{-1} per g C m^{-3})

K_{DON} = mineralization rate of dissolved organic nitrogen (day^{-1})

K_{DOP} = mineralization rate of dissolved organic phosphorus (day^{-1})

Kdotam = constant that relates total active metal solubility to dissolved oxygen concentration (per g O_2 m^{-3})

K_{DP} = minimum mineralization rate of dissolved organic phosphorus (day^{-1})

K_{DPalg} = constant that relates mineralization to algal biomass (day^{-1} per g C m^{-3})

Ke_b = background light extinction (m^{-1})

Ke_{Chl} = light extinction coefficient for chlorophyll 'a' (m^{-1} per mg Chl m^{-3})

Kess = total light extinction coefficient (m^{-1})

Ke_{TSS} = light extinction coefficient for total suspended solid (m^{-1} per g m^{-3})

KFCB = first order die-off rate at 20 °C (day^{-1})

KHbmf = dissolved oxygen concentration at which total active metal release is half the anoxic

KHbmf = release rate (g O_2 m^{-3})

KH_{COD} = half-saturation constant of dissolved oxygen required for oxidation of COD (g O_2 m^{-3})

$KHDN_N$ = denitrification half-saturation constant for nitrate (g N m^{-3})

KHN = mean half-saturation constant for algal nitrogen uptake (g N m^{-3})

$KHNit_{DO}$ = nitrification half-saturation constant for dissolved oxygen (g O_2 m^{-3})

$KHNit_N$ = nitrification half-saturation constant for ammonium (g N m^{-3})

KHN_x = half-saturation constant for nitrogen uptake for algal group x (g N m^{-3})

KHP = mean half-saturation constant for algal phosphorus uptake (g P m^{-3})

KHP_x = half-saturation constant for phosphorus uptake for algal group x (g P m^{-3})

K_{HR} = heterotrophic respiration rate of dissolved organic carbon (day^{-1})

KHR_x = half-saturation constant of dissolved oxygen for algal DOC excretion for group x (g O_2 m^{-3})

KHS = half-saturation constant for silica uptake for diatoms (g Si m^{-3}).

K_{LC} = minimum dissolution rate of labile particulate organic carbon (day^{-1})

K_{LCalg} = constants related dissolution of labile POC, to algal biomass (day^{-1} per g C m^{-3})

K_{LN} = minimum hydrolysis rate of labile particulate organic nitrogen (day^{-1})

K_{LNalg} = constants that relate hydrolysis of labile PON to algal biomass (day^{-1} per g C m^{-3})

K_{LP} = minimum hydrolysis rate of labile particulate organic phosphorus (day^{-1})

K_{LPalg} = constants that relate hydrolysis of labile POP to algal biomass (day^{-1} per g C m^{-3})

K_{LPOC} = dissolution rate of labile particulate organic carbon (day^{-1})

K_{LPON} = hydrolysis rate of labile particulate organic nitrogen (day^{-1})

K_{LPOP} = hydrolysis rate of labile particulate organic phosphorus (day-1)

KNit1 = effect of temperature below TNit on nitrification rate ($°C^{-2}$)

KNit2 = effect of temperature above TNit on nitrification rate ($°C^{-2}$)

K_r = reaeration coefficient (day^{-1}): the reaeration term is applied to the surface layer only

K_{RC} = minimum dissolution rate of refractory particulate organic carbon (day^{-1})

K_{RCalg} = constants related dissolution of refractory POC to algal biomass (day^{-1} per g C m^{-3})

K_{RN} = minimum hydrolysis rate of refractory particulate organic nitrogen (day^{-1})

K_{RNalg} = constants that relate hydrolysis of refractory PON to algal biomass (day^{-1} per g C m^{-3})

K_{ro} = proportionality constant = 3.933 in MKS unit

K_{RP} = minimum hydrolysis rate of refractory particulate organic phosphorus (day^{-1})

K_{RPalg} = constants that relate hydrolysis of refractory POP to algal biomass (day^{-1} per g C m^{-3})

K_{RPOC} = dissolution rate of refractory particulate organic carbon (day^{-1})

K_{RPON} = hydrolysis rate of refractory particulate organic nitrogen (day^{-1})

K_{RPOP} = hydrolysis rate of refractory particulate organic phosphorus (day^{-1})

K_{SAp} = empirical coefficient relating available silica sorption to total suspended solid (per g m^{-3})

K_{SAp} = or particulate total active metal (per mol m^{-3}) concentration

K_{SU} = dissolution rate of particulate biogenic silica at TR_{SUA} (day^{-1})

K_{SUA} = dissolution rate of particulate biogenic silica (day^{-1})

Ktam = effect of temperature on sediment release of total active metal ($°C^{-1}$)

KTB_x = effect of temperature on metabolism for algal group x ($°C^{-1}$)

KT_{COD} = effect of temperature on oxidation of chemical oxygen demand ($°C^{-1}$)

$KTG1_x$ = effect of temperature below TM_x on growth for algal group x ($°C^{-2}$)

$KTG2_x$ = effect of temperature above TM_x on growth for algal group x ($°C^{-2}$)

KT_{HDR} = effect of temperature on hydrolysis of particulate organic matter ($°C^{-1}$)

KT_{MNL} = effect of temperature on mineralization of dissolved organic matter ($°C^{-1}$)

KT_r = constant for temperature adjustment of DO reaeration rate

KT_{SUA} = effect of temperature on dissolution of particulate biogenic silica ($°C^{-1}$)

LPOC = concentration of labile particulate organic carbon (g C m^{-3})

LPON = concentration of labile particulate organic nitrogen (g N m^{-3})

LPOP = concentration of labile particulate organic phosphorus (g P m^{-3})

NH4 = ammonium nitrogen concentration (g N m^{-3})

Nit = nitrification rate (day^{-1}) given in Eq. 3-13g

Nit_m = maximum nitrification rate at TNit (g N m^{-3} day^{-1})

NO3 = nitrate nitrogen concentration (g N m^{-3})

PM_x = maximum growth rate under optimal conditions for algal group x (day^{-1})

PN_x = preference for ammonium uptake by algal group x ($0 \le PN_x \le 1$)

PO4d = dissolved phosphate phosphorus concentration (g P m^{-3})

PO4d = dissolved phosphate (g P m^{-3})

PO4p = particulate (sorbed) phosphate (g P m^{-3})

PO4t = total phosphate (g P m^{-3}) = PO4d + PO4p

PRR_x = predation rate at TR_x for algal group x (day^{-1})

PR_x = predation rate of algal group x (day^{-1})

P_x = production rate of algal group x (day^{-1})

RPOC = concentration of refractory particulate organic carbon (g C m^{-3})

RPON = concentration of refractory particulate organic nitrogen (g N m^{-3})

RPOP = concentration of refractory particulate organic phosphorus (g P m^{-3})

S = salinity in water column (ppt) provided from the hydrodynamic model

SA = concentration of available silica (g Si m^{-3}) = SAd + SAp

SAd = dissolved available silica (g Si m^{-3})

SAd = concentration of dissolved available silica (g Si m^{-3})

SAp = particulate (sorbed) available silica (g Si m^{-3})

SOD = sediment oxygen demand (g O_2 m^{-2} day^{-1}), applied to the bottom layer only

STOX = salinity at which Microcystis growth is halved (ppt)

SU = concentration of particulate biogenic silica (g Si m^{-3}).

t = time (day)

T = temperature (°C) provided from the hydrodynamic model

TAM = total active metal concentration (mol m^{-3}) = TAMd + TAMp

TAMd = dissolved total active metal (mol m^{-3})

TAMdmx = solubility of total active metal under anoxic conditions (mol m^{-3})

TAMp = particulate total active metal (mol m^{-3})

TFCB = effect of temperature on decay of bacteria ($°C^{-1}$)

TM_x = optimal temperature for algal growth for algal group x (°C)

TNit = optimum temperature for nitrification (°C)

TR_{COD} = reference temperature for oxidation of chemical oxygen demand (°C).

TR_{HDR} = reference temperature for hydrolysis of particulate organic matter (°C)

TR_{MNL} = reference temperature for mineralization of dissolved organic matter (°C)

TR_{SUA} = reference temperature for dissolution of particulate biogenic silica (°C)

TR_x = reference temperature for basal metabolism for algal group x (°C)

TSS = total suspended solid concentration (g m^{-3}) provided from the hydrodynamic model

Ttam = reference temperature for sediment release of total active metal (°C).

u_{eq} = weighted velocity over cross-section (m sec^{-1}) = $\sum(u_k V_k)/\sum(V_k)$

U_w = wind speed (m sec^{-1}) at the height of 10 m above surface

V = cell volume (m^3).

WB_x = external loads of algal group x (g C day^{-1})

WCOD = external loads of chemical oxygen demand (g O_2-equivalents day^{-1}).

WDO = external loads of dissolved oxygen (g O_2 day^{-1})

WDOC = external loads of dissolved organic carbon (g C day^{-1})

WDON = external loads of dissolved organic nitrogen (g N day^{-1})

WDOP = external loads of dissolved organic phosphorus (g P day^{-1})

WFCB = external loads of fecal coliform bacteria (MPN per 100 ml m^3 day^{-1})

WLPOC = external loads of labile particulate organic carbon (g C day^{-1})

WLPON = external loads of labile particulate organic nitrogen (g N day^{-1})

WLPOP = external loads of labile particulate organic phosphorus (g P day^{-1})

WNH4 = external loads of ammonium (g N day^{-1})

WNO3 = external loads of nitrate (g N day^{-1})

WPO4t = external loads of total phosphate (g P day^{-1})

W_{rea} = wind-induced reaeration (m day^{-1}) $= 0.728 U_w^{½} - 0.317 U_w + 0.0372 U_w^2$

WRPOC = external loads of refractory particulate organic carbon (g C day^{-1})

WRPON = external loads of refractory particulate organic nitrogen (g N day^{-1})

WRPOP = external loads of refractory particulate organic phosphorus (g P day^{-1})

WSA = external loads of available silica (g Si day^{-1})

WS_{LP} = settling velocity of labile particulate organic matter (m day^{-1})

WS_{RP} = settling velocity of refractory particulate organic matter (m day^{-1})

WS_s = settling velocity of particulate metal (m day^{-1})

WS_{TSS} = settling velocity of suspended solid (m day^{-1}), provided by the hydrodynamic model

WSU = external loads of particulate biogenic silica (g Si day^{-1})

WS_x = settling velocity of algal group x (m day^{-1})

WTAM = external loads of total active metal (mol day^{-1})

Δz = layer thickness (m)

Sediment Processes Model Parameters

$J_{POM,i}$ = depositional flux of POM (M = C, N or P) routed into the i^{th} G class (g m^{-2} day^{-1})

J_{PSi} = depositional flux of PSi (g Si m^{-2} day^{-1})

$FCLP_i$, = fraction of water column labile POC routed into the i^{th} G class in sediment

$FNLP_i$ = fraction of water column labile PON routed into the i^{th} G class in sediment

$FPLP_i$ = fraction of water column labile POP routed into the i^{th} G class in sediment

$FCRP_i$, = fraction of water column refractory POC routed into the i^{th} G class in sediment

$FNRP_i$ = fraction of water column refractory PON routed into the i^{th} G class in sediment

$FPRP_i$ = fraction of water column refractory POP routed into the i^{th} G class in sediment

$FCB_{x,i}$, = fraction of POC in the algal group x routed into the i^{th} G class in sediment

$FNB_{x,i}$ = fraction of PON in the algal group x routed into the i^{th} G class in sediment

$FPB_{x,i}$ = fraction of POP in the algal group x routed into the i^{th} G class in sediment

$G_{POM,i}$ = concentration of POM (M = C, N or P) in the i^{th} G class in Layer 2 (g m^{-3})

$K_{POM,i}$ = decay rate of the i^{th} G class POM at 20 °C in Layer 2 (day^{-1})

$\theta_{POM,i}$ = constant for temperature adjustment for $K_{POM,i}$

T = sediment temperature (°C)

W = burial rate (m day^{-1})

J_M =diagenesis flux (g m^{-2} day^{-1}) of carbon (M = C), nitrogen (M = N) or phosphorus (M = P)

Ct_1 & Ct_2 = total concentrations in Layer 1 and 2, respectively (g m^{-3})

Ct_o = total concentration in the overlying water (g m^{-3})

s = surface mass transfer coefficient (m day^{-1})

KL = diffusion velocity for dissolved fraction between Layer 1 and 2 (m day^{-1})

ϑ = particle mixing velocity between Layer 1 and 2 (m day^{-1})

fd_o = dissolved fraction of total substance in the overlying water ($0 \le fd_o \le 1$)

fd_1 = dissolved fraction of total substance in Layer 1 ($0 \le fd_1 \le 1$)

fp_1 = particulate fraction of total substance in Layer 1 (= 1 - fd_1)

fd_2 = dissolved fraction of total substance in Layer 2 ($0 \le fd_2 \le 1$)

fp_2 = particulate fraction of total substance in Layer 2 (= 1 - fd_2)

κ_1 = reaction velocity in Layer 1 (m day^{-1})

J_1 = sum of all internal sources in Layer 1 (g m^{-2} day^{-1})

J_{aq} =sediment flux of ammonium, nitrate, phosphate or sulfide/methane to the overlying water (g m^{-2} day^{-1})

κ_2 = reaction velocity in Layer 2 (m day^{-1})

J_2 = sum of all internal sources including diagenesis in Layer 2 (g m^{-2} day^{-1})

D_p = apparent diffusion coefficient for particle mixing (m^2 day^{-1})

θ_{Dp} = constant for temperature adjustment for D_p

$G_{POC,R}$ = reference concentration for $G_{POC,1}$ (g C m^{-3})

KM_{Dp} = particle mixing half-saturation constant for oxygen (g O_2 m^{-3})

Dp_{min} = minimum diffusion coefficient for particle mixing (m^2 day^{-1})

D_d = diffusion coefficient in pore water (m^2 day^{-1})

θ_{Dd} = constant for temperature adjustment for D_d

$R_{BI,BT}$ = ratio of bio-irrigation to bioturbation

$KM_{NH4,O2}$ = nitrification half-saturation constant for dissolved oxygen (g O_2 m^{-3})

$NH4_1$ = total ammonium nitrogen concentration in Layer 1 (g N m^{-3})

KM_{NH4} = nitrification half-saturation constant for ammonium (g N m^{-3})

κ_{NH4} = optimal reaction velocity for nitrification at 20 °C (m day^{-1})

θ_{NH4} = constant for temperature adjustment for κ_{NH4}

J_{Nit} = nitrification flux (g N m^{-2} day^{-1}).

$\kappa_{NO3,1}$ = reaction velocity for denitrification in Layer 1 at 20 °C (m day^{-1})

$\kappa_{NO3,2}$ = reaction velocity for denitrification in Layer 2 at 20 °C (m day^{-1})

θ_{NO3} = constant for temperature adjustment for $\kappa_{NO3,1}$ and $\kappa_{NO3,2}$

$J_{N2(g)}$ = denitrification flux (g N m^{-2} day^{-1})

$NO3_1$ = total nitrate nitrogen concentration in Layer 1 (g N m^{-3})

$NO3_2$ = total nitrate nitrogen concentration in Layer 2 (g N m^{-3}).

$a_{O2,C}$ = stoichiometric coefficient for carbon diagenesis consumed by

$a_{O2,C}$ = sulfide oxidation (2.6667 g O_2-equivalents per g C)

$a_{O2,NO3}$ = stoichiometric coefficient for carbon diagenesis consumed by denitrification (2.8571 g O_2-equivalents/g N).

$\kappa_{H2S,d1}$ = reaction velocity for dissolved sulfide oxidation in Layer 1 at 20 °C (m day^{-1})

$\kappa_{H2S,p1}$ = reaction velocity for particulate sulfide oxidation in Layer 1 at 20 °C (m day^{-1})

θ_{H2S} = constant for temperature adjustment for $\kappa_{H2S,d1}$ and $\kappa_{H2S,p1}$

$KM_{H2S,O2}$ = constant to normalize the sulfide oxidation rate for oxygen (g O_2 m^{-3}).

$H2S_1$ = total sulfide concentration in Layer 1 (g O_2-equivalents m^{-3})

$a_{O2,NH4}$ = stoichiometric coefficient for oxygen consumed by nitrification (4.33 g O_2 per g N)

$J_{aq,CH4}$ = aqueous methane flux (g O_2-equivalents m^{-2} day^{-1})

$J_{CH4(g)}$ = gaseous methane flux (g O_2-equivalents m^{-2} day^{-1})

$CSOD_{max}$ = maximum CSOD occurring when all the dissolved methane transported to the oxic layer is oxidized

κ_{CH4} = reaction velocity for dissolved methane oxidation in Layer 1 at 20 °C (m day^{-1})

θ_{CH4} = constant for temperature adjustment for κ_{CH4}

$CH4_{sat}$ = saturation concentration of methane in the pore water (g O_2-equivalents m^{-3})

PSi = concentration of particulate biogenic silica in the sediment (g Si m^{-3})

S_{Si} = dissolution rate of PSi in Layer 2 (g Si m^{-3} day^{-1})

J_{PSi} = depositional flux of PSi (g Si m^{-2} day^{-1})

J_{DSi} = detrital flux of PSi (g Si m^{-2} day^{-1}) to account for PSi settling to the sediment that is not associated with the algal flux of biogenic silica

K_{Si} = first order dissolution rate for PSi at 20 °C in Layer 2 (day^{-1})

θ_{Si} = constant for temperature adjustment for K_{Si}

KM_{PSi} = silica dissolution half-saturation constant for PSi (g Si m^{-3})

Si_{sat} = saturation concentration of silica in the pore water (g Si m^{-3})

D_T = heat diffusion coefficient between the water column and sediment (m^2 sec^{-1})

T_W = temperature in the overlying water column (°C)